

**ANALYSIS AND MODELING OF GNSS AUGMENTATION SYSTEM
FOR BANGLADESH**

A. A. M. SHAH SADMAN

**MILITARY INSTITUTE OF SCIENCE AND TECHNOLOGY (MIST)
DHAKA, BANGLADESH**

2021



**ANALYSIS AND MODELING OF GNSS AUGMENTATION
SYSTEM FOR BANGLADESH**

A. A. M. SHAH SADMAN
(BSc Engg., AUST)

**A THESIS SUBMITTED
FOR THE DEGREE OF MASTER OF
ENGINEERING**


**DEPARTMENT OF ELECTRICAL, ELECTRONIC AND
COMMUNICATION ENGINEERING
MILITARY INSTITUTE OF SCIENCE AND TECHNOLOGY**

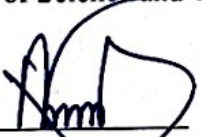
2021

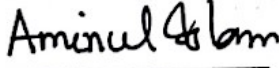
APPROVAL

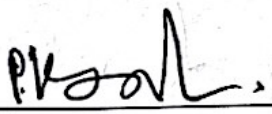
The thesis titled "Analysis and Modeling of GNSS Augmentation System for Bangladesh" submitted by A. A. M. Shah Sadman, Roll No: 1017160026, Session: 2016-2017 has been accepted as satisfactory in partial fulfillment of the requirement for the degree of Master of Science in Electrical, Electronic and Communication Engineering on June, 2021.

BOARD OF EXAMINERS

1. 

Dr. Md. Hossam-E-Haider
Professor
Department of Electrical, Electronic and Communication Engineering
Military Institute of Science and Technology, Dhaka
Chairman
2. 

Brigadier General A K M Nazrul Islam, PhD
Head of the Dept. and Senior Instructor
Department of Electrical, Electronic and Communication Engineering
Military Institute of Science and Technology, Dhaka
Member
(Ex-officio)
3. 

Major Md Aminul Islam, PhD, EME
Instructor Class 'B'
Department of Electrical, Electronic and Communication Engineering
Military Institute of Science and Technology, Dhaka
Member
(Internal)
4. 

Dr. Pran Kanai Saha
Professor
Department of Electrical and Electronic Engineering
Bangladesh University of Engineering and Technology, Dhaka
Member
(External)

DECLARATION

I hereby declare that this thesis is my original work and it has been written by me in its entirety. I have duly acknowledged all the sources of information which have been used in the thesis.

The thesis (fully or partially) has not been submitted for any degree or diploma in any university or institute previously.

ଡା.ଆ.ଋ ଶାହି ଆଦମାନ

A. A. M. Shah Sadman

Date: 26/06/2021

ACKNOWLEDGEMENTS

I would like to begin by uttering that all praise and glory go to Almighty Allah (s.w.t) for giving me the perseverance, strength, knowledge and capability to complete this research work successfully. My earnest gratefulness to my supervisor, Professor Dr. Md. Hossam-E-Haider for his timely valuable guidance, productive suggestions and inspirations in the journey of completing the work. Without his generous support this research work would not have been a success.

I am truly obliged to the rest of the members of my board of examination for reviewing this thesis and giving me support, suggestions and valuable time regarding this work.

Moreover, I would also like to acknowledge the contribution of the Department of Electrical, Electronic and Communication Engineering for the facilities provided to me for doing my research work.

Finally, I would like to thank my family who consistently supported and motivated me towards achieving my goal.

ABSTRACT

Satellite communication, certainly is one of the most reliable means of communication nowadays because of its larger coverage, broader bandwidth and ability to provide an incessant communication. In order to enhance the navigation accuracy, augmentation systems for Global Navigation Satellite System (GNSS) have been developed in many countries. These augmentation systems work locally to minimize the computational error so that extreme accuracy can be achieved. To establish an augmentation system is a complex task as many factors need to be considered. Bangladesh being a satellite owning country can aim for developing its own augmentation system provided the major requirements are studied as well as analyzed satisfactorily which will leverage the economic growth and can be a defense asset. Several navigation systems use different satellite constellations for navigation purpose but for an augmentation system the best one or combination should be selected by investigating some of the important relevant parameters. So, a comparison is required among the navigation systems over a particular period of time, surveying at different locations in Bangladesh to detect the best possible system as well as differentiate among the locations based on the parameters. As array antenna has been proven to be more beneficial than a single element antenna as it not only augments the directivity but also enables beam steering capability which is accomplished by establishing a phase difference relation among the antenna elements. Furthermore, selecting location for ground station is significant in augmentation system. The behavior of satellite signal differs in different locations as the environmental condition is not the same. Bangladesh is a subtropical monsoon country having variations in temperature, rainfall and humidity, so these factors along with the parameters will play a vital role in the selection of ground station. In a nut shell, this thesis work aims to perform some of the major criteria to setup an augmentation system for Bangladesh, from analyzing various satellite constellation and comparing among them in order to find out the performance parameters to developing some reference station antennas. Additionally, the atmospheric effects have also been evaluated to find out the signal propagation delay for different cities in order to compare among the cities to find out the location for reference station. Also, uplink and downlink loss analysis has been done by estimating the crucial factors.

TABLE OF CONTENTS

Certificate of Approval	i
Declaration	ii
Acknowledgements	iii
Abstract	iv
Table of Contents	v-viii
List of Figures	ix-xi
List of Tables	xii-xiii
Abbreviations	xiv
Chapter 1 Introduction	1
1.1 Global Navigation Satellite System (GNSS)	1
1.2 Limitations of GNSS Operation	2
1.3 GNSS Augmentation System	3
1.4 Types of Augmentation System	4
1.4.1 Ground Based Augmentation System (GBAS)	4
1.4.2 Satellite Based Augmentation System (SBAS)	4
1.5 Operation of SBAS	4
1.6 Necessity of SBAS	6
1.7 Motivation	7
1.8 Objectives of the Thesis	8
1.6 Organization of the Book	8
Chapter 2 Literature Review	10
2.1 Introduction	10
2.2 GNSS Constellations	10
2.2.1 Global Positioning System (GPS)	10
2.2.2 Galileo	11
2.2.3 GLONASS	11
2.2.4 BeiDou	12
2.2.5 Other constellations	12
2.3 Different Operational SBAS in the World	13
2.3.1 Wide Area Augmentation System (WAAS)	13

2.3.2	European Geostationary Navigation Overlay Service (EGNOS)	14
2.3.3	GPS Aided GEO Augmented Navigation (GAGAN)	14
2.3.4	African Satellite Augmentation System (ASAS)	15
2.3.5	SBAS for Australia	16
2.4	SBAS Implementation Recommendations	16
2.5	GNSS Parameters	17
2.5.1	MDB and MDE	17
2.5.2	Bias-to-Noise Ratio (BNR)	18
2.5.3	Number of in view satellites	18
2.5.4	Dilution of Precision (DOP)	18
2.5.5	User Equivalent Range Error (UERE)	19
2.5.6	Accuracy	20
2.6	SBAS Reference Station Antenna	20
2.6.1	Antenna parameters	20
2.6.2	Beam scanning of phased array antenna	21
2.7	Environmental Factors and Signal Loss	22
2.7.1	Tropospheric scintillation	23
2.7.2	Ionospheric delay	23
2.7.3	Rainfall attenuation	23
2.7.4	Uplink and downlink loss	23
Chapter 3	Methodology	25
3.1	Introduction	25
3.2	Segmentation of the Objectives	25
3.3	Analysis on GNSS Augmentation System and GNSS Parameters	25
3.4	Selection of the Surveyed Locations	25
3.5	Comparison of GNSS Parameters over Different Locations	26
3.6	Design of Reference Station Antenna and Observation of the Performance of Array Antenna as well as Beam Scanning	27
3.6.1	2x2 slotted microstrip patch antenna for different GNSS frequencies	29
3.6.2	Improved 2x3 phased array patch antenna to enhance the beam scanning range	31

3.7	Analysis on the Environmental Factors	32
3.7.1	Tropospheric scintillation model	32
3.7.2	Ionospheric delay	34
3.7.3	Rainfall attenuation	35
3.7.4	Simulation setup and data collection	36
3.8	Uplink and downlink loss estimation	38
3.9	Software Support	38
Chapter 4	Results and Discussion	39
4.1	Simulation Results of GNSS Parameters over Different Locations	39
4.1.1	Dhaka (23.8103 ⁰ N, 90.4125 ⁰ E)	39
4.1.2	Chattogram (22.3569 ⁰ N, 91.7832 ⁰ E)	42
4.1.3	Rajshahi (24.3745 ⁰ N, 88.6042 ⁰ E)	46
4.1.4	Sylhet (24.8949 ⁰ N, 91.8687 ⁰ E)	49
4.1.5	Khulna (22.8456 ⁰ N, 89.5403 ⁰ E)	52
4.1.6	Discussion on the results	55
4.1.7	Evaluation of the outcomes	56
4.2	Simulation Results of GNSS Accuracy	57
4.2.1	Dhaka (23.8103 ⁰ N, 90.4125 ⁰ E)	57
4.2.2	Chattogram (22.3569 ⁰ N, 91.7832 ⁰ E)	58
4.2.3	Rajshahi (24.3745 ⁰ N, 88.6042 ⁰ E)	59
4.2.4	Sylhet (24.8949 ⁰ N, 91.8687 ⁰ E)	60
4.2.5	Khulna (22.8456 ⁰ N, 89.5403 ⁰ E)	61
4.2.6	Discussion on the results	61
4.2.7	Evaluation of the outcomes	62
4.3	Simulation Results of Ground Station Phased Array Antenna for Different GNSS Constellations	62
4.3.1	Results analysis of a 2x2 slotted microstrip patch antenna for different GNSS frequencies	63
4.3.2	Simulation results of improved 2x3 phased array patch antenna to enhance the beam scanning range	72
4.4	Estimation of Atmospheric Factors of GNSS Signals over Bangladesh to Select Suitable Ground Station Location	74
4.4.1	Tropospheric Scintillation Fade Depth (SFD)	74

4.4.2	Discussion on the results	89
4.4.3	Ionospheric delay estimation	90
4.4.4	Discussion on the results	93
4.4.5	Rainfall attenuation	94
4.4.6	Discussion on the results	95
4.4.7	Evaluation of the outcomes	95
4.5	Estimation of Uplink and Downlink Loss over the Locations	96
4.5.1	Discussion on the results	97
Chapter 5	Conclusion and Future Recommendation	98
5.1	Conclusion	98
5.2	Significance of the Research	98
5.3	Scope for Future Work	99
	List of Publications	101
	List of References	102

LIST OF FIGURES

Figure No.	Name of Figure	Page No.
Fig. 1.1	Operation of SBAS	5
Fig. 1.2	Map of SBAS owned countries	6
Fig. 2.1	Coverage area map of WAAS	13
Fig. 2.2	Availability map of EGNOS	14
Fig. 2.3	GAGAN coverage map of GSAT 8, 10, 15	15
Fig. 3.1	U- slotted microstrip patch antenna (a) rotation angle $Z = 0^{\circ}$, (b) rotation angle $Z = 40^{\circ}$, (c) rotation angle $Z = 80^{\circ}$	28
Fig. 3.2	Designed 2x2 phased array antenna	29
Fig. 3.3	Designed rectangular slotted microstrip patch antenna	30
Fig. 3.4	Designed 2x3 phased array antenna	31
Fig. 4.1	GPS values over Dhaka (a) MDB, (b) MDE, (c) GDOP	39
Fig. 4.2	Galileo values over Dhaka (a) MDB, (b) MDE, (c) GDOP	40
Fig. 4.3	MDB value over Dhaka for combined GPS – Galileo	41
Fig. 4.4	MDE value over Dhaka for combined GPS – Galileo	41
Fig. 4.5	GDOP value over Dhaka for combined GPS – Galileo	42
Fig. 4.6	GPS values over Chattogram (a) MDB, (b) MDE and (c) GDOP	42
Fig. 4.7	GPS values over Chattogram (a) MDB, (b) MDE and (c) GDOP	43
Fig. 4.8	MDB value over Chattogram for combined GPS – Galileo ..	44
Fig. 4.9	MDE value over Chattogram for combined GPS – Galileo ..	45
Fig. 4.10	GDOP value over Chattogram for combined GPS – Galileo ..	45
Fig. 4.11	GPS values over Rajshahi (a) MDB, (b) MDE and (c) GDOP ..	46
Fig. 4.12	Galileo values over Rajshahi (a) MDB, (b) MDE and (c) GDOP	47
Fig. 4.13	MDB value over Rajshahi for combined GPS – Galileo	48
Fig. 4.14	MDE value over Rajshahi for combined GPS – Galileo	48
Fig. 4.15	GDOP value over Rajshahi for combined GPS – Galileo	48
Fig. 4.16	GPS values over Sylhet (a) MDB, (b) MDE and (c) GDOP ..	49

Fig. 4.17	Galileo values over Sylhet (a) MDB, (b) MDE and (c) GDOP	50
Fig. 4.18	MDB value over Sylhet for combined GPS – Galileo	51
Fig. 4.19	MDE value over Sylhet for combined GPS – Galileo	51
Fig. 4.20	GDOP value over Sylhet for combined GPS – Galileo	52
Fig. 4.21	GPS values over Khulna (a) MDB, (b) MDE and (c) GDOP	52
Fig. 4.22	Galileo values over Khulna (a) MDB, (b) MDE and (c) GDOP	53
Fig. 4.23	MDB value over Khulna for combined GPS – Galileo	54
Fig. 4.24	MDE value over Khulna for combined GPS – Galileo	55
Fig. 4.25	GDOP value over Khulna for combined GPS – Galileo	55
Fig. 4.26	Accuracy results over Dhaka (a) GPS and (b) Galileo	57
Fig. 4.27	Accuracy results over Chattogram (a) GPS and (b) Galileo	58
Fig. 4.28	Accuracy results over Rajshahi (a) GPS and (b) Galileo	59
Fig. 4.29	Accuracy results over Sylhet (a) GPS and (b) Galileo	60
Fig. 4.30	Accuracy results over Khulna (a) GPS and (b) Galileo	61
Fig. 4.31	Far field radiation pattern (polar) for $Z = 80^0$ of (a) L1, (b) L2 and (c) L5	64
Fig. 4.32	S- parameters of the antenna for $Z = 80^0$ for GPS frequencies	65
Fig. 4.33	Far field radiation pattern (polar) for $Z = 80^0$ of (a) E5, (b) E6 and (c) L3	66
Fig. 4.34	S-parameters of the antenna for $Z = 80^0$ for Galileo and GLONASS frequencies	67
Fig. 4.35	Radiation pattern (polar) of array antenna for GPS L1 (a) $\theta = +21^0$ and (b) $\theta = -21^0$	69
Fig. 4.36	Radiation pattern (polar) of array antenna for Galileo E6 (a) $\theta = +21^0$ and (b) $\theta = -21^0$	70
Fig. 4.37	Radiation pattern (polar) of array antenna for GLONASS L3, (a) $\theta = +21^0$ and (b) $\theta = -21^0$	71
Fig. 4.38	Far field polar radiation pattern (a) and 3D radiation pattern (b) of the array antenna for $\theta = +24^0$	73
Fig. 4.39	Far field polar radiation pattern (a) and 3D radiation pattern (b) of the array antenna for $\theta = +15^0$	73

Fig. 4.40	Far field polar radiation pattern (a) and 3D radiation pattern (b) of the array antenna for $\theta = -25^0$	74
Fig. 4.41	SFD for different elevation angle in Dhaka for L1 (a) Maximum and (b) Minimum	75
Fig. 4.42	SFD for different elevation angle in Dhaka for E5 (a) Maximum and (b) Minimum	77
Fig. 4.43	SFD for different elevation angle in Chattogram for L1 (a) Maximum and (b) Minimum	78
Fig. 4.44	SFD for different elevation angle in Chattogram for E5 (a) Maximum and (b) Minimum	80
Fig. 4.45	SFD for different elevation angle in Rajshahi for L1 (a) Maximum and (b) Minimum	81
Fig. 4.46	SFD for different elevation angle in Rajshahi for E5 (a) Maximum and (b) Minimum	83
Fig. 4.47	SFD for different elevation angle in Khulna for L1 (a) Maximum and (b) Minimum	84
Fig. 4.48	SFD for different elevation angle in Khulna for E5 (a) Maximum and (b) Minimum	86
Fig. 4.49	SFD for different elevation angle in Sylhet for L1 (a) Maximum and (b) Minimum	87
Fig. 4.50	SFD for different elevation angle in Sylhet for E5 (a) Maximum and (b) Minimum	89
Fig. 4.51	Ionospheric delay for L1	91
Fig. 4.52	Ionospheric delay for E5	92
Fig. 4.53	Ionospheric delay for L3	92
Fig. 4.54	Rainfall attenuation delay over different locations	94
Fig. 4.55	Downlink loss over different locations	96
Fig. 4.56	Uplink loss over different locations	97

LIST OF TABLES

Table No.	Name of Table	Page No.
Table 3.1	Typical GPS C/A – code UERE budget	26
Table 3.2	Typical UERE budget for Galileo	26
Table 3.3	Optimized physical dimension of U-slotted microstrip patch antenna	29
Table 3.4	Optimized physical dimension of rectangular slotted microstrip patch antenna	30
Table 3.5	Geographical position of the surveyed locations	35
Table 3.6	Average maximum temperature (t_{max}) of the surveyed locations	35
Table 3.7	Average minimum temperature (t_{min}) of the surveyed locations	35
Table 3.8	Average relative humidity, H (%) of the surveyed locations	36
Table 3.9	Average maximum TEC of the surveyed locations	36
Table 3.10	Average rainfall rate (mm/hr) of the surveyed locations	36
Table 4.1	Summary of the simulation results for Dhaka	41
Table 4.2	Summary of the simulation results for Dhaka	42
Table 4.3	Summary of the simulation results for Chattogram	44
Table 4.4	Summary of the simulation results for Chattogram	45
Table 4.5	Summary of the simulation results for Rajshahi	47
Table 4.6	Summary of the simulation results for Rajshahi	49
Table 4.7	Summary of the simulation results for Sylhet	51
Table 4.8	Summary of the simulation results for Sylhet	52
Table 4.9	Summary of the simulation results for Khulna	54
Table 4.10	Summary of the simulation results for Khulna	55
Table 4.11	Overall comparison among the locations on the parameters	56
Table 4.12	Overall comparison among the locations on accuracy	62
Table 4.13	Parametric study of antenna for GPS signals	63
Table 4.14	Parametric study of antenna for Galileo and GLONASS signals	66
Table 4.15	2x2 array antenna performance for GPS signals	68

Table 4.16	2x2 array antenna performance for Galileo and GLONASS signals	70
Table 4.17	Scan angle determination of 2x3 phased array antenna	72
Table 4.18	SFD value of Dhaka using L1 for different elevation angle	75
Table 4.19	SFD value of Dhaka using E5 for different elevation angle	76
Table 4.20	SFD value of Chattogram using L1 for different elevation angle	78
Table 4.21	SFD value of Chattogram using E5 for different elevation angle	79
Table 4.22	SFD value of Rajshahi using L1 for different elevation angle	81
Table 4.23	SFD value of Rajshahi using E5 for different elevation angle	82
Table 4.24	SFD value of Khulna using L1 for different elevation angle	84
Table 4.25	SFD value of Khulna using E5 for different elevation angle	85
Table 4.26	SFD value of Sylhet using L1 for different elevation angle	87
Table 4.27	SFD value of Sylhet using E5 for different elevation angle	88
Table 4.28	Average SFD comparison among the locations per year	90
Table 4.29	Ionospheric delay of all the locations for L1, E5 and L3	91
Table 4.30	Average ionospheric delay comparison among the locations per year	93
Table 4.31	Rain attenuation (db/km) of individual locations	94
Table 4.32	Average rainfall attenuation comparison among the locations per year	95
Table 4.33	Overall comparison among the locations on environmental factors	96

ABBREVIATIONS

ASAS	African Satellite Augmentation System
BNR	Bias-to-Noise Ratio
EGNOS	European Geostationary Navigation Overlay Service
GAGAN	GPS Aided GEO Augmented Navigation
GBAS	Ground Based Augmentation System
GDOP	Geometric Dilution of Precision
GEO	Geostationary Earth Orbit
GLS	GNSS Landing System
GNSS	Global Navigation Satellite System
GPS	Global Positioning System
ICAO	International Civil Aviation Organization
IRNSS	Indian Regional Navigation Satellite System
SBAS	Satellite Based Augmentation System
MDB	Minimal Detectable Bias
MDE	Minimal Detectable Effect
QZSS	Quasi-Zenith Satellite System
SFD	Scintillation Fade Depth
TEC	Total Electron Content
UERE	User Equivalent Range Error
WAAS	Wide Area Augmentation System

CHAPTER 1

INTRODUCTION

1.1 Global Navigation Satellite System (GNSS)

At present, satellite navigation has become one of the most sophisticated means of technologies all over the world. Due to its vast significance in aviation, maritime, public safety and other civil activities, countries are opting to invest in developing satellite navigation system. It all started back in 1978 with the launch of first GPS satellite, solely developed by the USA, into the orbit. Afterwards, the GPS constellation has been completed within upcoming years which has 31 satellites in space giving full global coverage. A Global Navigation Satellite System (GNSS) is a satellite navigation system that has global coverage. GNSS is capable of providing positioning, navigation, and timing (PNT) services which means that geographic location can be calculated from anywhere on the earth using a GNSS receiver. Most of the developed countries have developed or trying to develop their own satellite navigation system. Among them, Galileo of European Union, GLONASS of Russia, IRNSS of India and Beidou of China are fully operational GNSS [1].

GNSS systems are continuously being upgraded from to newer generations of better services, as well as being made compatible and interoperable with one another so that receivers can use two or more constellations. If the receivers are capable of receiving the various GNSS signals, this increases efficiency and services.

GNSS architecture consists of three segments- space segment, control segment and user segment [2]. The space segment is made up of GNSS satellites that orbit the earth at an altitude of about 20,000 kilometers. Each satellite in a GNSS constellation sends out a signal that identifies it as well as provides information on its time, orbit, and status.

The control segment is a combination of a ground-based network of master control stations, data uploading stations, and monitor stations. The master control station in each GNSS system monitors the satellites' orbit parameters and onboard high-precision clocks as required to maintain accuracy.

The signals and status of the satellites are tracked and relayed to the master control station by monitor stations, which are typically spread out over a wide geographic area. The signals are analyzed by the master control station, which then sends a time correction.

The user segment is made up of the receiving equipment. A GNSS receiver is a piece of equipment that processes signals emitted from satellites to determine the user's position in space. Though PVT determination is the most popular use, receivers may also be used for other purposes.

1.2 Limitations of GNSS Operation

The Global Navigation Satellite System (GNSS) is a complicated system that relies on data messages sent from a constellation of satellites. There is a risk of failure at any step, starting with the creation of data messages and upload to GPS satellites, transmission, reception, and processing by user receiving equipment. The failures can be at system level that occurs at the space segment due to the erroneous clock. As a result, the timing calculation of the satellite and ground station is not accurate. In any GNSS constellation, the position is calculated using four in view satellites. The visibility of these satellites are not the same all the time and despite having more in view satellite, the system calculates position data with four, which has error in it. Moreover, while traveling the signal through space and earth environment, a lot of interference happen which degrades the signal quality. As a consequence, a GNSS receiver can lose track on a satellite.

Also, signal transmission is often influenced by the media between the satellite and the receiver antenna which includes ionosphere, troposphere, and multipath effect. All these reasons give birth to error in the navigational data which is sent to the user segment, misguides the user. If the user is relying on only one navigation system then it will be difficult for the user to get the correct solution. A multiple constellation GNSS system can be a relief but it is also prone to error like single constellation.

As precision has become very important in many sectors such as aviation, maritime, a small error in position calculation is not accepted at all. Due to this reason, an augmentation system has been developed which reduces the error and confirms precise positioning.

1.3 GNSS Augmentation System

In order to make position determination more accurate, a system has been developed which not only improves the PNT of the GNSS but also enhances the sectors which includes safety of life (SOL). The system is called GNSS augmentation system. It was created to provide consistent, reliable, and safe navigation, particularly when high precision and increased coverage are needed. Many of the common error sources in GNSS are attempted to be corrected by augmentation systems. It is effectively achieved by placing a reference station in close proximity to a user, or where high-accuracy is necessary. GNSS augmentation system has found its application mostly in aviation industries as it provides some chief performance parameters which an individual GPS or GLONASS constellation cannot fully deliver. They are [3]:

- a) **Integrity:** Integrity refers to the ability to protect users from incorrect data in a timely manner. Since not all GPS satellites are tracked at all times, integrity cannot be guaranteed. A navigation system must, in particular, provide users with a warning of any failure within a certain amount of time (time-to-alert). If the navigation positioning error reaches the warning limit and that the event is not detected is identified as the integrity risk, also known as the probability of misleading information.
- b) **Accuracy:** It refers to the difference between measured and true positions at any given time to a defined reference value. Ideally, this reference value should be a true value, if known, or some agreed-upon standard value. Accuracy should not be confused with precision, which denotes a measurement quality that describes how well repeated measurements agree with themselves rather than with a reference value.
- c) **Continuity:** The ability of a navigation device to perform its work without unscheduled interruptions for the duration of its planned service is known as continuity. It refers to the navigation system's ability to provide a navigation output with the specified level of accuracy and integrity, assuming it was available when the operation began.
- d) **Availability:** The percentage of time that a service is available for use is referred to as availability. If the accuracy, integrity, and continuity standards are met, the service is available. Unlike land navigational aid structure, GNSS availability is

complicated by satellite movement relative to a coverage area and the potential for a long time to recover a satellite in the event of a failure. Due to the weather condition and variation in elevation angle, the availability of satellite varies time to time.

1.4 Types of Augmentation System

Augmentation system can be divided into two major types,

1.4.1 Ground Based Augmentation System (GBAS):

A GBAS is a local augmentation system in which the correction data is transferred to the user through the reference station. The reference station receives the position data from the satellites and corrects the data as the location of the reference station is known precisely. The reference stations are distributed around the desired locations such as airports. The correction message that is then sent to users via a VHF Data Link. This knowledge is used by an aircraft receiver to correct GPS signals. One of the best operational GBAS systems is Local Area Augmentation System (LAAS), developed by USA.

1.4.2 Satellite Based Augmentation System (SBAS):

In SBAS, the correction data is broadcasted through a geo stationary satellite. Similar to GBAS, the reference stations collect the navigational data from the satellite constellations. Then these data are transferred to the master station where the correction happens. From the master station, the data is transmitted to the geo stationary satellite and then it is broadcasted to the coverage area by that satellite. Thus SBAS improves the GNSS range accuracy. SBAS is discussed in more details in the next section.

1.5 Operation of Satellite Based Augmentation System (SBAS)

As mentioned in section 1.4.2, a SBAS corrects the navigational data with the help of a geo stationary satellite. SBAS is a regional system that is developed to meet the required accuracy in aviation and other activities. Two basic functions of an SBAS system are ranging and integrity channel [4]. It uses geo-stationary satellites to provide additional ranging signals to increase availability. The integrity channel is used to send GPS and integrity data to navigators. Major components of a SBAS system are:

- a) The **Ground Segment (GS)** consists of reference stations for ranging and integrity monitoring that are placed at specifically surveyed locations.
- b) The **Master Control Station (MCS)** gathers, calculates and processes data in order to deliver wide-area correction messages and credibility information to the user.
- c) The **Navigation Land Earth Station (NES)** uplinks messages to geostationary satellites (GEO) for transmission.

The concept of SBAS is described below:

- a) SBAS reference stations are placed at pre-surveyed locations in the desired region to measure pseudoranges and carrier phases from all visible satellites.
- b) SBAS master station calculates clock and ephemeris corrections for each GPS satellite monitored, as well as ephemeris information for each GEO and ionospheric vertical delays, using data from the reference stations.
- c) Users receive these corrections and error bounds from the master station via GEO communication satellites. In order to increase the precision of their location estimates, user avionics apply these corrections to their pseudoranges obtained from GPS measurements.

The SBAS signal that the user receives looks just like a GPS signal, with the exception that the transmitted message modulation rate is 250 bps instead of 50 bps for the GPS data stream and the data are error coded. The operation of SBAS is shown in Fig. 1.1.

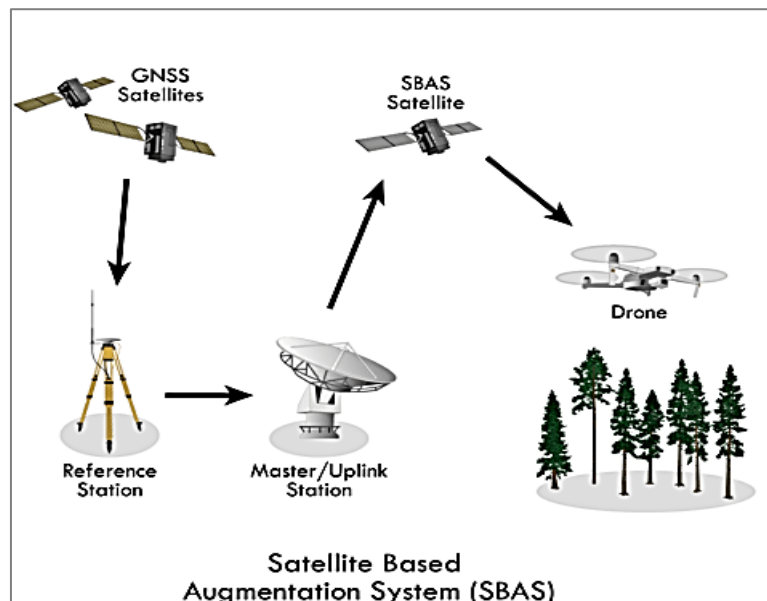


Fig. 1.1: Operation of SBAS (Source: <https://www.researchgate.net/publication>)

1.6 Necessity of SBAS

SBAS offers a more precise navigation service than simple GNSS-RAIM systems, as well as the high degree of integrity needed for most aviation navigation operations. Because of the advantages they offer, many interoperable SBAS have been or are being introduced around the world.

SBAS technology allows for the coverage of very wide areas of airspace and areas. In certain cases, it also provides more capability, versatility and cost-effective navigation options than ground-based navigation aids. SBAS is an important component of Performance Dependent Navigation (PBN).

SBAS minimizes dependency on obsolete, ground-based, and legacy infrastructure, allowing ground-based technology to be rationalized. SBAS navigation based on efficiency improves operating efficiencies, resulting in cost savings and emissions reductions.

SBAS is becoming more widely used in aviation to support a variety of other applications. Satellite navigation service availability will improve in areas with active ionospheres and during ionosphere storms with the possible launch of dual-frequency multiple constellation (DFMC) SBAS service. Fig. 1.2 displays a map of SBAS owned countries of the world.

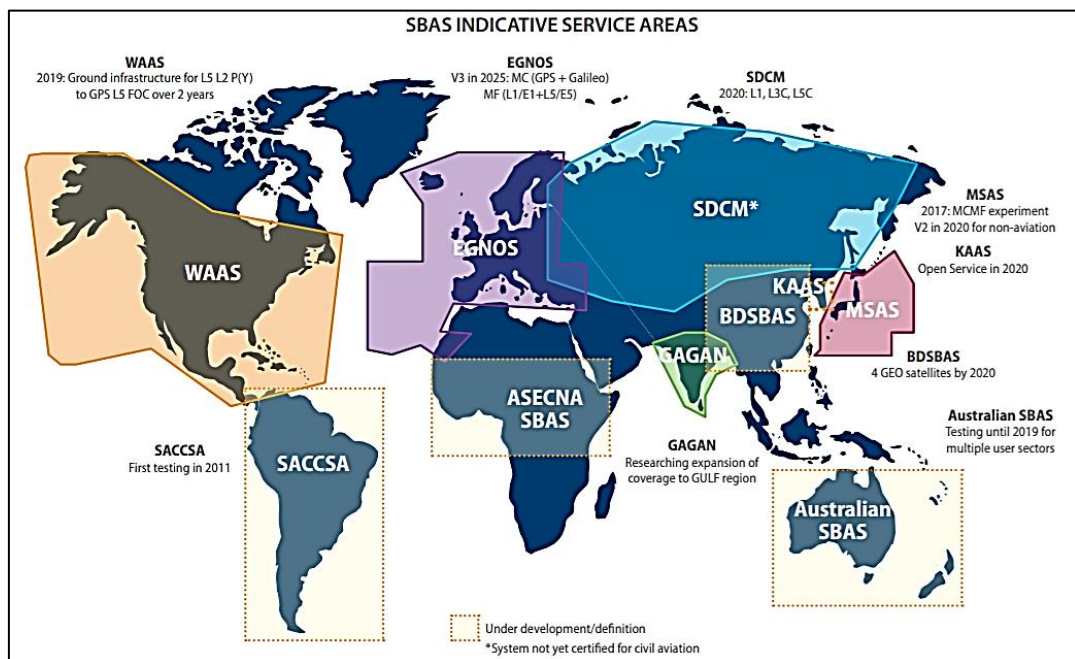


Fig. 1.2: Map of SBAS owned countries (Source: <https://www.euspa.europa.eu/europe>)

From the Fig. 1.2 above, it can be understood that most of the developed as well as developing countries have established or on the way to establish SBAS due to its vast importance in navigation sector.

1.7 Motivation

From the above study, it has appeared that the importance of developing a SBAS is inevitable for countries who are planning to leverage their aviation activities, public safety and defense strategy. Bangladesh being a developing country can also aim for building its own augmentation system. Bangladesh has launched its first geo stationary satellite, Bangabandhu Satellite – 1 on May 12, 2018. This satellite is a communication and broadcasting satellite. Development of another geo stationary satellite is also being planned and aimed to launch within upcoming years. For establishing a SBAS, geo stationary satellites are a must. So with proper planning on transponder utilization, in future a SBAS can be established. Apart from the reason, a SBAS will be essential for the further development of Bangladesh because:

- a) The expansion of the main airport of Bangladesh, Hazrat Shahjalal International Airport is taking place due to the increase of air traffic. According to a report of JICA [5], the number of international passengers reached 8 million in 2020 and are expected to reach 20 million by 2035. In addition, the airport's annual average air cargo volume reached approximately 420,000 tons in 2020. In order to maintain the air traffic in future, a planned SBAS system is indispensable. Also, in developing the GNSS landing system (GLS), SBAS plays key role.
- b) GNSS, when used with SBAS, can provide accurate and reliable positioning not only for ocean navigation but also for port approaches. In Matarbari, Bangladesh, a deep sea port is being constructed. This port have to maintain the huge traffic of ships which will anchor there. This port will no doubt will increase the economic growth of Bangladesh. So to aptly handle the situation a SBAS can be a fine and effective system. Moreover, Bangladesh is also giving emphasis on the blue economy concept [6] which includes monitoring sea resources, oil and gas mining etc. where SBAS can find its application too.
- c) Developing a SBAS will also help Bangladesh in defense and security sector. Along with GNSS, SBAS can be used in defense applications, from conventional military

uses in avionics and other guidance systems, to personal warfighter and convoy navigation, to asset monitoring and rescue.

- d) Bangladesh is geopolitically an important country. In order to tackle the pressure from unwanted enemies, SBAS can be established. Combined with GNSS, SBAS can be used to monitor and guard environmentally vulnerable areas.
- e) In addition to that, there are a number of sectors in Bangladesh where SBAS can be utilized. Such as land mapping, surveying, autonomous driving and GIS.

Overall, the application of SBAS in Bangladesh is extensive. To sustain the economic growth in future as well as maintain the leading position in the world, this system can be initiated. These are the motivations that worked as fuel behind the research work.

1.8 Objectives of the Thesis

The specific objectives of the thesis are following:

- a) To examine and compare the major existing satellite constellations to identify the best possible constellation for Bangladesh and to investigate various types of GNSS augmentation systems to develop a theoretical model for Bangladesh.
- b) To design and simulate a range of reference station antenna keeping crucial factors in mind to transmit and receive signal from Bangabandhu satellite.
- c) To analyze and develop signal propagation model as well as link budget.

1.9 Organization of the Thesis

The layout of the thesis is as follows:

Chapter 1 comprises of introduction to the thesis topic and the motivation behind the research. Also, the objectives of the thesis have been included in this chapter.

Chapter 2 consists of the theoretical studies that are required for the research work. It describes different GNSS constellations as well as some of the operational SBAS around the world. Also, the parameters and the atmospheric factors that dominate the GNSS performance have been included in this chapter. The theoretical aspects of designing phased array antenna has been discussed too.

Chapter 3 is comprised of the computational methods of the research work. It deals with the process of completing the research in a comprehensive manner. The surveyed locations for which this research has been done, are mentioned with their geographical condition. The design method of phased array antenna has also been included in this chapter as well. The troposphere and ionosphere delay models have been analyzed with proper equations. Finally the simulation setup and required data tables are incorporated.

Chapter 4 is solely dedicated to the simulation and estimated results and discussion on those outcomes. The results have been displayed in graphs as well as in tables where it is needed. Each of the segments has been evaluated after the illustration of the results entirely.

Chapter 5 concludes the research work where the whole work has been summarized. Also, some of the recommendations have been provided in this chapter to carry forward the research in future.

CHAPTER 2

LITERATURE REVIEW

2.1 Introduction

This chapter focuses on the theoretical studies that are required to complete the research work. Since GNSS is such an important building block of an SBAS, the latest active constellations have been investigated. The model of different SBAS-owning countries has been discussed to gather operational knowledge of SBAS, as the research's main objective is to examine SBAS over Bangladesh. The parameters which are important in order to observe the performance parameters of GNSS, have been extracted from the literatures and discussed afterwards. Later on, the atmospheric variables which plays a key role in selecting the ground station have been reviewed along with some major phased array antenna parameters.

2.2 GNSS Constellations

With a view to having full global coverage and accurate position calculation, a number of satellite constellations have been developed which are being used to navigate as well as communicate. The major satellite constellations are discussed briefly below:

2.2.1 Global Positioning System (GPS):

The Global Positioning System (GPS), formerly known as Navstar GPS, is a satellite-based radio navigation system owned and operated by the United States Space Force. It offers geolocation and time information to a GPS receiver anywhere on or near the Earth. From the website of NASA, it is found that the GPS space section currently consists of 31 satellites (January 2021) orbiting the earth about 12,000 miles above. A total number of at least 24 operational satellites are needed for full global coverage. They travel at a speed of 7,000 miles per hour. The health and status of the satellites are tracked by a global ground control/monitoring network which also sends data to the satellites for navigation and other purposes. A GPS satellites transmit signals which travel by line of sight [2]. The signals are:

- a) L1 Signal: The carrier frequency is 1575.42 MHz and the C/A code is transmitted at this frequency using a BPSK modulation.

- b) L2 Signal: After the L1 frequency, the L2 frequency was introduced. A military code and a civilian use code are also included. The L2 operates at a higher frequency of 1227.60 MHz than the L1.
- c) L5 Signal: One of the latest signals included in the GPS upgrade plan is the GPS L5 (1176.45 MHz). The signal is thought to be used in conjunction with L1 and is transmitted in a radio band reserved solely for aviation safety services.

2.2.2 Galileo:

The European Union (EU) agreed in 1998 to pursue a satellite navigation system that was not based on GPS and was planned exclusively for civilian use around the world. Galileo, Europe's own global navigation satellite system, which provides a highly accurate and efficient global positioning service under civilian control. Galileo has 24 operating satellites and six in-orbit spares when fully deployed, placed in three circular Medium Earth Orbit (MEO) planes at 23,222 km altitude above the Earth [2]. The major signals transmitted by Galileo are:

- a) E1 Signal: The open services are realized by this signal with a carrier frequency of 1575.42 MHz.
- b) E5 Signal: The carrier frequency is 1191.795 MHz and also used in open services and safety of life (SOL).
- c) E6 Signal: This is the commercial service band with a carrier frequency of 1278.75 MHz.

2.2.3 Global Navigation Satellite System (GLONASS):

GLONASS, like GPS, was developed by the Russians to provide PVT data to suitably equipped civil and military users. On October 12, 1982, the Soviet Union launched the first GLONASS satellite. From the official website of GLONASS, as of March 2021, there are total 28 satellites in space among them 23 are operational. Each GLONASS satellite is in a 19,100-kilometer circular orbit with a 64.8-degree inclination relative to the Earth's surface. The time of the orbit is 11 hours and 15 minutes. The major signals transmitted by GLONASS constellation are:

- a) L1 Signal: the GLONASS L1 band ranges from 1592.9525 MHz to 1610.485 MHz.
- b) L3 Signal: The GLONASS L3 signal is centered at 1207.14 MHz.

2.2.4 BeiDou:

China designed and operates the BeiDou Navigation Satellite System (BDS) independently, with an emphasis on the country's national security and economic and social development. The BDS offers all-time, all-weather, and high-accuracy positioning, navigation, and timing services to global users. By 2000, the construction of BDS-1 was completed to provide services to China. A number of satellites in the Geostationary Earth Orbit (GEO), Inclined Geo-Synchronous Orbit (IGSO), and Medium Earth Orbit (MEO) make up the BDS space portion (MEO). From the government website of BeiDou, as of June 2020, there are total 35 satellites of BeiDou constellation in space. BeiDou signal bands are:

- a) B1 band: 1559.05 MHz to 1563.15 MHz with a center frequency of 1561.1 MHz.
- b) B2 band: 1195.14 MHz to 1219.14 MHz with a center frequency of 1207.14 MHz.
- c) B3 band: 1256.52 MHz to 1280.52 MHz with a center frequency of 1268.52 MHz.

2.2.5 Other constellations:

Apart from the above mentioned constellations, there are some other constellations which are being developed. The Indian Regional Navigation Satellite System (IRNSS) is an autonomous regional satellite navigation system that offers accurate real-time positioning and timing services. Its operational name is NavIC. It includes India and a 1,500-kilometer (930-mile) radius around it, with proposals for further expansion. There are 7 active satellites in the constellation. Three of the constellation's seven satellites are in geostationary orbit (GEO) and four are in inclined geosynchronous orbit (IGSO). The Quasi-Zenith Satellite System (QZSS) is a Japanese government-developed 4 satellite constellation system.

These satellite constellations can determine position with good precision for regular activities such as driving, location search, delivering products etc. But when it comes to the question of pinpoint positioning such as airplane landing, air fleet operation, ballistic missile guidance etc. SBAS is essential. For example, a standalone GPS receiver's positional accuracy is usually about 10 meters with no integrity. A SBAS system increases accuracy to better than 5 meters [3] and prevents the user from using unreliable satellites. In order to make navigation system more precise, most of the developed countries have developed or in the way of developing their own regional satellite based augmentation

system. All SBAS systems broadcast augmentation data via GEO on a continuous basis (geostationary satellite).

2.3 Different Operational SBAS in the World

2.3.1 Wide Area Augmentation System (WAAS):

The U.S. Wide Area Augmentation System is the first SBAS. WAAS was developed to help with air navigation in North America, but it's now being used for a number of land and sea-based operations. According to FAA testing, WAAS accuracy is usually higher than 7 meters, with findings showing that "the 95 percent horizontal and vertical accuracy at both measured sites is less than 2 meters. For WAAS, strong satellite geometry with a low DOP value is needed [7]. WAAS is made up of 38 WAAS reference stations (WRS) spread throughout the continental US, Alaska, Puerto Rico, Hawaii, Canada, and Mexico, three master control stations, two geostationary Earth orbit (GEO) satellites, and four ground uplink stations (GUS). The coverage area map of WAAS is displayed in Fig. 2.1 collected from FAA.

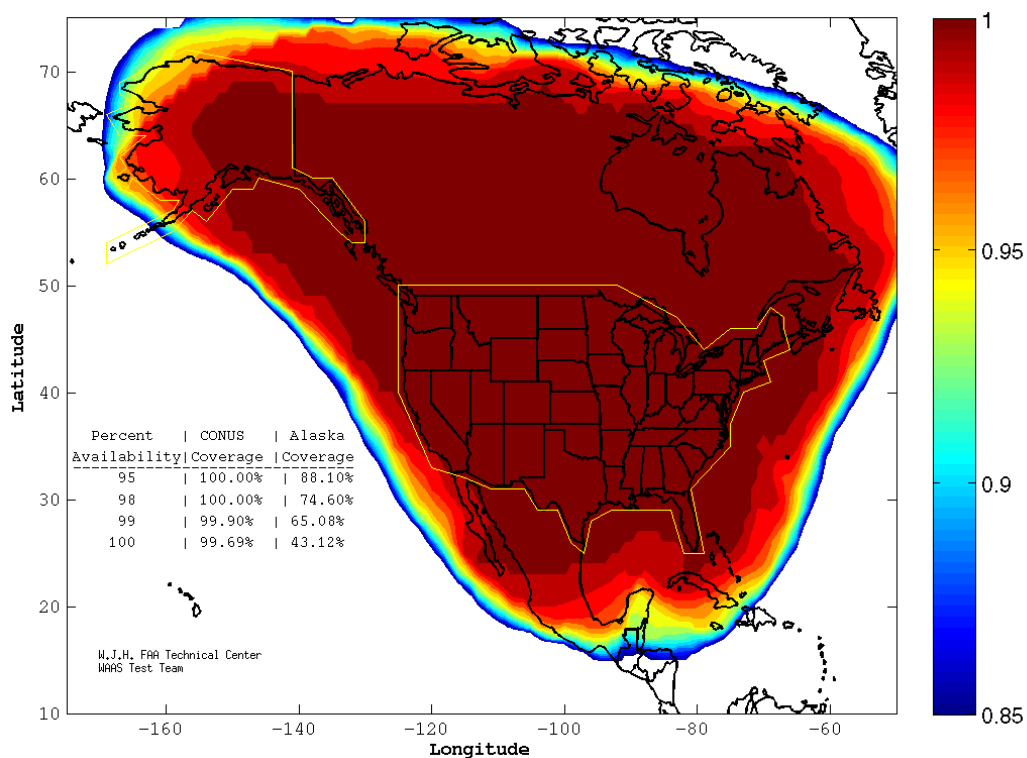


Fig. 2.1: Coverage area map of WAAS (Source: <https://www.boldmethod.com/>)

2.3.2 European Geostationary Navigation Overlay Service (EGNOS):

EGNOS is a satellite-based augmentation system (SBAS) developed for the European Commission by the European Space Agency and EUROCONTROL. It currently works in conjunction with the GPS, reporting on the accuracy and reliability of their positioning data and sending out corrections. The Open Service (OS) is a free service accessible to the general public in Europe. On October 1, 2009, this service became operational. 40 Ranging Integrity Monitoring Stations, 2 Mission Control Centers, 6 Navigation Land Earth Stations, the EGNOS Wide Area Network (EWAN), and three geostationary satellites make up EGNOS [8]. The performance parameters vary in these reference stations due to the geography and due to this reason the availability fluctuates. EGNOS availability map is displayed in Fig. 2.2 [9] which has been described as the minimum area where the user can measure its position at least 99 percent of the time.

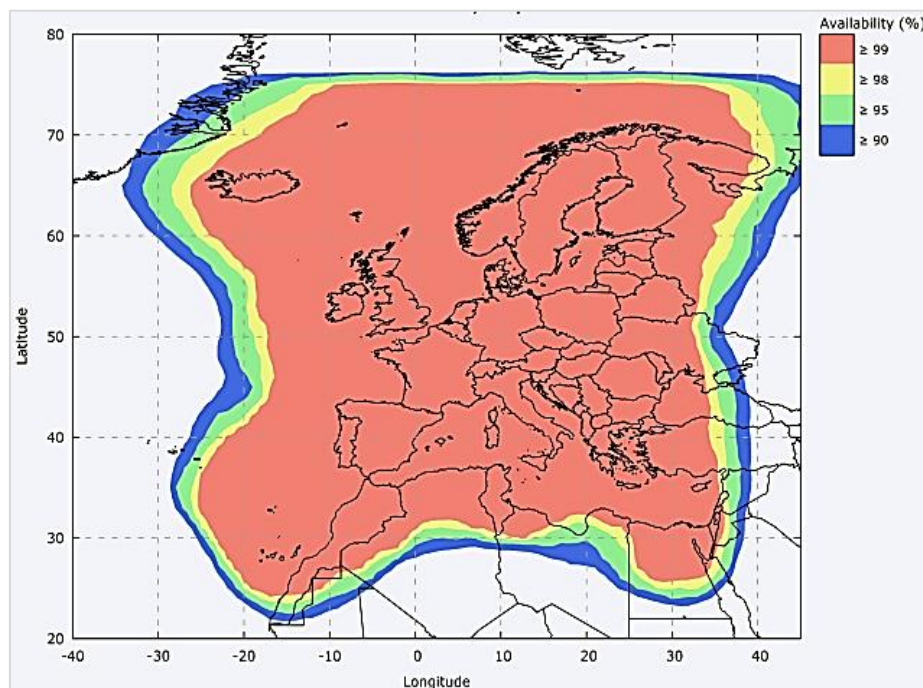


Fig. 2.2: Availability map of EGNOS (Source: <https://gssc.esa.int/navipedia>)

2.3.3 GPS Aided GEO Augmented Navigation (GAGAN):

The Indian Space Research Organization (ISRO) and the Airports Authority of India (AAI) have partnered on a proposal to deploy the Satellite Based Augmentation System (SBAS) over Indian airspace using GPS/GLONASS. While being designed for civil aviation, the device can be used by a wide range of users, including private and public vehicles, railways,

shipping, surveys and more. The GAGAN payload is carried by three GEO satellites: GSAT-8, GSAT-10, and GSAT-15. GAGAN has 15 reference stations spread across the world. At Kundalahalli in Bangalore, two mission control centers have been created, along with associated uplink stations [10]. Since India is situated in the equatorial ionospheric anomaly belt, one of the key concerns about an SBAS implementation in India is ionospheric behavior at these latitudes. The coverage area of GAGAN is shown in Fig. 2.3 [11].

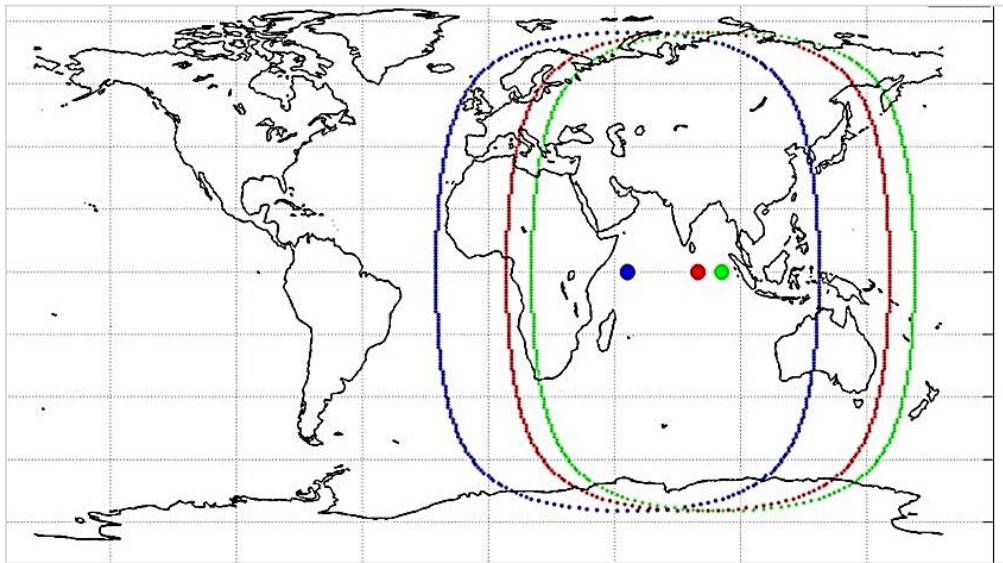


Fig. 2.3: GAGAN coverage map of GSAT 8, 10, 15 (Source: <https://www.icao.com>)

2.3.4 African Satellite Augmentation System (ASAS):

The ASAS network will cover the entire African continent as well as the Middle East. The ASAS network will be identical in terms of system and service to the US WAAS, providing solutions for maritime, land (road, rail and ground) and aeronautical applications. The ASAS service is being designed to correct GNSS signals from the 24 GPS and 24 GLONASS orbiting satellites, which can be inaccurate due to satellite orbit and clock drift, as well as signal delays caused by the atmosphere and ionosphere. A minimum of 50 Ground Monitoring Stations (GMS) or reference stations, 5 Ground Control Stations (GCS) or master stations, and 5 Ground Earth Stations must be included in the ASAS ground network (GES) [12]. In Nigeria, the Nigerian Communications Satellite (NIGCOMSAT) LTD is a Federal Ministry of Communications-owned company. The company operates and manages the NigComSat-1 and NigComSat1R geostationary communications

satellites. As a SBAS, NIGCOMSAT-1 was Africa's first contribution to the Global Navigation Satellite System (SBAS).

2.3.5 SBAS for Australia:

Australia is one of the few major Organization for Economic Cooperation and Development (OECD) countries that does not have SBAS services, which include both wide-area DGNSS and ranging and integrity services via satellites. Australia is considering developing an SBAS capability that is: exclusively owned and controlled by Australia or an expansion of existing SBAS systems. Ground stations in Australia are needed to track satellite and monitor as well as measure atmospheric delay [13]. As of now, the Australian SBAS is currently in test mode and will not be accredited as a critical aviation safety device until it is operational.

2.4 SBAS Implementation Recommendations

The International Civil Aviation Organization (ICAO) is a specialized agency that modifies international air navigation principles and techniques and promotes the planning and development of international air transport to ensure safe and orderly growth. The ICAO Council adopts standards and best practices in air navigation, infrastructure and flight inspection, among other things. As the major application of SBAS is to provide precise positioning in aviation sector, ICAO delivers guidelines in terms of developing the system. Some of the foremost recommendations are discussed below [14]:

- a) SBAS performance depends on a number of parameters which oscillates from constellation to constellations. Also, the improvement of measurement relies on the satellite geometry.
- b) Continuity is the ability of a system to perform its function without unplanned interruptions during the intended operation. In the case of SBAS, the number of satellites in view determines the level of continuity [15].
- c) The availability of GNSS satellites are not the same throughout the world. The variation in the availability of satellite results in erroneous data from location to location. It is recommended to analyze the visible satellites of desired locations.
- d) It's critical to understand that GNSS can be affected by a variety of error sources. The error sources make the accuracy to swing.

- e) The SBAS signals are broadcasted at the center frequency of the GNSS signals for which the receiver/user device need to be constructed.
- f) SBAS provides users with improved ionospheric delay calculations based on real-time observation in order to improve position accuracy and system availability. Several theoretical and empirical ionosphere models have been developed which needs to be analyzed for establishing a regional SBAS.

2.5 GNSS Parameters

Some major criteria must be evaluated in order to make a distinguishing approach to the performance of satellite constellations. These parameters aid in the evaluation of satellite constellations for various locations, resulting in the establishment of an SBAS. They are discussed below:

2.5.1 MDB and MDE:

One of the parts of reliability of GNSS system is internal reliability that can be represented by minimal detectable bias (MDB). MDB is a measurement of the size of the error that can be detected. MDB can be written as (Baarda, 1967; Teunissen, 1998) [16]:

$$|\nabla| = \frac{\lambda_0}{c^T Q_y^{-1} P_A^\perp} \quad (2.1)$$

Where,

$P_A^\perp = I - P_A = I - A(A^T Q_y^{-1} A)^{-1} A^T Q_y^{-1}$, here, P_A is the orthogonal projector on the range space of the design matrix A .

c = model error.

λ_0 = non-centrality parameter which depends on chosen values of the confidence level α_0 and detection power γ_0 .

Q_y = covariance matrix.

Another part of the reliability is the external reliability that is applied to determine systematic error of observation on adjusted co-ordinate. It can be expressed by minimal detectable effect (MDE) which is computed as [16]:

$$\nabla \hat{x} = \begin{pmatrix} \nabla \hat{b} \\ \nabla \hat{a} \end{pmatrix} \quad (2.2)$$

Where,

$\nabla \hat{b}$ is the bias in the float baseline solution.

$\nabla \hat{a}$ is the bias in the float ambiguity solution.

If the values of the MDB and MDE are decreased, then the positioning accuracy, reliability and efficiency can be further improved [16].

2.5.2 Bias-to-Noise Ratio (BNR):

A dimensionless parameter known as bias to noise ratio (BNR) is used to measure external reliability. A scalar bias-to-noise ratio is [17],

$$C_{BNR} = \Delta \hat{x}^T Q_{\hat{x}}^{-1} \Delta \hat{x} \quad (2.3)$$

Where,

$\Delta \hat{x}$ = estimate correction term induced by bias vector.

$Q_{\hat{x}}$ = covariance matrix of bias free state.

The external reliability of a system is considered as good if C_{BNR} has a small value.

2.5.3 Number of in view satellites:

Satellite visibility is defined as the ground station's capability to receive a signal from the satellite. The visibility of satellite is an important aspect of determining the location of ground station [18]. Many satellite constellations such as GPS, GALILEO and GLONASS are providing complete global coverage but visibility of satellites in all the area are not same. Satellite visibility depends on many things, for example location of the place on earth, environmental condition, receiver strength etc. The declining of the number of in view satellite not only effects the system's availability but also degrades the total performance [18]. For a good navigation solution, a minimum of four satellites are required but a better solution can be achieved if the number increases.

2.5.4 Dilution of Precision (DOP):

Along with the visibility of satellite, it is also important how the satellites are positioned in the space. If the visible satellites are close together, the error in the navigational message is greater. To measure the error in the signal propagation due to the satellite geometry, geometric dilution of precision (GDOP) is used. The calculation of GDOP starts by estimating the position offset which is denoted as [19],

$$\Delta x = (H^T H)^{-1} H^T \Delta \rho \quad (2.4)$$

Where, $(H^T H)$ is a 4 X 4 matrix. The pseudorange measurement can be viewed as a linear computation of three terms,

$$\Delta \rho = \rho_T - \rho_L - d\rho \quad (2.5)$$

Where,

ρ_T = vector error from pseudorange value

ρ_L = vector of pseudorange values computed at the linearization point.

$d\rho$ = net error in the pseudorange value.

Using the equation (2.4) and (2.5), least square solution matrix can be obtained as,

$$dx = [(H^T H)^{-1} H^T] d\rho \quad (2.6)$$

The covariance matrix can be written as

$$cov(dx) = (H^T H)^{-1} H^T cov(d\rho) H (H^T H)^{-1} \quad (2.7)$$

After deriving the equations, GDOP can be derived in terms of $(H^T H)^{-1}$ component,

$$GDOP = \sqrt{D_{11} + D_{22} + D_{33} + D_{44}} \quad (2.8)$$

A low value of GDOP indicates a good geometry as well as low navigational error and vice versa. The more the number of in view satellites, the better the value of GDOP which ensures a good accuracy. GDOP value varies from 1-20.

2.5.5 User Equivalent Range Error (UERE):

There is a need for a unique parameter which justifies the effect of all the errors. One such parameter is known as UERE. Each satellite signal suffers from different type of errors. The errors involved in each satellite are summed up and converted into the unit of distance to develop UERE. The UERE for a given satellite is considered to be the square root of the sum different error sources. UERE is symbolized as ‘ σ ’ [20]. UERE is divided into two types [21], which are:

- a. The signal in space ranging error called User Range Error (URE). URE sources are clock error, ephemeris error and group delay error.
- b. User Equipment Error (UEE). The error sources are ionosphere, troposphere, multipath, group delay and noise and interference error.

2.5.6 Accuracy:

In order to develop a good accuracy performance for GNSS, a good satellite geometry is a must. A good satellite geometry can be attained when the satellites are spread in the sky, not clustered together. But only DOP cannot provide all the information required to determine the accurate position. To determine the position, pseudorange is calculated. As the radio signal from satellite has to travel a long distance to the receiver, it suffers from error inclusion. These errors degrades the quality of a signal hence the quality of the accuracy reduces. So, to get a satisfactory level of accuracy these errors should also be taken into consideration which paved the way to the concept of UERE. Both the UERE and DOP then can be used to find the GNSS position accuracy. Multiplying the UERE with appropriate DOP will provide accuracy within one sigma ($1-\sigma$) level which is depicted below [22]:

$$\text{Position Accuracy} = \text{DOP} \times \text{UERE} \quad (2.9)$$

2.6 SBAS Reference Station Antenna

In satellite communication, receivers contain antenna to receive signal. As different satellite constellation has different transmission frequency, the performance of an antenna varies. On the other hand, an array of patch antenna can also be used in the ground station to transmit and receive the satellite signal for purposes like SBAS, GNSS landing system etc. An important aspect of antenna system for SBAS ground station is the fact that how wide the antenna beam can scan. The antennas in an array must be designed by following specific design rules and to attain the beam steering each antenna must be fed with different phased signals. A number of reference station antennas are utilized according to the requirement such as helix antenna, microstrip patch antenna, parabolic antenna etc. [23].

2.6.1 Antenna parameters:

Antenna is one of the most fundamental components of a SBAS reference station which is used to receive navigation data from different constellations and transmit the corrected data to the geo stationary satellite. The design of a reference station antenna thus depends on the frequency of the constellation. To analyze the results of an antenna, a number of parameters need to be evaluated. A few of the most relevant parameters are briefly discussed below [24].

- a) **Directivity:** The directivity is defined as the ratio of the subject antenna's maximum radiation intensity to that of an isotropic or reference antenna radiating the same total power. When transmitting or receiving, the radiation intensity is directed in a specific direction. As a consequence, the antenna's directivity is said to be in that direction.
- b) **Impedance matching:** Impedance matching occurs when the approximate value of a transmitter's impedance equals the approximate value of a receiver's impedance, or vice versa. The antenna, transmission line, and circuitry impedances should all be the same to ensure optimal power transfer between the antenna and the receiver or transmitter.
- c) **Voltage Standing Wave Ratio (VSWR):** The voltage standing wave ratio (VSWR) is a calculation of how well radio-frequency power is transmitted from a source of power to a load through a transmission network. VSWR has a number of values ranging from 1 to ∞ . For most antenna applications, a VSWR of less than 2 is considered appropriate. It is possible to characterize the antenna as having a good match.
- d) **Scattering Parameter:** Scattering parameters or S-parameters denotes the relationship between ports in antenna system. If in a system there are two ports, port 1 and port 2, then S21 means the power transferred from port 1 to port 2. For antenna, the most common term is S11 which denotes how much power is reflected from antenna. It is also known as reflection coefficient or return loss.

2.6.2 Beam scanning of phased array antenna:

The controlling factor of radiation pattern of an array antenna are the antenna element, the geometry of the array and the amplitude and phase of the excitation of each antenna. If the elements of the array antenna are set up in such a way that the radiation pattern of each antenna sums up with adjacent antenna to develop a pattern known as main beam, then it is called phased array antenna. In the case of a phased array antenna, the main beam direction can be rotated if the phase of individual antenna is changed. Using the classical analysis where the main radiation pattern is obtained by vector adding the individual pattern, the final field (E_t) can be written as [25],

$$E_t = E_{se} \times AF \tag{2.10}$$

Here, E_{se} is the field strength of a single element and AF is the array factor which can be represented as below where N is the total number of elements,

$$AF = \frac{1}{N} \left[\frac{\sin\left(\frac{N}{2}\Psi\right)}{\sin\left(\frac{1}{2}\Psi\right)} \right] \quad (2.11)$$

Here, $\Psi = k_0 d \sin\theta + \beta$ where β and d are the phase difference and distance between elements respectively. So the directivity of the antenna can be increased by increasing either N or d [20]. The first maximum which is the major lobe occurs when $\Psi = 0$,

$$0 = k_0 d \sin\theta + \beta \quad (2.12)$$

By varying β , the direction of the major lobe can be manipulated that allows to change the direction without moving the antenna mechanically which is known as beam steering. For a scan angle θ_s , the phase difference can be solved as,

$$\beta = -k_0 d \cos\theta_s \quad (2.13)$$

To get a scan range from $0 - 180^\circ$, β has to vary from $-k_0 d$ to $k_0 d$.

2.7 Environmental Factors and Signal Loss

There are often losses in satellite transmissions due to a variety of factors. Some of these losses may be constant, while others are affected by weather conditions, especially rain. So environmental factors play an important role in developing SBAS for a particular region. As the atmospheric condition is not the same all over the world, the GNSS signal propagation delay is also not similar hence the losses also are not alike. For example, weather condition affects the GNSS signal differently in urban and forest environment [26]. The signals from satellite has to pass through ionosphere and troposphere where the maximum delay as well as loss occur. A signal suffers scintillation in these regions which is the change in amplitude and phase due to the variations in dielectric components. Some of the major environmental factors which are essential in selecting SBAS ground station, discussed below.

2.7.1 Tropospheric scintillation:

The troposphere is the lowest layer of the atmosphere. The troposphere has a temperature gradient that decreases with altitude. It consists the majority of clouds and weather systems. Tropospheric scintillation is a phenomenon that causes signal loss in satellite communication systems that have a small fade margin. Due to tropospheric scintillation, rapid amplitude and phase changes in received signal occur which affects the communication. Scintillation Fade Depth (SFD) is calculated in order to find out the tropospheric effects on signal propagation. A number of model is being used to find out the SFD for a particular region [27].

2.7.2 Ionospheric delay:

Ionosphere is the most upper part of the Earth's atmosphere which is ionized with electrons. The total number of electrons present in a path between a radio transmitter and receiver is known as the Total Electron Content (TEC). The presence of electrons has an effect on radio waves. The radio signal would be influenced further if there are more electrons in the direction of the radio wave. TEC is an important parameter to monitor for ground-to-satellite communication and satellite navigation. Furthermore, the SBAS system may be needed to deal with substantial total electron content (TEC) depletion in limited, localized areas. The ionospheric delay calculation over the area is critical to the SBAS's efficient implementation.

2.7.3 Rainfall attenuation:

Rain particle attenuation is non-uniform and can only be calculated experimentally from rain rate measurements. Rain attenuation has the following effects: loss of signal strength at the receiver, wastage of transmitting power in an attempt to solve this form of attenuation, and in extreme cases, total signal loss at the receiver [28]. Also it causes in unavailability of satellite for a long time. Since rain rates differ, this criterion is critical when choosing an SBAS ground station.

2.7.4 Uplink and downlink loss:

The signals from satellite has to travel a long way, passing through the free space and then the atmosphere. In this journey, losses occur which need to be considered during

development of a SBAS system. The free space path loss is the loss when the signal travels through vacuum, with no objects nearby to cause any reflection or diffraction. This loss is dependent on the distance of satellite from the earth and signal frequency. The atmospheric losses depends on the factors mentioned above. Overall, these losses should be considered while estimating uplink and downlink loss for SBAS [29]. The loss will vary from location to location due to the fluctuation of weather condition.

CHAPTER 3

METHODOLOGY

3.1 Introduction

This chapter demonstrates the computational method of the research work. The objectives of the work have been achieved by a number of a sequential processes which includes the selection of the surveyed locations, analysis and comparison of the GNSS parameters, designing of phased array antenna to observe the beam steering and study of the environmental factors as well as link losses over Bangladesh. Also the data which are essential for the analysis have been listed in the chapter. The overall simulation setup that is comprised of the time frame of the work and different software has also been included in this chapter.

3.2 Segmentation of the Objectives

In order to successfully attain the desired goals of the research, the objectives listed in Chapter 1 have been dissected into segments. This segmentation will aid to complete the work in a sequential way which is described below.

3.3 Analysis on GNSS Augmentation System and GNSS Parameters

The work will start with investigating different GNSS augmentation systems. As most of the countries develop augmentation system according to their requirement, it is important to know and understand the major criteria behind the development. It is also crucial to recognize the performance parameters of the SBAS system which will defy the present condition of GNSS system for a particular region. After a number of literature reviews, some major parameters have been fixed which will be simulated and analyzed over Bangladesh. Among these parameters MDB, MDE, DOP, BNR, number of visible satellites, accuracy have been analyzed over Bangladesh for different GNSS constellation for over two years' of average data.

3.4 Selection of the Surveyed Locations

For the analysis over Bangladesh, five major cities have been selected. In order to select the cities, it has been kept in mind so that it covers the whole country. Moreover, the weather condition of these cities are not the same throughout the year, so the performance of GNSS parameters and environmental factors are tend to vary which will provide a picture of the GNSS signal performance. The surveyed cities are:

Dhaka (23.8103⁰N, 90.4125⁰E): Dhaka is the capital and largest city of Bangladesh which is situated at the center of the country. The land is flat and close to sea level, with tropical vegetation and damp soils. Due to heavy rainfall and cyclones, Dhaka is vulnerable to flooding during the monsoon season. Dhaka has a tropical climate that is hot, rainy, and humid. Dhaka has a tropical wet and dry climate, as per the Köppen climate classification.

Chittagong (22.3569⁰N, 91.7832⁰E): Chittagong is the second largest city of Bangladesh. It is located in southeastern Bangladesh, along the coast of the Chittagong Hill Tracts. Chittagong has a tropical monsoon climate, according to the Köppen climate classification.

Rajshahi (24.3745⁰N, 88.6042⁰E): Rajshahi has a tropical wet and dry climate, according to the Köppen climate classification. Rajshahi's climate is characterized by monsoons, high temperatures, high humidity, and moderate rainfall.

Khulna (22.8456⁰N, 89.5403⁰E): After Dhaka and Chittagong, Khulna is Bangladesh's third-largest district. In the country's south-western region. The city is warm and humid and pleasant in the winter.

Sylhet (24.8949⁰N, 91.8687⁰E): Sylhet is a city in Bangladesh's north-eastern province. Sylhet has a tropical monsoon climate like the rest of Bangladesh. The terrain is mainly hilly.

3.5 Comparison of GNSS Parameters over Different Locations

After selecting the surveyed locations, the simulation have been done to observe the results of the parameters over the five locations. The constellations analyzed are GPS and Galileo system. For estimating the accuracy over the locations, the typical UERE budget of GPS and Galileo have been used which are tabulated in Table 3.1 and Table 3.2.

Table 3.1. Typical GPS C/A – code UERE budget

Error Sources	GPS 1 σ Error (m)
Ephemeris Error	1.4
Satellite Clock Error	1.8
Ionospheric Delay	0.5
Tropospheric Delay	0.2
Receiver Noise	0.6
Multipath	1.5
Total	2.84

Table 3.2: Typical UERE budget for Galileo

Error Source	Galileo 1 σ Error (m)
Signal in Space Ranging Error (SISE)	0.67
Residual Ionosphere Error	6
Residual Troposphere Error	1.35
Thermal Noise, Interference, Multipath	0.35
Multipath Bias Error	0.59
Satellite BGD Error	0.30
Code-Carrier Ionospheric Divergence Error	0.30
Total:	6.26

Taking the values of both the UERE budget, finally the accuracy has been calculated for the particular time period over the five locations using equation 2.9.

3.6 Design of Reference Station Antenna and Observation of the Performance of Array Antenna as well as Beam Scanning

In this section, development of GNSS antenna which can be used in reference stations, has been studied in order to observe the array performance. The major aim of this section is to perceive how a patch array antenna behaves to different GNSS signals and how to increase the overall beam scanning angle range. For doing that, various approaches have been taken starting from implementing slots and taper in patch antenna. The design of the array antenna starts by designing a single patch antenna with the specified dielectric constant (ϵ_r) and

height (h_s). To design a rectangular microstrip patch antenna for a specific resonant frequency (f_r), the width (W) and length (L) of the patch should be computed. The dimension of the patch has been calculated using the formula given below [30] [31]:

Width of the patch,

$$W = \frac{c}{2} \sqrt{\frac{2}{\epsilon_r + 1}} \quad (3.1)$$

Length of the patch is determined by,

$$\epsilon_{eff} = \frac{\epsilon_r + 1}{2} + \frac{\epsilon_r - 1}{2} \left\{ \sqrt{1 + 12 \left(\frac{h_s}{W} \right)} \right\}^{-1} \quad (3.2)$$

$$\Delta L = h_s (0.412) \frac{(\epsilon_{eff} + 0.3) \left(\frac{W}{h_s} + 0.264 \right)}{(\epsilon_{eff} - 0.258) \left(\frac{W}{h_s} + 0.8 \right)} \quad (3.3)$$

$$L_{eff} = \frac{c}{2f_r \sqrt{\epsilon_{eff}}} \quad (3.4)$$

$$L = L_{eff} - 2\Delta L \quad (3.5)$$

Where,

ϵ_{eff} is the effective dielectric constant.

L_{eff} is the effective length.

c is the speed of light.

Ground plane width (W_g) and length (L_g) are calculated using the formulas below,

$$W_g = 6h_s + W \quad (3.6)$$

$$L_g = 6h_s + L$$

Following the equations, two array antennas have been designed and analyzed which are discussed below.

3.6.1 2x2 slotted microstrip patch antenna for different GNSS frequencies

An inset fed microstrip patch antenna using copper has been constructed on a FR-4 dielectric substrate. A U-slot is etched on the patch after a number of optimization which can be rotated along the z-axis. An L-shaped notch is added at the left corner of the patch. To observe the variations in performance, the slot is rotated by angles from 0° to 90° at an interval of 5° . The reason for doing this is to detect the best reflection coefficient of the patch antenna as the angle rotation determines the position of the S-parameter curve. From simulation, no substantial change has been found from 5° to 35° but a good change is observed at 40° angle. Similar type of change are found for 80° angle as well. Because of this reason, three angles which are 0° , 40° and 80° have been chosen for final design. The final structures of the patch antenna with three different rotation angles are displayed below in Fig. 3.1.

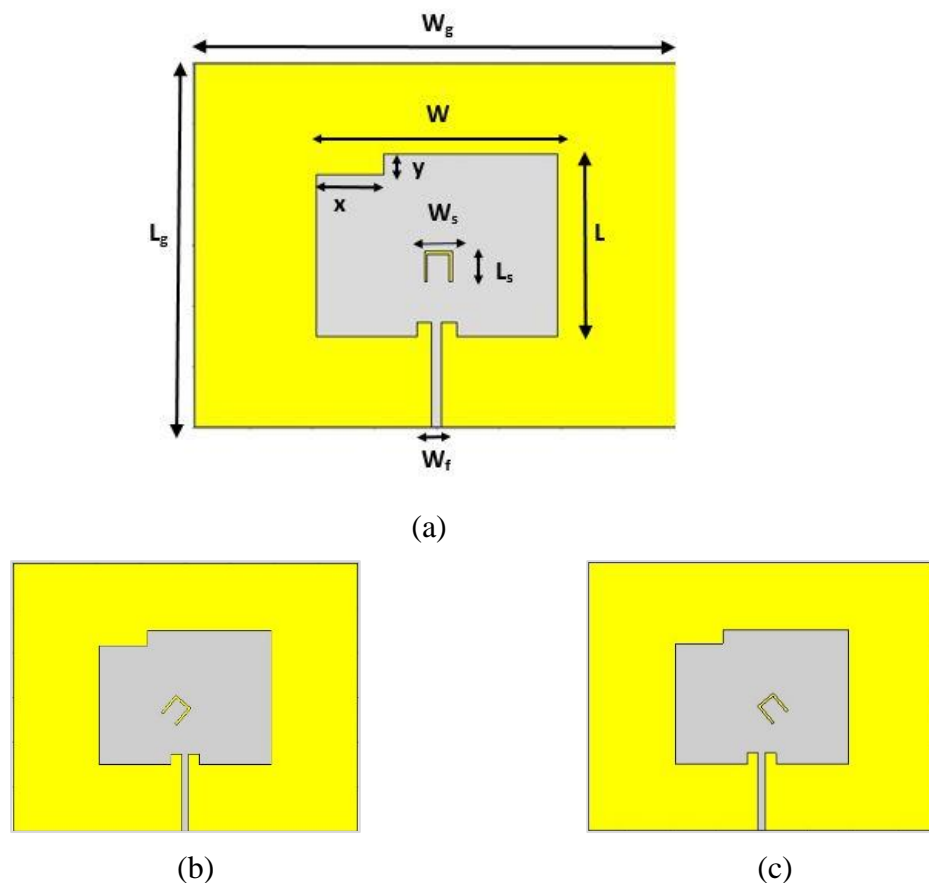


Fig. 3.1: U- slotted microstrip patch antenna (a) rotation angle $Z = 0^{\circ}$, (b) rotation angle $Z = 40^{\circ}$, (c) rotation angle $Z = 80^{\circ}$

Table 3.3 lists the physical dimension of the antenna. Most of the dimensions remain unchanged during the simulation whereas the length and width varies as the frequency changes.

Table 3.3: Optimized physical dimension of U-slotted microstrip patch antenna

Parameters	Dimensions
Dielectric constant, ϵ_r	4.4
Substrate thickness, h_s	1.6 mm
Input impedance, Z_0	50 ohm
Microstrip feed width, W_f	3.08 mm
Slot length, L_s	6.42 mm
Slot width, W_s	3.70 mm
Thickness of the patch, h_t	0.03 mm
Notch width, x	19.5 mm
Notch length, y	6.35 mm

Keeping the above values fixed, the antenna is designed for different constellation frequencies. Afterwards, analyzing the parameters and finding the optimum orientation, 2x2 array antennas are constructed for each constellation frequency to observe the array performance. In Fig. 3.2, the 2x2 array antenna is illustrated.

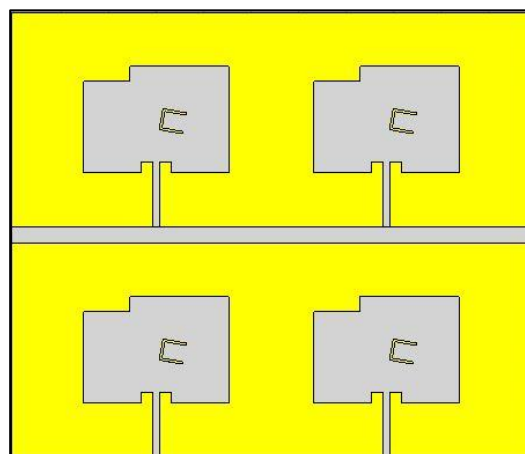


Fig. 3.2: Designed 2x2 phased array antenna

3.6.2 Improved 2x3 phased array patch antenna to enhance the beam scanning range

This antenna is a modified and improved version of the previous antenna which has been designed to improve the overall performance. A single rectangular inset fed patch antenna using copper has been constructed on a FR-4 dielectric substrate which is shown in Fig. 3.3 with the dimensions in Table 3.4.

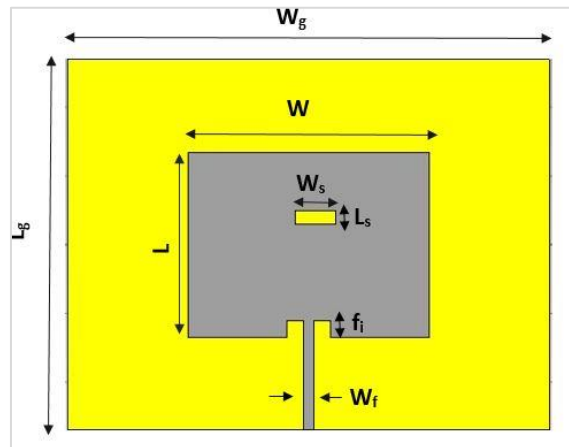


Fig. 3.3: Designed rectangular slotted microstrip patch antenna

Table 3.4: Optimized physical dimension of rectangular microstrip patch antenna

Parameters	Dimensions
Dielectric constant, ϵ_r	4.4
Substrate thickness, h_s	1.6 mm
Width of the patch, W	70 mm
Length of the patch, L	53.89 mm
Thickness of the patch, h_t	0.03 mm
Width of the ground plane, W_g	140 mm
Length of the ground plane, L_g	107.78 mm
Microstrip feed width, W_f	3.08 mm
Slot length, L_s	4 mm
Slot width, W_s	12 mm

After observing the analytical parameters of a single patch antenna, the antenna array is constructed using the similar patch antenna. Six antennas are arranged in a 2x3 matrix where each antenna is equally spaced from the adjacent antenna and the antennas are excited

separately using six dielectric ports. There is a gap on the substrate in between the two rows but the ground plane is uniform. The antennas are connected to the ground such that 50 ohm impedance matching is maintained [32]. Some of the dimensions are optimized slightly to get appropriate results. Fig. 3.4 shows the optimized version of the array antenna.

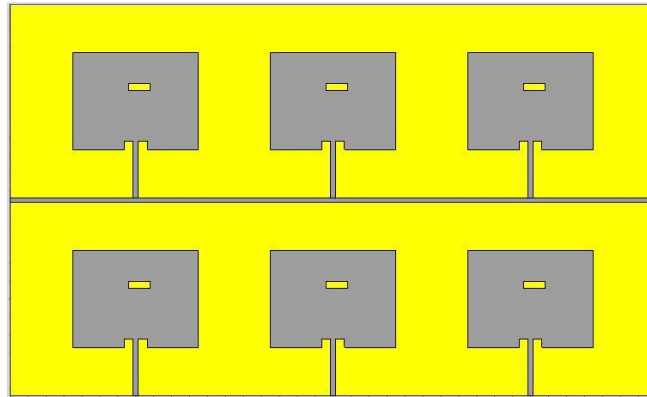


Fig. 3.4: Designed 2x3 phased array antenna

Both the antennas are simulated and the results have been discussed in Chapter 4 in details with the radiation pattern and beam scanning.

3.7 Analysis on the Environmental Factors

In order to make a comparison among the locations regarding the selection of ground station for SBAS, environmental factors play major role. The behavior of satellite signal differs in different locations as the environmental condition is not the same. That is why the selection of ground station depends on a number of environmental criteria like ionospheric and tropospheric scintillation, rain attenuation etc. Bangladesh is a subtropical monsoon country having variations in temperature, rainfall and humidity, so these factors will play a vital role in the selection of ground station for augmentation system. In this work, a number of model has been used to estimate the variation of these factors.

3.7.1 Tropospheric scintillation model

Troposphere is the lowest layer of the atmosphere and reason of signal delay in this region is due to the change in refractive index. The scintillation fade in this region is calculated using meteorological parameters such as temperature and humidity. A number of established models are International Telecommunication Union (ITU) Model [33], OTUNG Model [34] and Karasawa Prediction Model [35]. Among these, ITU model is the

most broadly exploited model to estimate the scintillation fade depth (SFD) [36] of a specific region. ITU is an organization that is responsible for all the standards for information and communication sectors. For measuring various atmospheric factors, a number of models have been recognized by ITU. Among them the ITU model to measure the SFD have been well established and implemented worldwide. ITU model is based on average temperature t (C^0) and relative humidity H of a region for a wider period of time. Since the average temperature and relative humidity changes over time, the value of SFD also fluctuates. The model also estimates SFD for antenna elevation angle equal or greater than 5^0 . Major computational parameters that are essential to estimate SFD using the model are denoted below

t = average temperature (C^0) of the location

H = average relative humidity (%d) of the location

f = frequency of operation (GHz)

D = earth station antenna diameter (m)

θ = earth station antenna elevation angle

η = antenna efficiency

In order to compute SFD, a number of steps need to be followed which are demonstrated sequentially below [8]:

- a. Calculate the saturation water vapor pressure, e_s , [hPa],

$$e_s = 6.11e^{\frac{19.7t}{t+273}} \quad (3.7)$$

- b. Calculate the wet term of the radio refractivity, N_{wet} , [ppm],

$$N_{wet} = \frac{3730 \times H \times e_s}{(t + 273)^2} \quad (3.8)$$

- c. Calculate the standard deviation of the reference signal amplitude, σ_{ref} , [dB],

$$\sigma_{ref} = 3.6 \times 10^{-3} + 10^{-4} \times N_{wet} \quad (3.9)$$

- d. Calculate the effective path length L , [m],

$$L = \frac{2000}{\sqrt{\sin^2\theta + 2.35 \times 10^{-4} + \sin\theta}} \quad (3.10)$$

- e. Estimate the effective antenna diameter [m] as follows,

$$D_{eff} = \sqrt{\eta}D \quad (3.11)$$

- f. Calculate the antenna averaging factor,

$$g(x) = \sqrt{3.86(x^2 + 1)^{11/12} \sin \left[\frac{11}{6} \arctan \frac{1}{x} \right] - 7.08x^{5/6}} \quad (3.12)$$

Where, $x = 1.22D_{eff}^2 \frac{f}{L}$

- g. Calculate the standard deviation of the signal for desired period,

$$\sigma = \sigma_{ref} f^{7/12} \frac{g(x)}{(\sin\theta)^{1.2}} \quad (3.13)$$

- h. Compute the time percentage factor $a(p)$, for the time percentage p , in the range between $0.01\% < p < 50\%$.

$$a(p) = -0.061(\log_{10}p)^3 + 0.072(\log_{10}p)^2 - 1.71\log_{10}p + 3 \quad (3.14)$$

- i. Compute the scintillation fade depth in dB using the equation below,

$$A_s(p) = a(p)\sigma \quad (3.15)$$

The SFD is calculated according to the requirement considering a number of aspects such as elevation angle, percentage of time, antenna diameter etc. so that a wider picture can be developed. It is also recommended to use ITU model for frequencies up to 20 GHz.

3.7.2 Ionospheric delay

The ionosphere is partially ionized medium and the propagation velocity of GNSS signals depend on the density of total electron content (TEC). The longer a signal is in the ionosphere, the greater the influence of the ionosphere on it. The value of TEC is not the same all over the day so the delay is also variable. The delay caused by ionosphere can be described using the model by Klobuchar [37]. As ionosphere is a dispersive medium, the angular frequency ' ω ' and wave number ' k ' is related by,

$$\omega^2 = c^2k^2 + (2\pi f_p)^2 \quad (3.16)$$

Where, $f_p = 8.98\sqrt{N_e}$, N_e is the electron density.

Taking $\omega = 2\pi f$, the phase refractive index and group refractive index of the ionosphere can be written as,

$$N_{ph} = 1 - \frac{40.3}{f^2} N_e \quad (3.17)$$

The difference between the measured length and Euclidean distance between the receiver and the satellite can be measured as,

$$\Delta_{ph,f}^{iono} = -\frac{40.3}{f^2} \int N_e dl \quad (3.18)$$

$$\Delta_{gr,f}^{iono} = \frac{40.3}{f^2} \int N_e dl \quad (3.19)$$

The differences $\Delta_{ph,f}^{iono}$ and $\Delta_{gr,f}^{iono}$ are called phase and code ionospheric refraction. After a number of derivational steps, the relation between ionospheric delay and TEC can be drawn as,

$$I_f = \alpha_f TEC = \frac{40.3}{f^2} TEC \quad (m) \quad (3.20)$$

The ionospheric delay is also frequency dependent as the delay is inversely proportional to the square of frequency. As the value of TEC is not the same all over the world, the ionospheric effect is also not similar [37]. It is also not similar throughout the whole day. Due to its importance in communication sector, a number of models have been developed to estimate.

3.7.3 Rainfall attenuation

The existence of rain in the propagation path causes scattering and absorption of the satellite signal because the raindrops behave as dissipative dielectric media to the signal. In subtropical country like Bangladesh, rainfall becomes a key factor of signal attenuation which causes signal degradation. Moreover the rain rate throughout the year is not the same in all the places. A number of models like ITU-R, Ajayi method are being utilized in order to compute rain attenuation. According to ITU-R model, to measure the rain attenuation for a specific period of time, the rain rate (mm/hr) data is required and the specific rain attenuation (db/km) can be approximated by,

$$A_{rain} = KR^\alpha \quad (3.21)$$

Where, R is the rain rate in mm/hr and K and α are frequency and temperature dependent constant with values 1.076 and 0.67 respectively [38] and for this research these values are taken to observe the attenuation scenario. The values are used to determine the rain attenuation which is obtained following some steps described in [33]. The rain attenuation is calculated for a 0.01% of the time.

3.7.4 Simulation setup and data collection

Before stepping into the analysis and simulation part, a set of pre-requisites have been established and noted. The study of SFD is done for two constellation signals- L1 (1.575 GHz) which is the signal of GPS and E5 (1.191 GHz) which is the signal of Galileo. For ionospheric delay, L3 (1.202 GHz) has also been added. To formulate this study, the latitude, longitude and the height from the sea level of the selected cities are listed and displayed in Table 3.5.

Table 3.5: Geographical position of the surveyed locations

Location	Latitude, Longitude	Height
Dhaka	23.8103° N, 90.4125° E	4 meter
Chattogram	22.3569° N, 91.7832° E	29 meter
Rajshahi	24.3745° N, 88.6042° E	18 meter
Khulna	22.8456° N, 89.5403° E	9 meter
Sylhet	24.8949° N, 91.8687° E	35 meter

To calculate the SFD, ionospheric delay and rain attenuation of signals in these locations, the temperature, relative humidity, TEC and rain rate have been collected from Bangladesh Agricultural Research Council (BARC). The average data of each month of the year is collected for a period of last 20 years (1998-2018). The average maximum temperature, average minimum temperature and average relative humidity data are showed in Table 3.6, Table 3.7 and Table 3.8 respectively.

Table 3.6: Average maximum temperature (t_{max}) of the surveyed locations

Location	Jan	Feb	Mar	Apr	May	Jun	Jul	Aug	Sep	Oct	Nov	Dec
Dhaka	24.6	27.8	31.8	33.8	32.8	31.9	31.8	31.7	31.8	31.9	28.6	25.4
Chattogram	25.4	27.7	31.6	31.4	31.8	32	30.8	30.6	31.8	31.7	29.8	26.5
Rajshahi	23.6	27.6	32.4	35.6	34.7	34	31.6	32.4	31.7	31.6	28.8	25.4
Khulna	26.5	28.9	33.1	34.5	34.5	32.5	32.7	32.7	32.7	32.7	30.5	27.2
Sylhet	24.7	27.5	30.6	30.8	31	30.7	31.6	31.6	30.6	30.5	28.8	26.6

Table 3.7: Average minimum temperature (t_{\min}) of the surveyed locations

Location	Jan	Feb	Mar	Apr	May	Jun	Jul	Aug	Sep	Oct	Nov	Dec
Dhaka	12.9	16.1	21.1	24.1	25	26	25.7	26.2	26	23.4	18.7	13.1
Chattogram	13.7	15.7	20.7	24.2	24.9	25.2	24.9	25	25	24.2	19	15.6
Rajshahi	11.3	12.9	17.7	22.7	23.7	25.7	26	25.7	26	23.2	17.6	13.2
Khulna	14.8	15.4	20.2	24.1	24.3	25.6	26.3	26.3	25.7	24.6	20.5	14.1
Sylhet	12.9	14.7	17.8	20.7	22.8	23.4	25	24.7	25	23	18.7	13.7

Table 3.8: Average relative humidity, H (%) of the surveyed locations

Location	Jan	Feb	Mar	Apr	May	Jun	Jul	Aug	Sep	Oct	Nov	Dec
Dhaka	71.6	66.7	62.5	71.9	77.1	83.1	81	81	79	73	72	73
Chattogram	72.1	69.2	71.3	76.5	79.5	82.3	86	84.7	83	82.3	77.6	74.7
Rajshahi	75.7	68	63	65	73.7	82.3	86.3	85.7	85	82	76.7	75.9
Khulna	77.3	73.3	71.2	77.1	79.8	88.1	88	86.7	87.1	85.2	81.9	80.1
Sylhet	73.6	67.3	67	75	81.6	86.3	86.5	85	86.2	83	76	75

To calculate the ionospheric delay and rain attenuation, average maximum TEC data and rain rate of the surveyed areas have been registered in Table 3.9 and Table 3.10.

Table 3.9: Average maximum TEC of the surveyed locations

Location	Jan	Feb	Mar	Apr	May	Jun	Jul	Aug	Sep	Oct	Nov	Dec
Dhaka	16.9	18.4	30.1	37.7	36.6	24.8	23.1	26.3	24.6	19.7	19.6	18.1
Chattogram	16.5	19.1	29.5	32	23	24	22.1	25.3	23.6	19.2	19	17.2
Rajshahi	16.2	20.4	23.6	35.8	24.1	22.8	21.8	21.3	25.1	18.3	16.1	15.7
Khulna	17.9	22.3	25.9	37.1	24.4	22.2	23.5	21.8	25.4	20.1	17.6	16.9
Sylhet	16	21	23.5	33.3	23	21.5	21.8	20.6	26	16.8	16.3	15.2

Table 3.10: Average rainfall rate (mm/hr) of the surveyed locations

Location	Jan	Feb	Mar	Apr	May	Jun	Jul	Aug	Sep	Oct	Nov	Dec
Dhaka	6	21	57	138	272	367	377	317	271	157	32	7
Chattogram	5.6	15	48	126	219	583	743	530	261	203	48	12
Rajshahi	9	13	21	61	210	326	397	302	257	145	15	6
Khulna	13.3	44.4	52	87	200	335	329	323	254	129	32	6
Sylhet	13	27	108	319	549	780	751	595	468	227	31	8

3.8 Uplink and Downlink Loss Estimation

The link loss estimation has been done in this section for three constellations over the five locations. The free space path loss for both the downlink and uplink have been estimated using the equations below [29] respectively,

$$L_D = 10 \log \left(\frac{4\pi d}{c/f} \right)^2 \quad (3.22)$$

$$L_U = 10 \log \left(\frac{4\pi d c}{f} \right)^2 \quad (3.23)$$

The calculated free space path loss and the estimated loss from the tropospheric and rainfall attenuation discussed earlier have been added to finally produce the uplink and downlink loss. The estimated losses are then represented in a graphical way.

3.9 Software Support

A number of simulation software have been used to observe the outcomes of the GNSS parameters. MATLAB is the major software which has been used to analyze the signal performance. To study the simulation results of the GNSS parameters, an extension tool of MATLAB named Visual has been used. CST Microwave Studio has been exploited to design, examine and observe the crucial antenna parameters such as S parameters, VSWR, radiation pattern, beam scanning etc.

CHAPTER 4

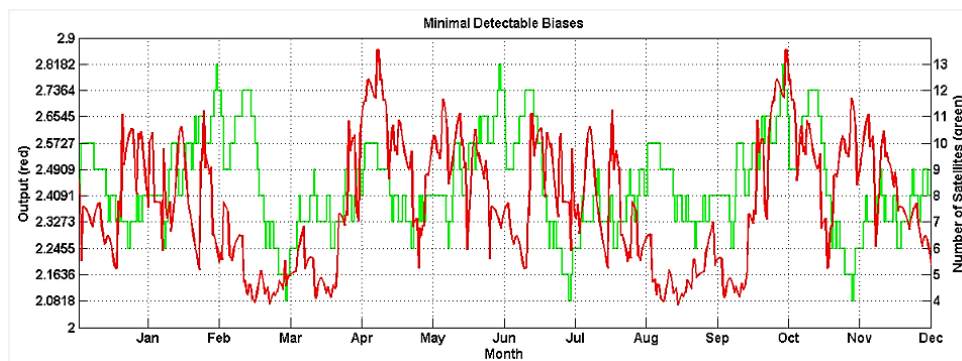
RESULTS AND DISCUSSIONS

4.1 Simulation Results of GNSS Parameters over Different Locations

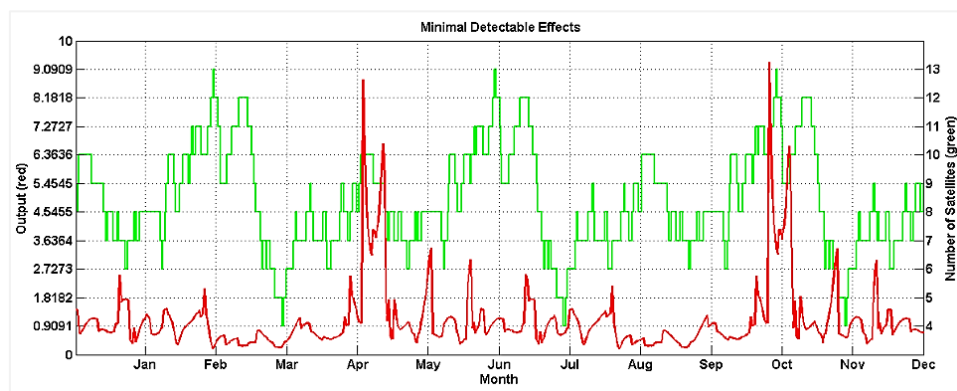
The result of this analysis is done for the five selected locations of Bangladesh using GPS (L1) and Galileo (E5) constellations. The simulation is done in two ways - using individual GPS and Galileo constellation and a combined GPS – Galileo constellation. The performance parameters that have been simulated are – MDB, MDE, GDOP, number of visible satellites and BNR. In every case, the results are showed in both graphical and tabular form.

4.1.1 Dhaka (23.8103°N, 90.4125°E)

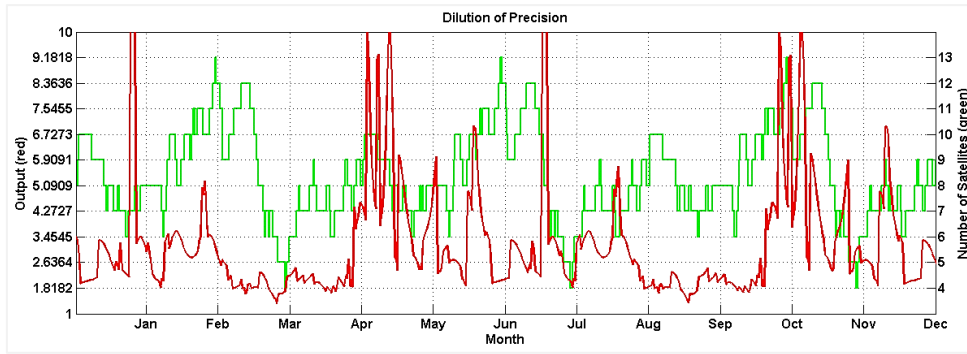
GPS and Galileo: Simulation is done to observe the parameters using individual GPS and Galileo constellation over Dhaka. The simulation results in graphical form are displayed below in Fig. 4.1 (a ~ c) and Fig. 4.2 (a ~ c) respectively.



(a)

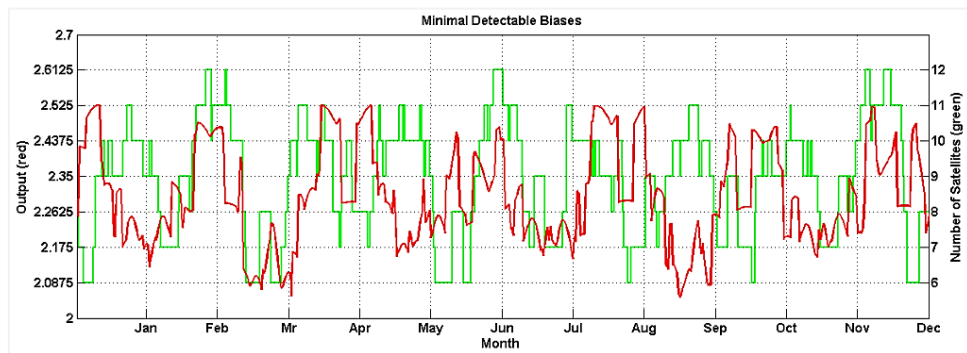


(b)

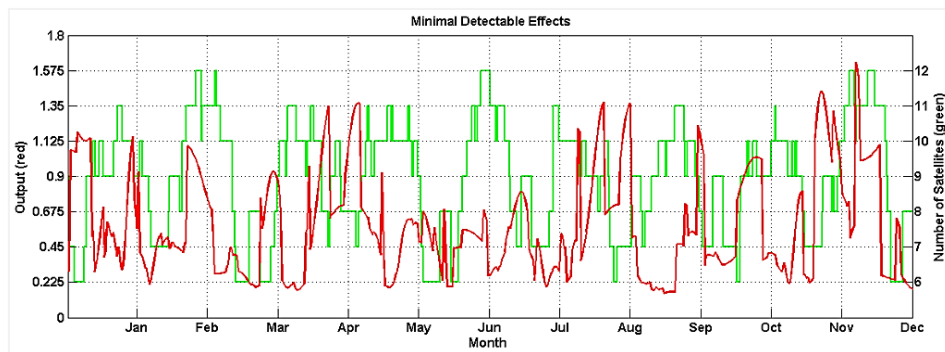


(c)

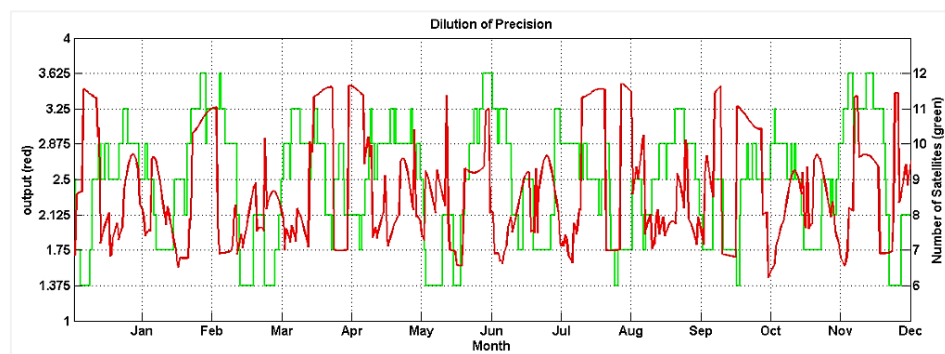
Fig. 4.1: GPS values over Dhaka (a) MDB, (b) MDE and (c) GDOP



(a)



(b)



(c)

Fig. 4.2: Galileo values over Dhaka (a) MDB, (b) MDE and (c) GDOP

The simulation results are listed in Table 4.1 below to display some of the major outputs from the graphs.

Table 4.1: Summary of the simulation results for Dhaka

Parameters	GPS		Galileo	
	Highest Value	Lowest Value	Highest Value	Lowest Value
MDB	2.863	2.069	2.525	2.055
MDE	9.67	0.259	1.621	0.176
GDOP	10	1.449	3.516	1.462
No. of Visible Satellites	13	4	12	6
BNR	4.132		3.626	

The table shows the highest and lowest value of the simulated parameters for both the constellations. In the case of MDB, MDE, GDOP and BNR, Galileo has better results than GPS though GPS has more number of in view satellites.

Combined GPS and Galileo: The combined GPS – Galileo simulation is done to observe the parameters over Dhaka and the results in are displayed below in Fig. 4.3 to Fig. 4.5.

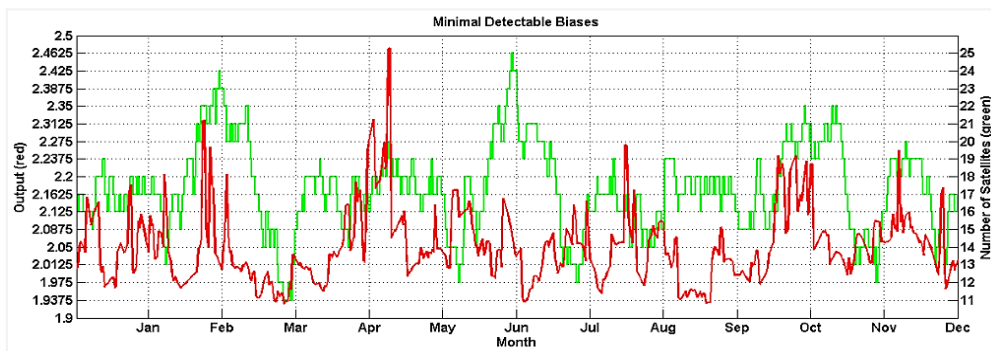


Fig. 4.3: MDB value over Dhaka for combined GPS - Galileo

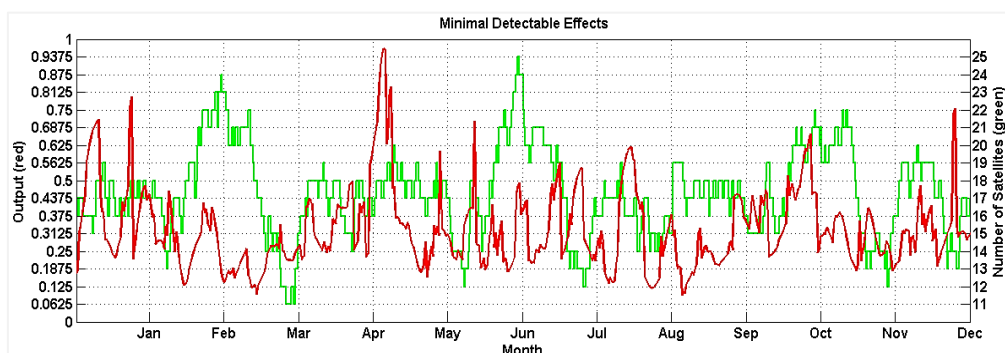


Fig. 4.4: MDE value over Dhaka for combined GPS - Galileo

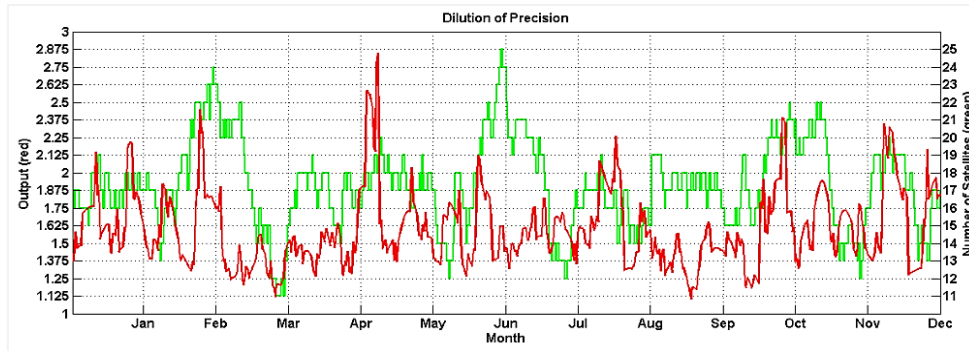


Fig. 4.5: GDOP value over Dhaka for combined GPS - Galileo

From the graphical representations of the simulated parameters, Table 4.2 has been constructed to show the important observables.

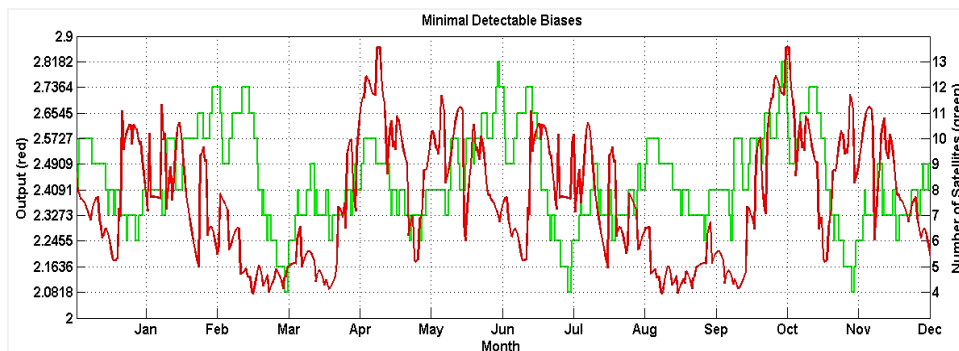
Table 4.2: Summary of the simulation results for Dhaka

Parameters	Highest Value	Lowest Value
MDB	2.473	1.931
MDE	0.967	0.094
GDOP	2.847	1.103
No. of Visible Satellites	25	11
BNR	3.171	

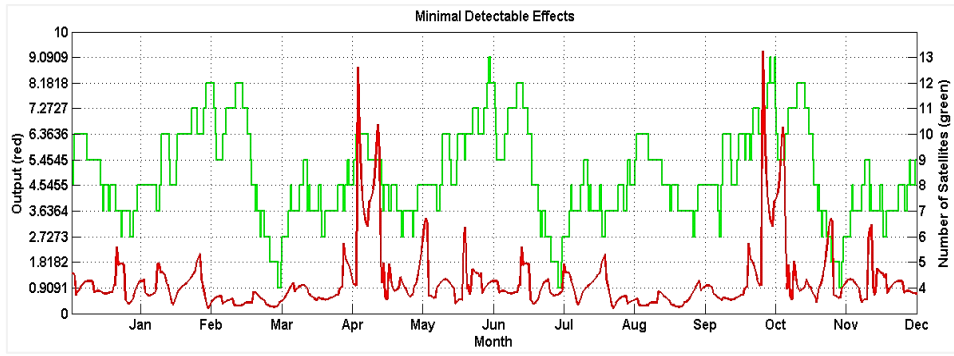
It has appeared that a combined constellation provides the best result. Number of in view satellites has increased significantly to a maximum of 24 satellite. The highest MDB value is 2.473 which is less than the individual constellations. GDOP value has also decreased.

4.1.2 Chattogram (22.3569⁰N, 91.7832⁰E)

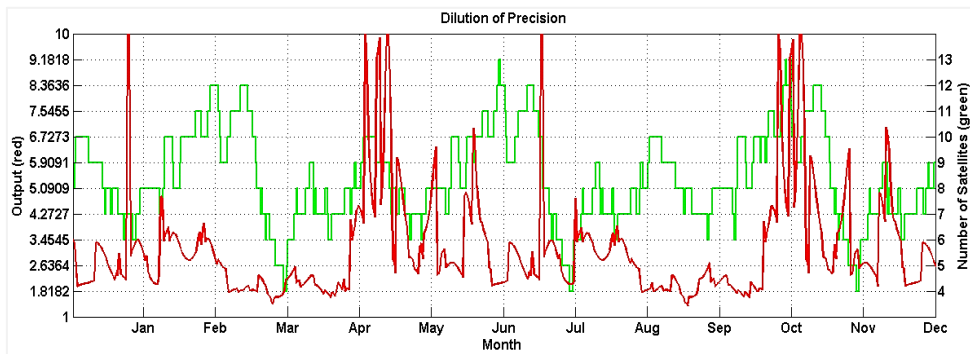
GPS and Galileo: Simulation is done to observe the parameters using individual GPS and Galileo constellation over Dhaka. The simulation results in graphical form are displayed below in Fig. 4.6 (a ~ c) and Fig. 4.7 (a ~ c) respectively.



(a)

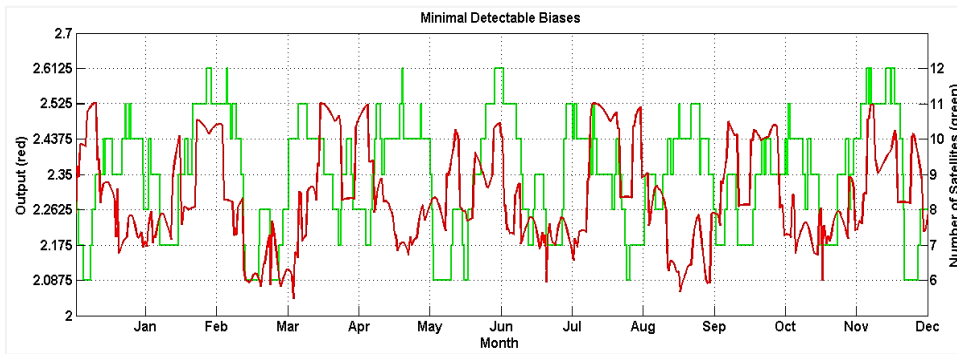


(b)

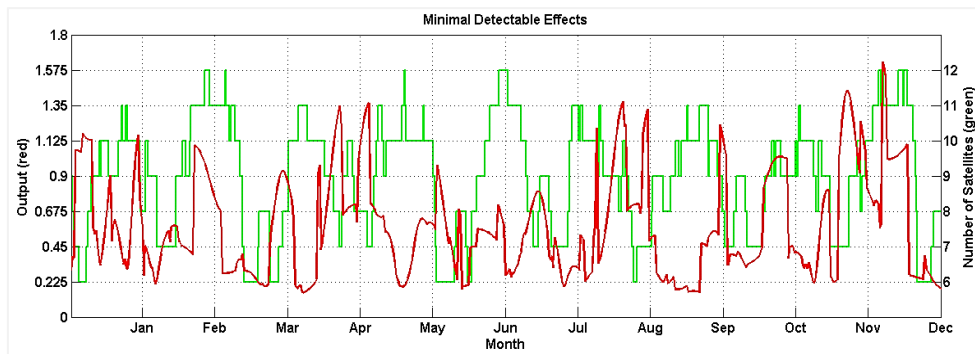


(c)

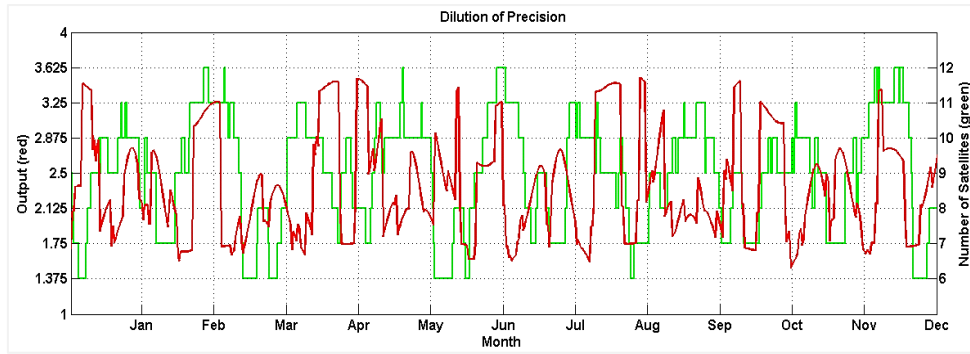
Fig. 4.6: GPS values over Chattogram (a) MDB, (b) MDE and (c) GDOP



(a)



(b)



(c)

Fig. 4.7: Galileo values over Chattogram (a) MDB, (b) MDE and (c) GDOP

Table 4.3 displays some of the major outputs from the graphs based on the simulation performance.

Table 4.3: Summary of the simulation results for Chattogram

Parameters	GPS		Galileo	
	Highest Value	Lowest Value	Highest Value	Lowest Value
MDB	2.863	2.071	2.528	2.029
MDE	9.854	0.187	1.628	0.015
GDOP	10	1.344	3.481	1.492
No. of Visible Satellites	13	4	12	6
BNR	4.132		3.536	

The results here has also followed the similar trend as the previous one where Galileo performs better than GPS in all except for number of in view satellites.

Combined GPS and Galileo: The parameter results over Chattogram that are observed using combined GPS – Galileo simulation are shown in Fig. 4.8 to Fig. 4.10.

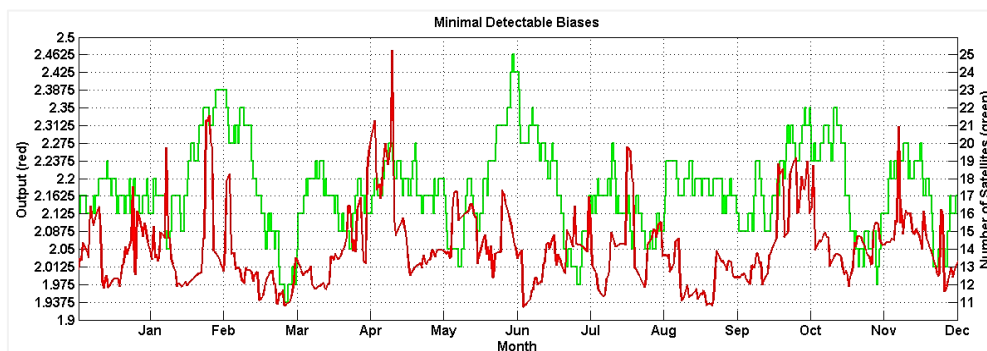


Fig. 4.8: MDB value over Chattogram for combined GPS - Galileo

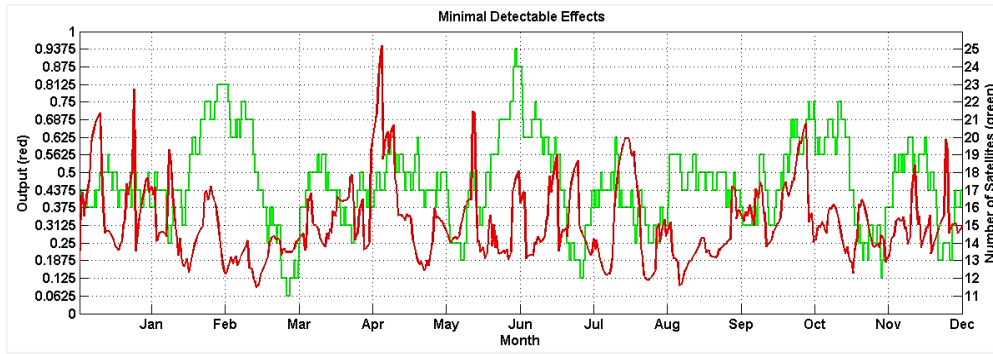


Fig. 4.9: MDE value over Chattogram for combined GPS - Galileo

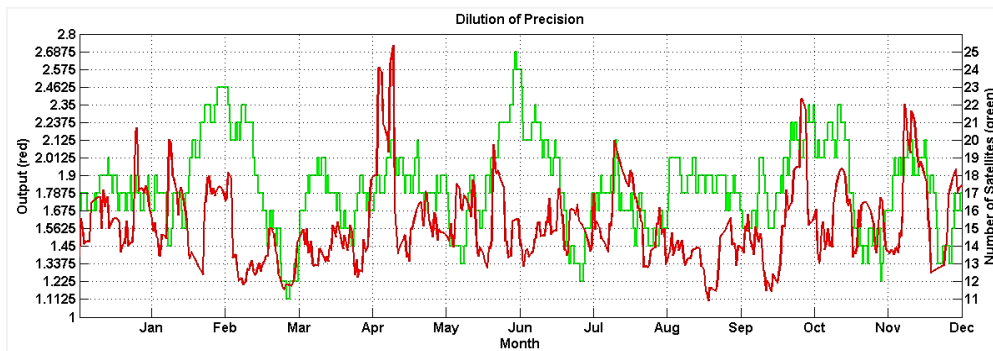


Fig. 4.10: GDOP value over Chattogram for combined GPS - Galileo

Table 4.4 below has been generated using the graphical representations of the simulated parameters to display the relevant observables.

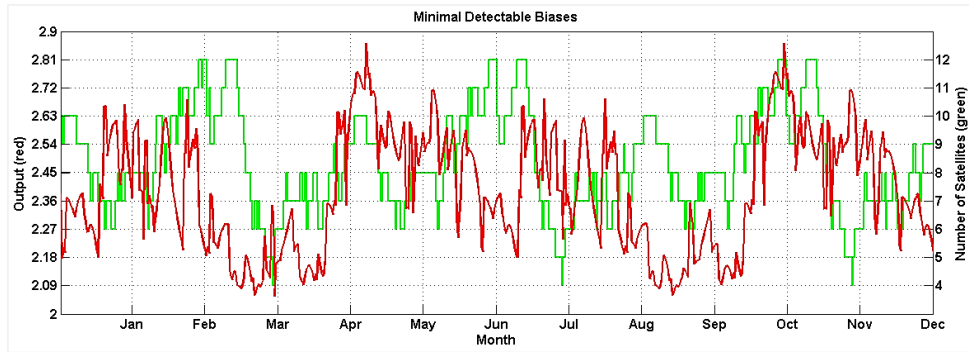
Table 4.4: Summary of the simulation results for Chattogram

Parameters	Highest Value	Lowest Value
MDB	2.472	1.928
MDE	0.949	0.093
GDOP	2.726	1.103
No. of Visible Satellites	25	11
BNR	3.175	

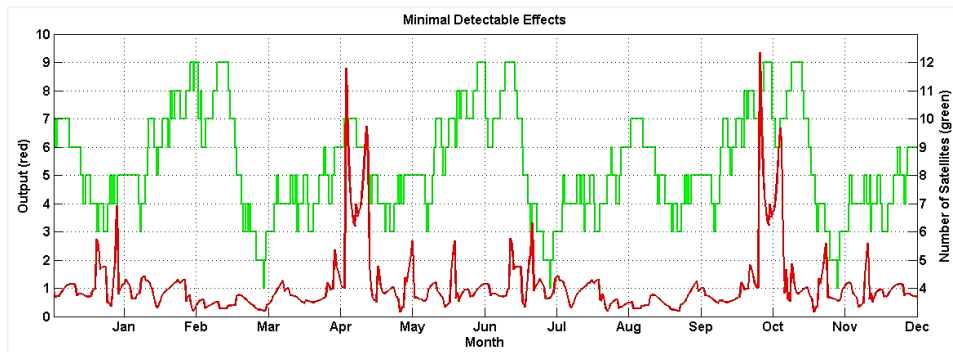
The above table, is evident of a combined constellation being much better than individual. The value of MDE is reduced to a maximum value of 0.949. The number of in view satellite has increased to 25. The maximum value of GDOP is 2.726 which is lower than individual constellation as well as Dhaka.

4.1.3 Rajshahi (24.3745°N, 88.6042°E)

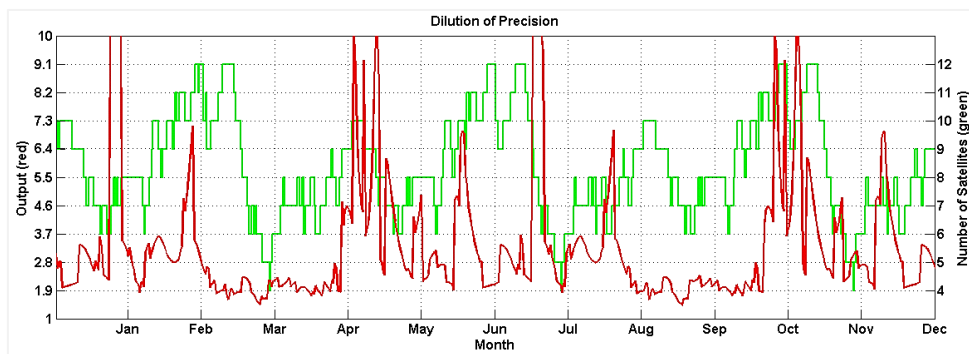
GPS and Galileo: To observe the parameters using individual GPS and Galileo constellation over Rajshahi, simulation has been done. The simulation results in graphical form are displayed below in Fig. 4.11 (a ~ c) and Fig. 4.12 (a ~ c) respectively.



(a)

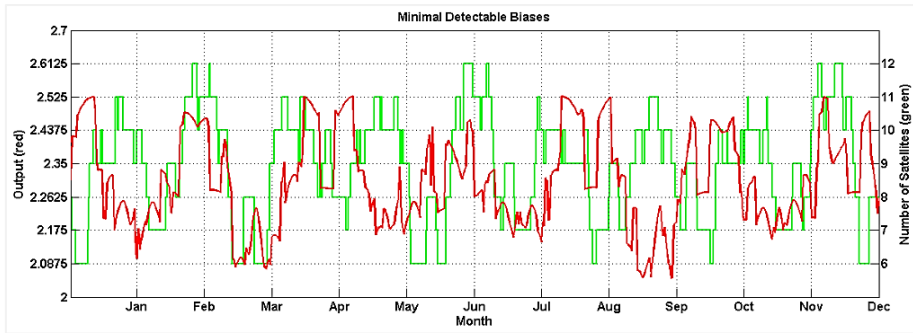


(b)

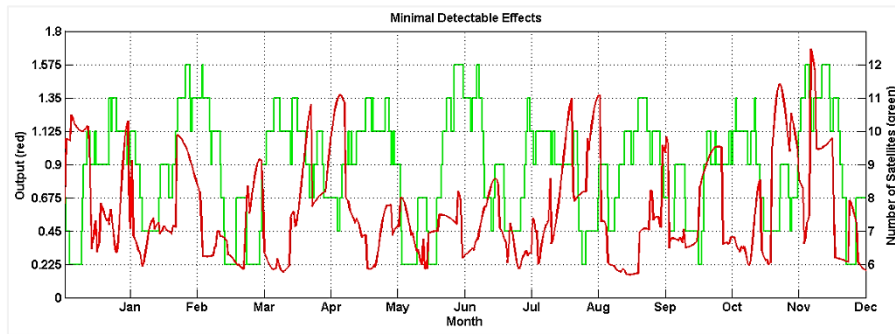


(c)

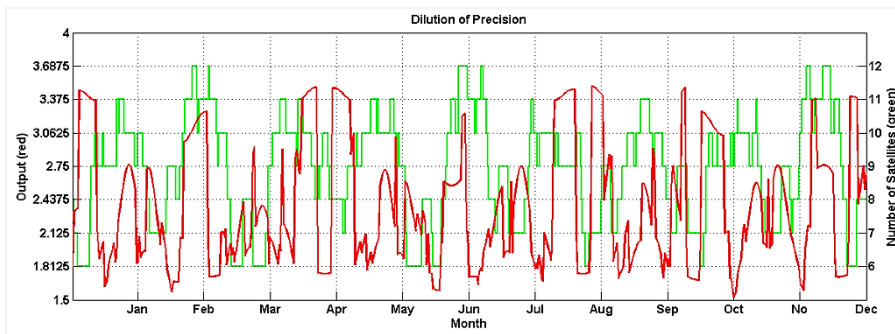
Fig. 4.11: GPS values over Rajshahi (a) MDB, (b) MDE and (c) GDOP



(a)



(b)



(c)

Fig. 4.12: Galileo values over Rajshahi (a) MDB, (b) MDE and (c) GDOP

To display the major outputs from the graphs, the simulation results are listed in Table 4.5.

Table 4.5: Summary of the simulation results for Rajshahi

Parameters	GPS		Galileo	
	Highest Value	Lowest Value	Highest Value	Lowest Value
MDB	2.863	2.058	2.525	2.052
MDE	9.344	0.188	1.647	0.017
GDOP	10	1.426	3.461	1.571
No. of Visible Satellites	12	4	12	6
BNR	4.141		3.517	

The number of in view satellites for GPS is lower than the previous simulations and as a whole, Galileo is ahead of GPS.

Combined GPS and Galileo: The combined GPS – Galileo simulation is done to observe the parameters over Rajshahi and the results in are displayed below in Fig. 4.13 to Fig. 4.15.

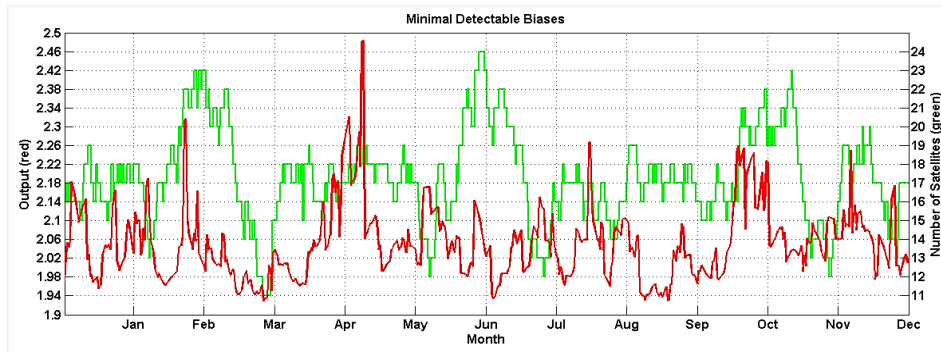


Fig. 4.13: MDB value over Rajshahi for combined GPS - Galileo

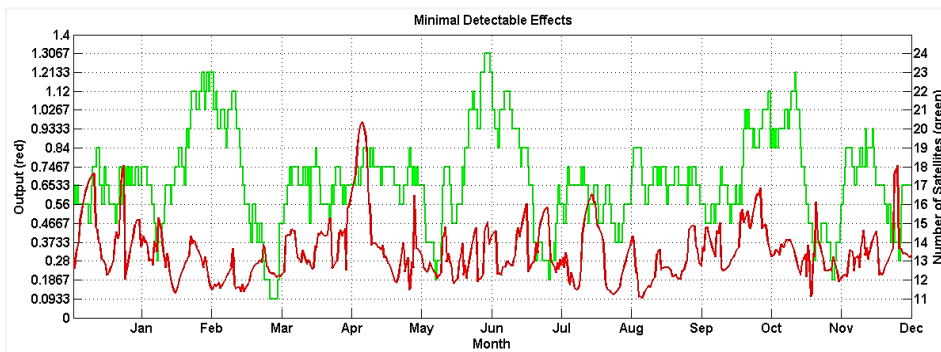


Fig. 4.14: MDE value over Rajshahi for combined GPS - Galileo

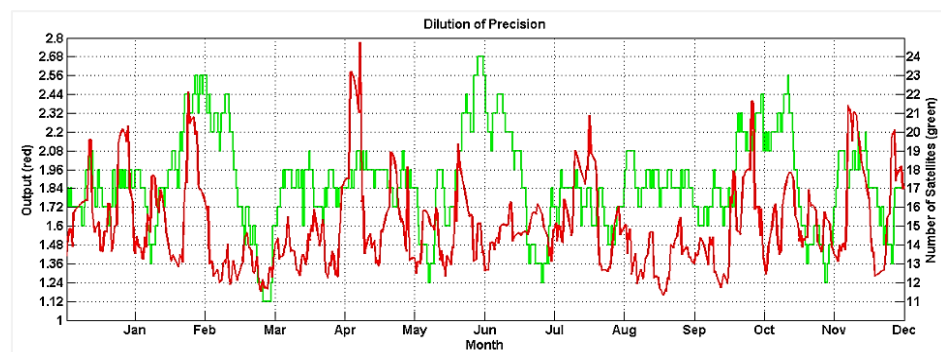


Fig. 4.15: GDOP value over Rajshahi for combined GPS - Galileo

From the graphical representations of the simulated parameters, Table 4.6 has been constructed to show the important observables.

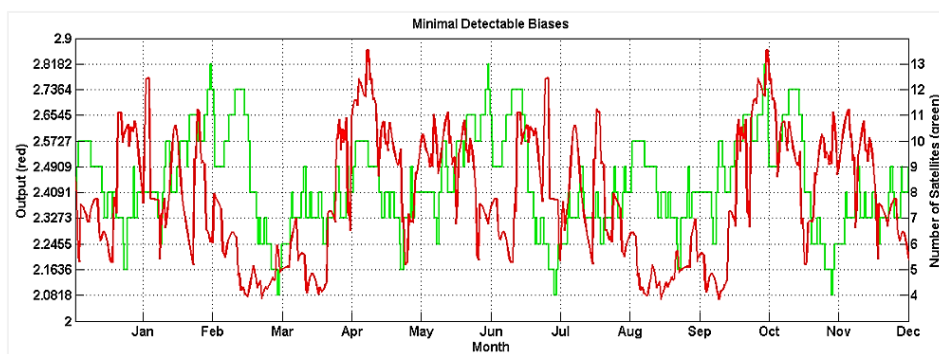
Table 4.6: Summary of the simulation results for Rajshahi

Parameters	Highest Value	Lowest Value
MDB	2.481	1.934
MDE	0.966	0.105
GDOP	2.771	1.156
No. of Visible Satellites	24	11
BNR	3.214	

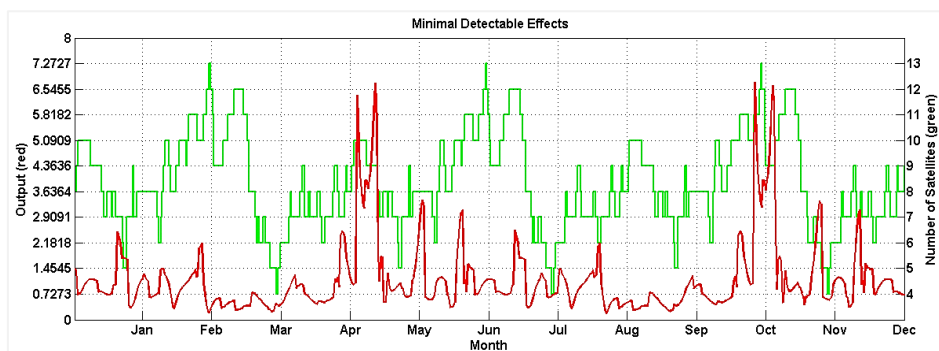
By comparing among the results for Rajshahi, it has appeared that combined constellation provides the finest result with decent values of the parameters. The maximum value of GDOP and MDE are lower than individual constellation but a little higher than Chattogram.

4.1.4 Sylhet (24.8949⁰N, 91.8687⁰E)

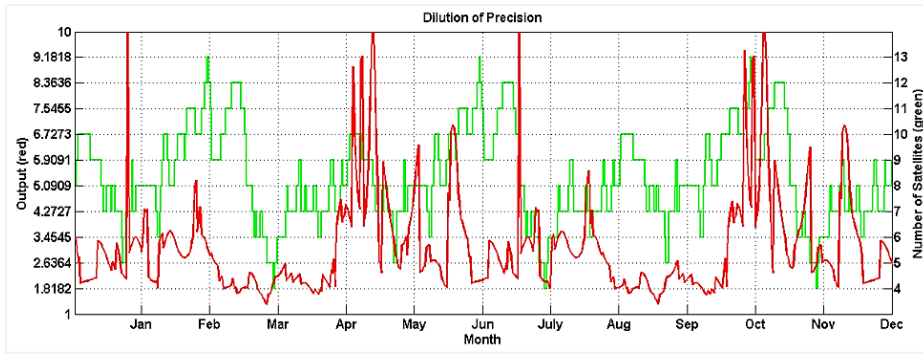
GPS and Galileo: The simulation results over Sylhet is displayed in graphical form are below in Fig. 4.16 (a ~ c) and Fig. 4.17 (a ~ c) respectively.



(a)

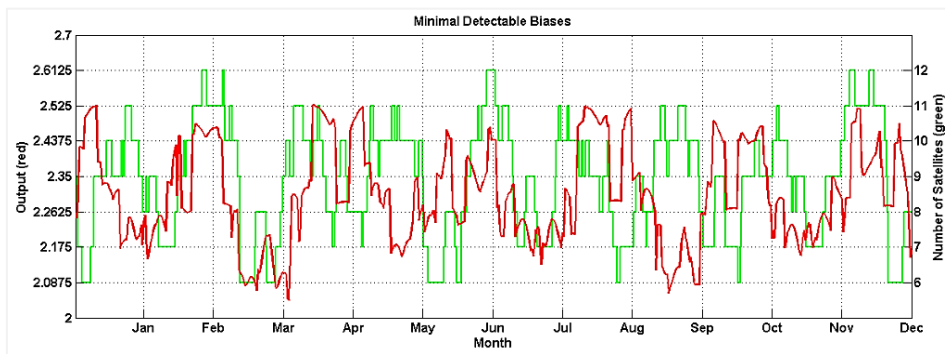


(b)

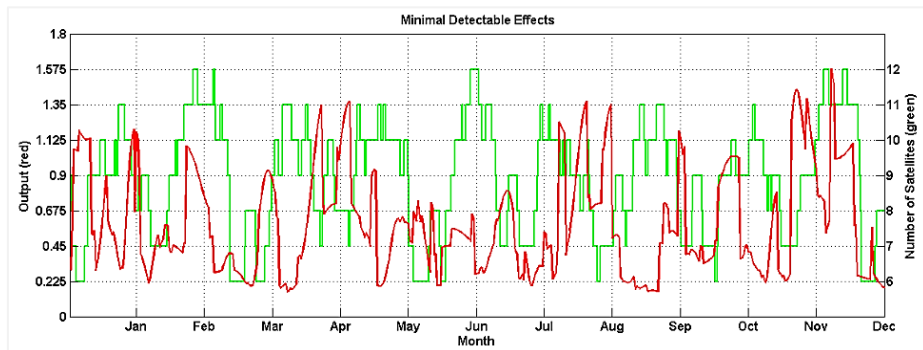


(c)

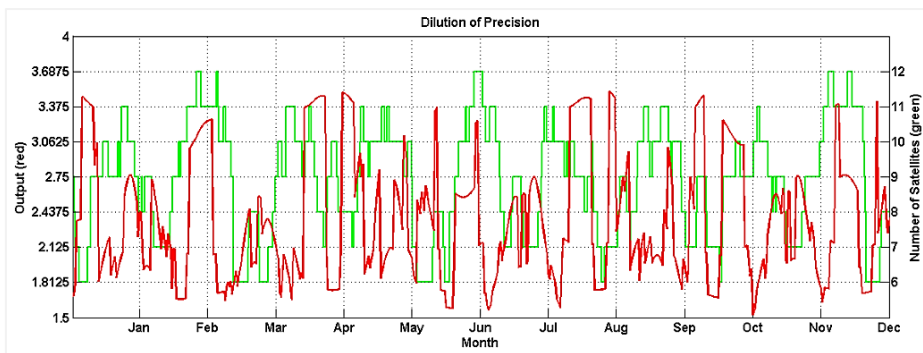
Fig. 4.16: GPS values over Sylhet (a) MDB, (b) MDE and (c) GDOP



(a)



(b)



(c)

Fig. 4.17: Galileo values over Sylhet (a) MDB, (b) MDE and (c) GDOP

Table 4.7 shows some of the main outputs from the graphs based on the simulation performance.

Table 4.7: Summary of the simulation results for Sylhet

Parameters	GPS		Galileo	
	Highest Value	Lowest Value	Highest Value	Lowest Value
MDB	2.861	2.071	2.525	2.044
MDE	6.711	0.189	1.579	0.156
GDOP	10	1.321	3.509	1.555
No. of Visible Satellites	13	4	12	6
BNR	4.131		3.521	

The number of in view satellites in both the cases has reduced to a value of 11 which is lower than the previous locations. A noticeable change has been observed in the value of MDE.

Combined GPS and Galileo: The parameters over Sylhet are observed using a combined GPS – Galileo simulation, and the findings are shown in Fig. 4.18 to Fig. 4.20.

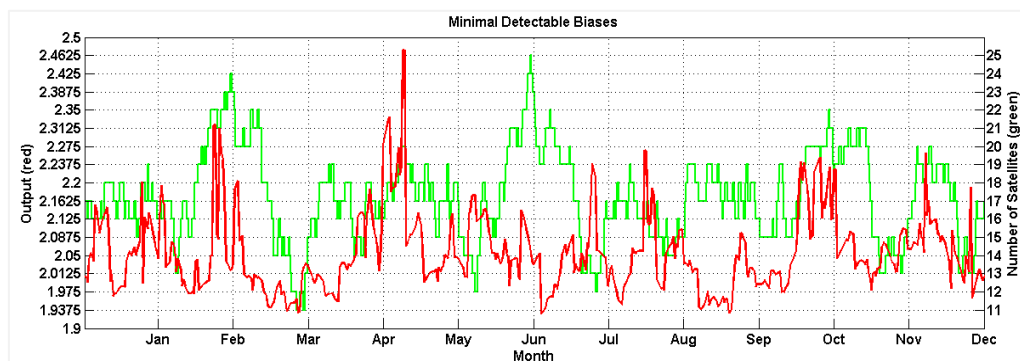


Fig. 4.18: MDB value over Sylhet for combined GPS - Galileo

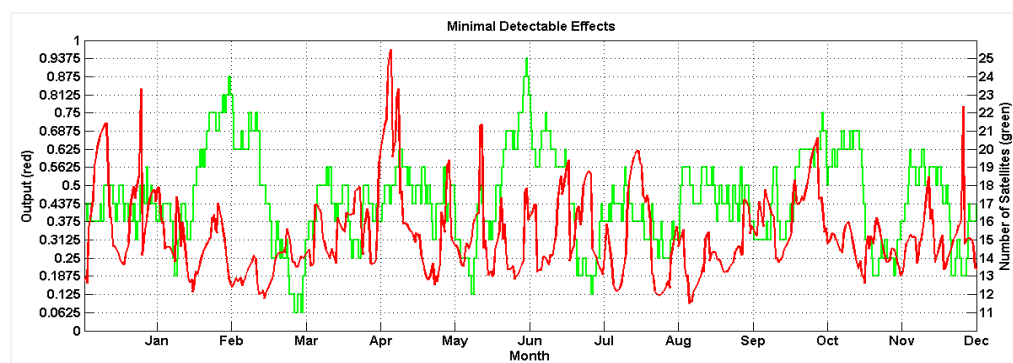


Fig. 4.19: MDE value over Sylhet for combined GPS - Galileo

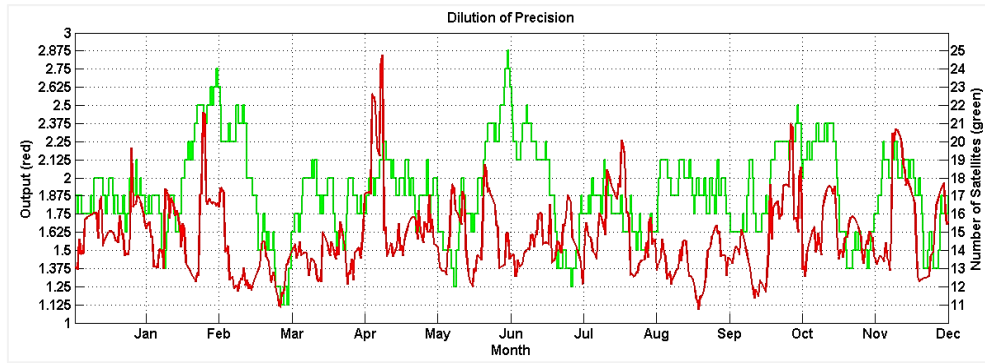


Fig. 4.20: GDOP value over Sylhet for combined GPS - Galileo

From the graphical representations of the simulated parameters, Table 4.8 has been constructed to show the important observables.

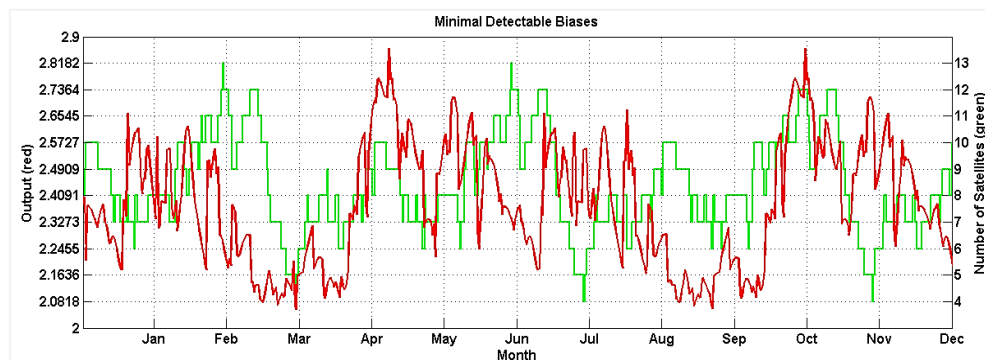
Table 4.8: Summary of the simulation results for Sylhet

Parameters	Highest Value	Lowest Value
MDB	2.473	1.929
MDE	0.969	0.096
GDOP	2.849	1.109
No. of Visible Satellites	25	11
BNR	3.174	

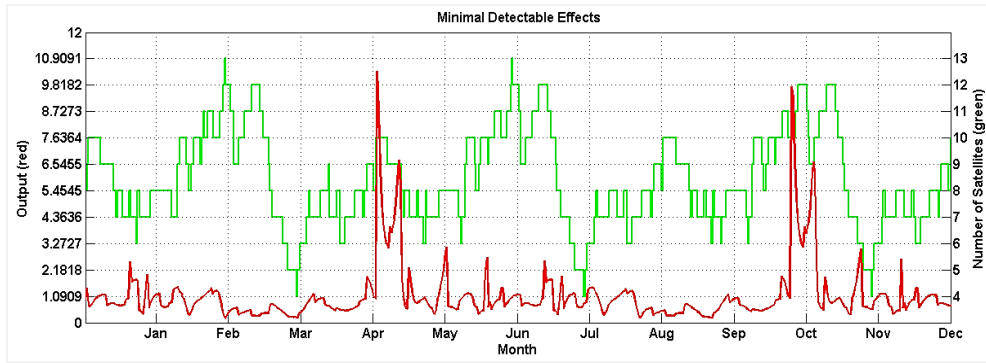
By comparing among the results for Rajshahi, it has appeared that combined constellation provides the finest result with decent values of the parameters. The maximum value of GDOP and MDE are lower than individual constellation but a little higher than Chattogram.

4.1.5 Khulna (22.8456⁰N, 89.5403⁰E)

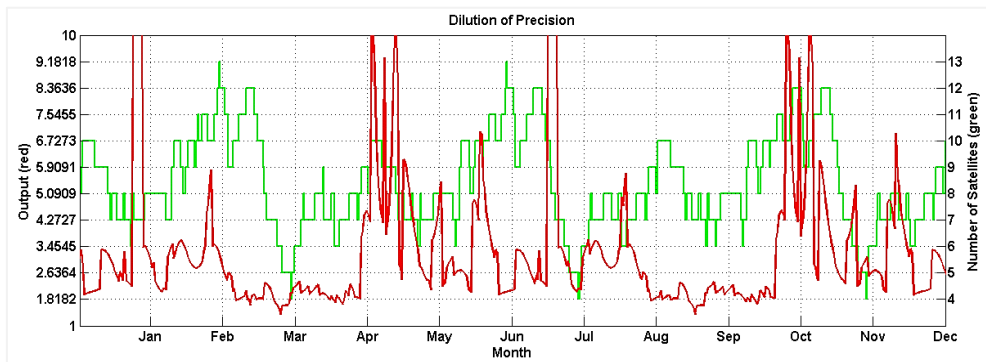
GPS and Galileo: The simulation is carried out to observe the parameters for Khulna and the simulation results are shown in graphical form in Fig. 4.21(a ~ c) and Fig. 4.22 (a ~ c).



(a)

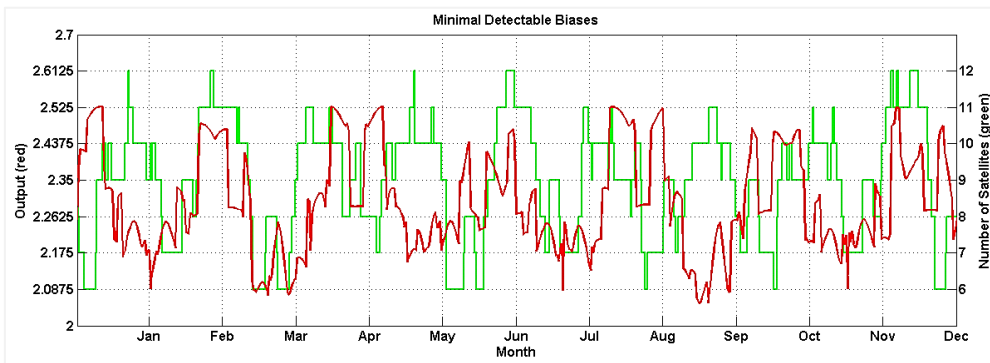


(b)

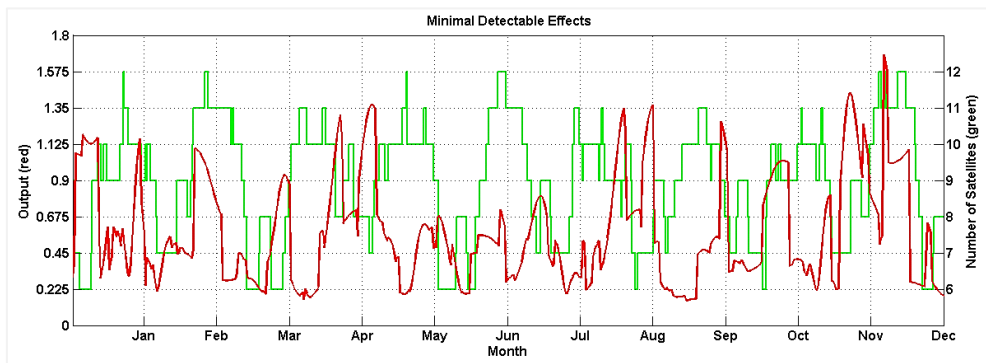


(c)

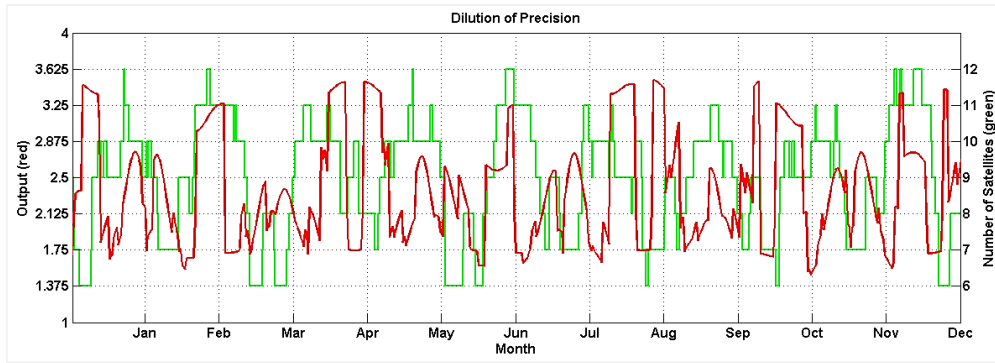
Fig. 4.21: GPS values over Khulna (a) MDB, (b) MDE and (c) GDOP



(a)



(b)



(c)

Fig. 4.22: Galileo values over Khulna (a) MDB, (b) MDE and (c) GDOP

The simulation results are listed in Table 4.9 below to display some of the major outputs from the graphs.

Table 4.9: Summary of the simulation results for Khulna

Parameters	GPS		Galileo	
	Highest Value	Lowest Value	Highest Value	Lowest Value
MDB	2.863	2.059	2.528	2.053
MDE	10.4	0.336	1.678	0.165
GDOP	10	1.361	3.506	1.491
No. of Visible Satellites	13	4	12	6
BNR	4.132		3.528	

Number of in view satellites in both the cases has reduced to a value of 11 which is lower than the previous locations. A noticeable change has been observed in the value of MDE.

Combined GPS and Galileo: The parameters over Khulna are observed using a combined GPS–Galileo simulation, as shown in Fig. 4.23 to Fig. 4.25.

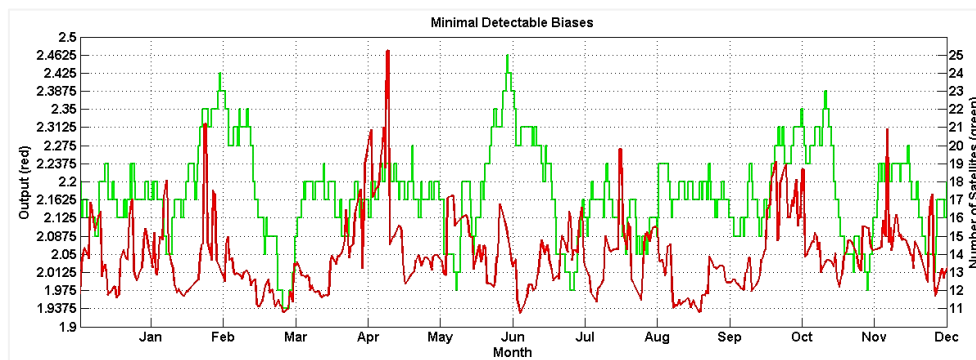


Fig. 4.23: MDB value over Khulna for combined GPS - Galileo

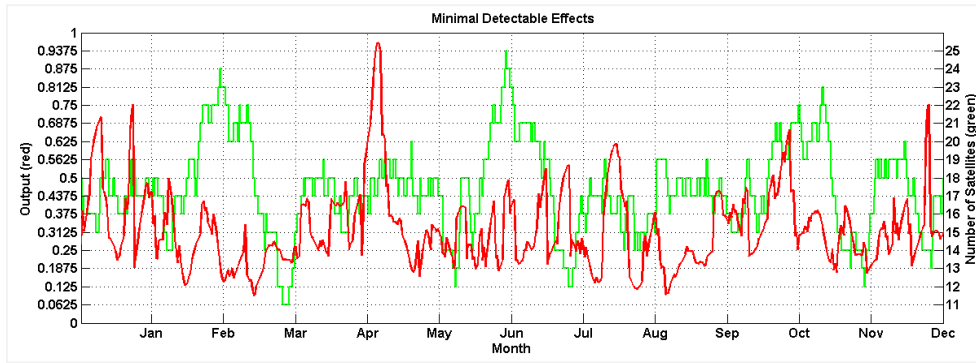


Fig. 4.24: MDE value over Khulna for combined GPS - Galileo

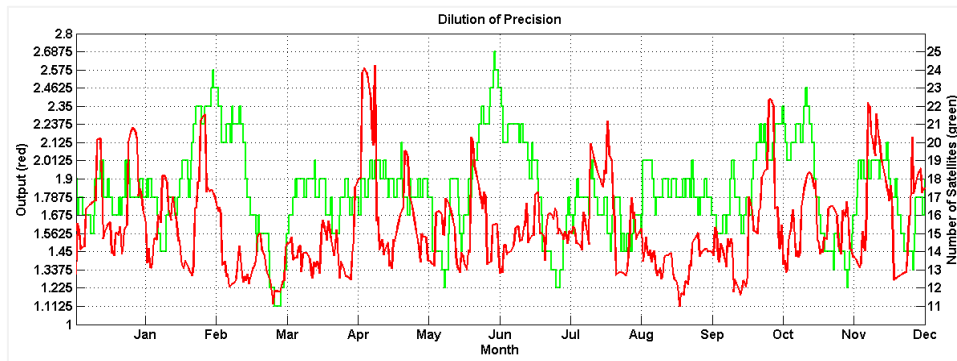


Fig. 4.25: GDOP value over Khulna for combined GPS - Galileo

From the graphical representations of the simulated parameters, Table 4.10 has been constructed to show the important observables.

Table 4.10: Summary of the simulation results for Khulna

Parameters	Highest Value	Lowest Value
MDB	2.472	1.929
MDE	0.966	0.098
GDOP	2.605	1.112
No. of Visible Satellites	25	11
BNR	3.175	

By comparing among the results for Khulna, it has appeared that combined constellation provides the finest result with decent values of the parameters. The maximum value of GDOP and MDE are lower than individual constellation but a little higher than Chittagong.

4.1.6 Discussion on the results

From the above analysis, a number of judgements can be taken. Primarily, we can observe variation in the results of GPS and Galileo but most of the parameter values of Galileo are

better than the GPS constellation except the number of in view satellites. The highest and lowest number of visible satellites of GPS constellation are 13 and 4. The highest value of GDOP for GPS constellation is 10 in all the results whereas the lowest value is around 1.34. In the case of Galileo constellation, the value of GDOP is lower than GPS which means that this constellation has good satellite geometry. The external and internal reliability values are not the same in both the cases but certainly better for Galileo system. Finally, the outputs from combined GPS-Galileo provides the best results in terms of the measured parameters for every simulated location. The highest value of MDB has decreased to a value of around 2.47 and MDE has reduced to around 0.96. Also, the highest value of GDOP has reduced to a value of around 2.771 which indicates if combined constellations are used, good geometry can be obtained. In this case, the highest value of visible satellites is 25 and the lowest value is 11.

4.1.7 Evaluation of the outcomes:

Revising the simulation and calculated data from section 4.1, some conclusions can be drawn. All the results varied from location to location since the position of the location are not the same at all. Because of this reason, the performance of the ground station will not be alike. Because of the aim to compare among the results to find out a better ground station location, a compact data consists of the important outcomes from the above analysis is needed. To do so a scale containing five measurement levels - best, good, average, not good and worst value is applied to the outcomes of the locations which is shown in Table 4.11 below. The values considered here are the highest value of each parameter.

Table 4.11: Overall comparison among the locations on the parameters

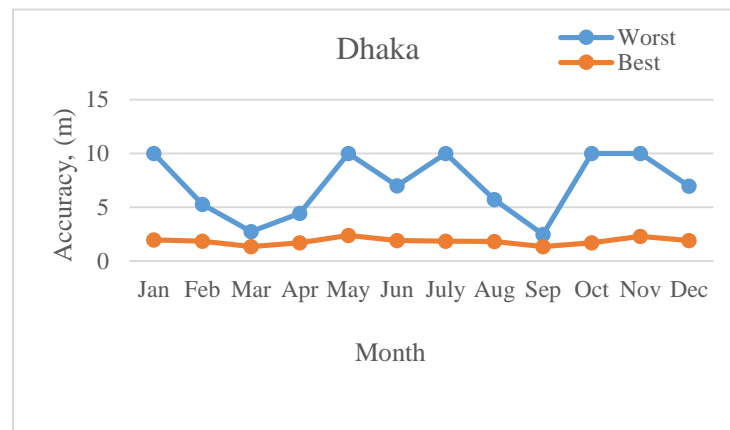
Parameter	Dhaka	Chattogram	Rajshahi	Khulna	Sylhet
MDB	Good	Best	Average	Best	Good
MDE	Good	Best	Average	Good	Average
Visible Satellite	Best	Best	Good	Best	Best
GDOP	Not Good	Good	Average	Best	Worst
BNR	Best	Average	Not Good	Good	Average

4.2 Simulation Results of GNSS Accuracy over Different Locations

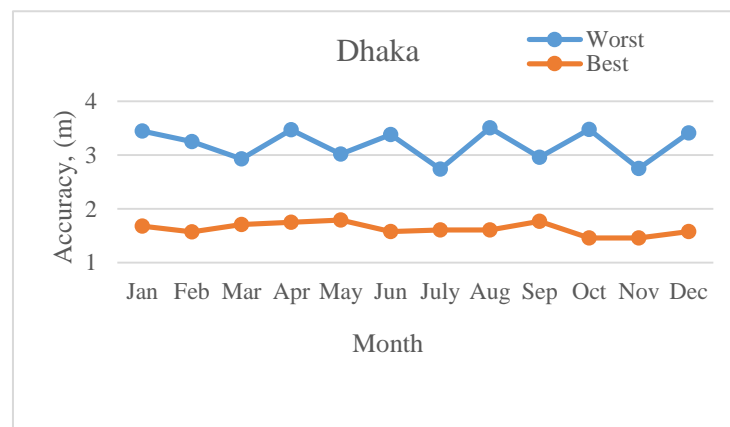
The results of GNSS accuracy calculation in the five major cities of Bangladesh is presented in this section. The estimation has been accomplished using the theory discussed in Chapter 2. Both the GPS (L1) and Galileo (E5) constellations have been used. The GDOP values are extracted from the simulation results of section 4.1. As maximum and minimum accuracy have been estimated, so both the highest and lowest values of GDOP of each month have been taken. The GDOP values for GPS and Galileo are listed below in Table 11 and Table 12 respectively. The accuracy of individual location is then represented in graphs where x-axis indicates the months and the y-axis indicates the accuracy in meter.

4.2.1 Dhaka (23.8103°N, 90.4125°E)

Accuracy calculated over Dhaka for GPS and Galileo are represented in Fig. 4.26 (a ~ b).



(a)



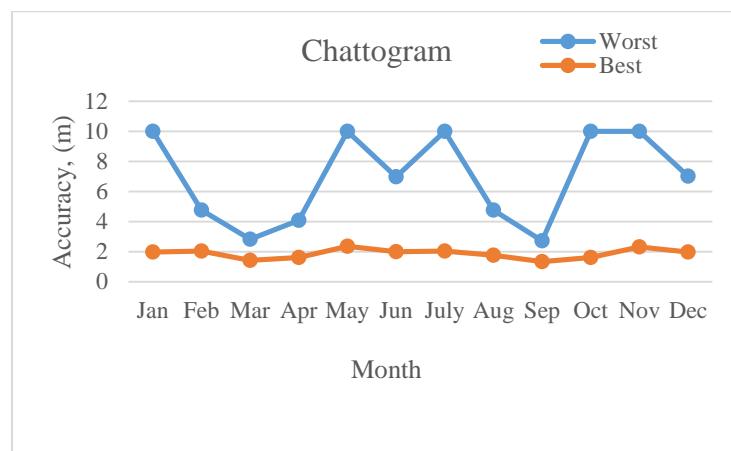
(b)

Fig. 4.26: Accuracy results over Dhaka (a) GPS and (b) Galileo

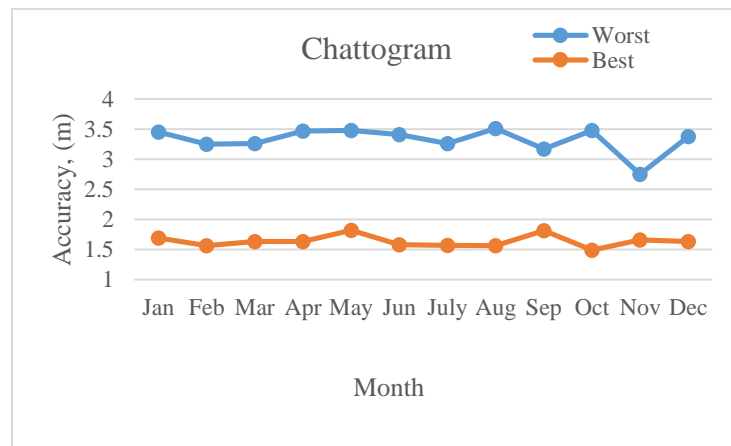
By analyzing the data, it has been observed that GPS has the best accuracy in the range of 1.33 to 2.38 meter whereas the worst accuracy lies in between 2.45 to 10 meter. The best accuracy value has been observed in March. On the other hand, Galileo has the best value which is 1.46 meter observed in October and November. The worst value for Galileo is 3.51 meter.

4.2.2 Chattogram (22.3569⁰N, 91.7832⁰E)

Similarly, the accuracy calculated over Chattogram for GPS and Galileo are displayed in Fig. 4.27 (a ~ b).



(a)



(b)

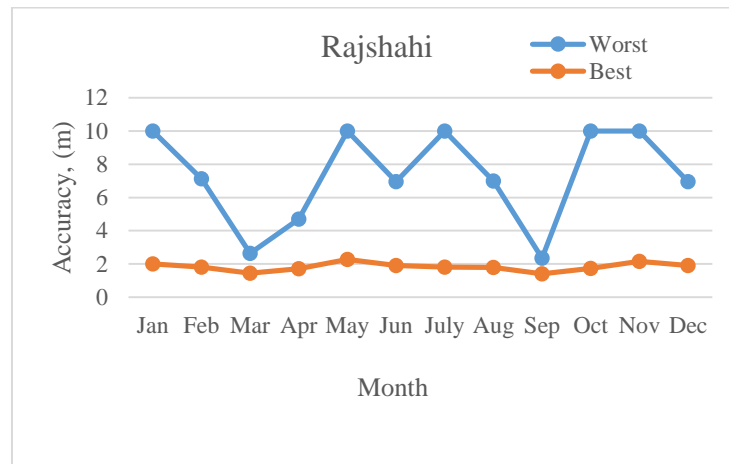
Fig. 4.27: Accuracy results over Chattogram (a) GPS and (b) Galileo

From the simulation data, a variation in the accuracy over Chattogram can be observed. For GPS, the best value is 1.34 meter which is observed in September. The worst value ranges

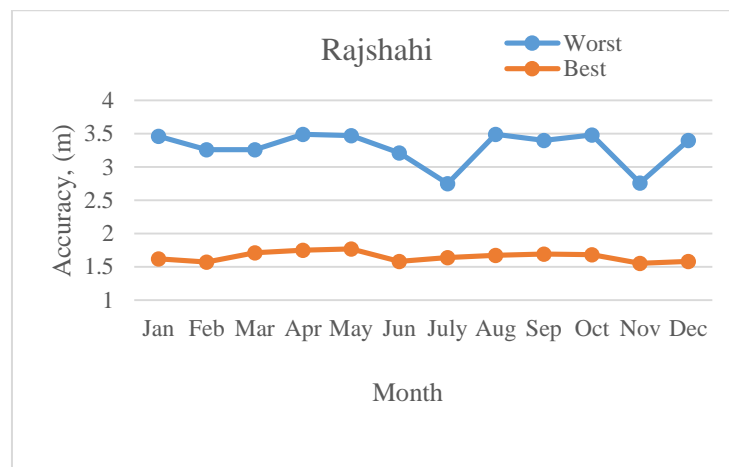
in between 2.71 meter to 10 meter. The best accuracy value for Galileo is 1.56 meter and the worst value is 3.48 meter. Overall the accuracy of Galileo is better than GPS.

4.2.3 Rajshahi (24.3745°N, 88.6042°E)

Fig. 4.28 (a ~ b) displays the accuracy results over Rajshahi for both the constellations analyzed.



(a)



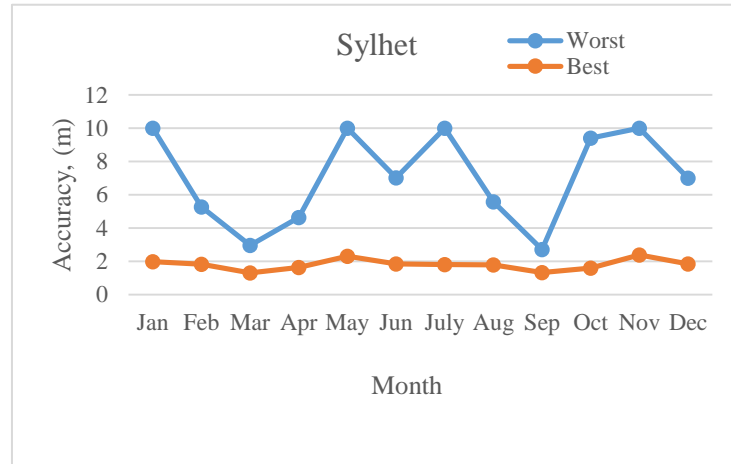
(b)

Fig. 4.28: Accuracy results over Rajshahi (a) GPS and (b) Galileo

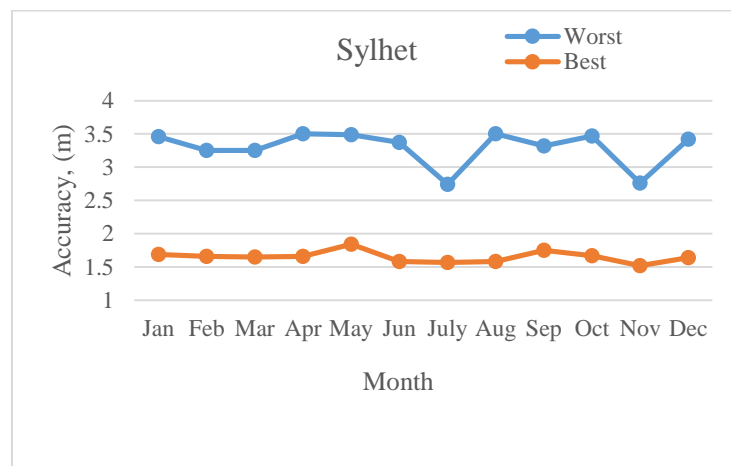
From the graphical information, a variety in the accuracy over Rajshahi can be noticed. For GPS, the best value is 1.42 meter that is slightly higher than the previous two observations. The worst result is in the middle of 2.36 meter to 10 meter. On the contrary, the best precision value for Galileo is 1.55 meter and the worst value is 3.49 meter. Overall, the values over Rajshahi are higher than Dhaka and Chattogram.

4.2.4 Sylhet (24.8949⁰N, 91.8687⁰E)

Below is Fig. 4.29 (a ~ b) that shows the accuracy results over Sylhet for both the investigated GPS and Galileo constellations.



(a)



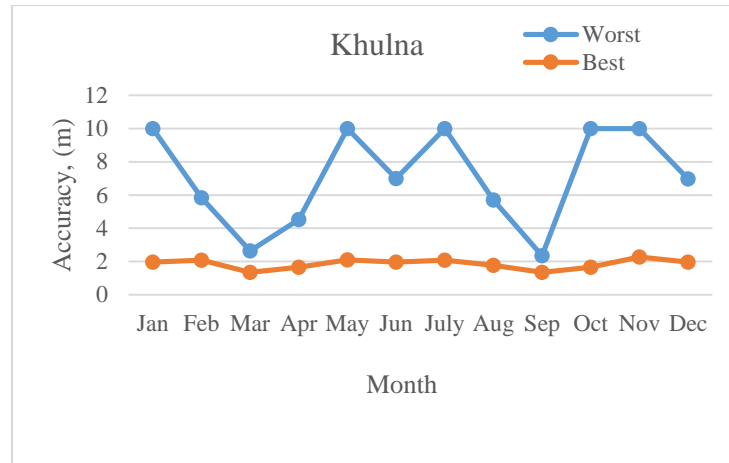
(b)

Fig. 4.29: Accuracy results over Sylhet (a) GPS and (b) Galileo

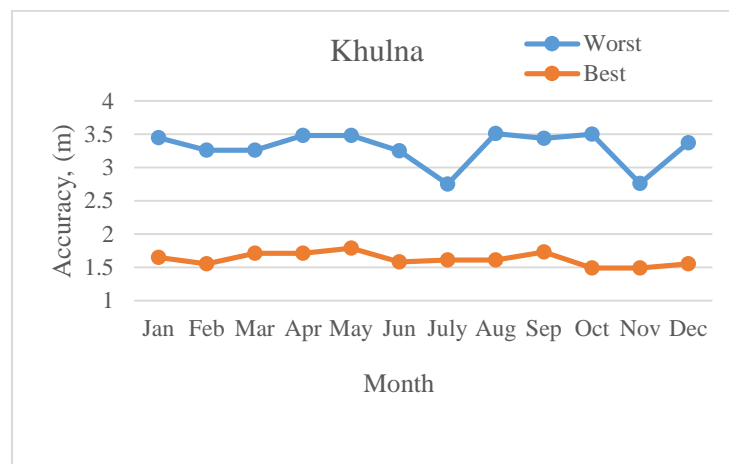
From the graphical data, an assortment in the preciseness over Sylhet can be taken into account. For GPS, the best value is 1.32 meter which is observed in September. The worst accuracy outcome is in the range of 2.71 meter to 10 meter. Moreover, the best and worst accuracy for Galileo are 1.52 meter and 3.5 meter respectively.

4.2.5 Khulna (22.8456⁰N, 89.5403⁰E)

Fig. 4.30 (a ~ b) displays the accuracy results over Khulna for both the constellations analyzed.



(a)



(b)

Fig. 4.30: Accuracy results over Khulna (a) GPS and (b) Galileo

From the graphical information, a variety in the accuracy over Khulna can be noticed. For GPS, the best value ranges from 1.35 meter to 2.27 meter. The worst result is in the middle of 2.36 meter to 10 meter. On the contrary, the best precision value for Galileo is 1.49 meter and the worst value is 3.51 meter.

4.2.6 Discussion on the results:

The above simulation results indicates the variation of accuracy in the surveyed regions for GPS and Galileo constellations. As GDOP value of different locations play an important

role in accuracy calculation, this type of variation has been observed. The region where highest GDOP has been recorded in the previous section, worst accuracy has been estimated there. Also, values of UERE for both GPS and Galileo have influenced the accuracy results. For GPS the accuracy fluctuates in between 1.34 to 10 meter whereas for Galileo the value is in between 1.4 to 3.51 meter. The accuracy results are better in case of Galileo than GPS. In Dhaka, the best accuracy has been calculated for Galileo which is 1.46 meter in October and November due to the low GDOP values.

4.2.7 Evaluation of the outcomes:

Revising the simulation and calculated data from section 4.2, a similar assessment can be made among the locations in terms of accuracy. Due to the variation of GDOP, the accuracy differs from location to location. Using the comparison Table 4.12, the accuracy condition is displayed below. The best accuracy values have been considered for this assessment for both the constellations.

Table 4.12: Overall comparison among the locations on accuracy

Location	Accuracy (GPS)	Accuracy (Galileo)
Dhaka	Good	Best
Chattogram	Good	Good
Rajshahi	Not Good	Not Good
Sylhet	Best	Average
Khulna	Average	Good

4.3 Simulation Results of Ground Station Phased Array Antenna for Different GNSS Constellations

In this section, the simulation outcomes of the design phased array microstrip patch antenna will be discussed. The design of the antenna dimension have been discussed broadly in the previous chapter. The major aim of the results is to find out how the antennas performs in different GNSS frequencies. Furthermore, the beam steering capability of the antennas is also a key observable.

4.3.1 Results analysis of a 2x2 slotted microstrip patch antenna for different GNSS frequencies

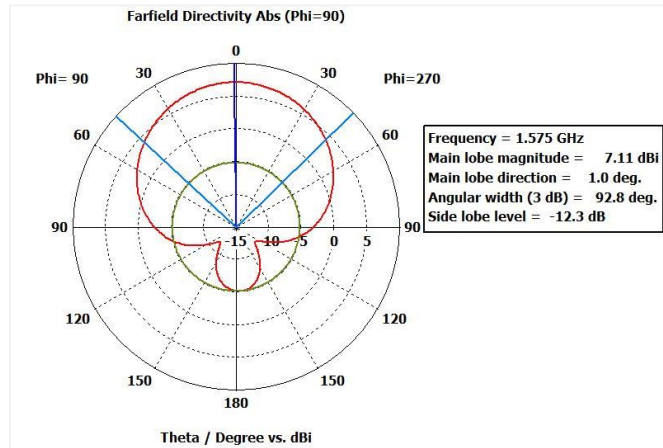
The results in this section is arranged in two parts for each constellation. Firstly, the simulation outcomes of the single U-slotted inset fed microstrip patch antenna by varying the slot angle for GPS (L1, L2 and L5), Galileo (E5, E6) and GLONASS (L3) signals are observed. To observe the variations in performance, the slot is rotated by three angles which are 0° , 40° and 80° . Finally, the best slot orientation is selected with which the phased array antenna is constructed in order to observe the beam steering range and the results are displayed.

GPS (L1, L2 and L5): The change in length and width of the antenna due to slot rotation and major excerpts from the radiation patterns are listed in Table 4.13 below to simplify the analysis.

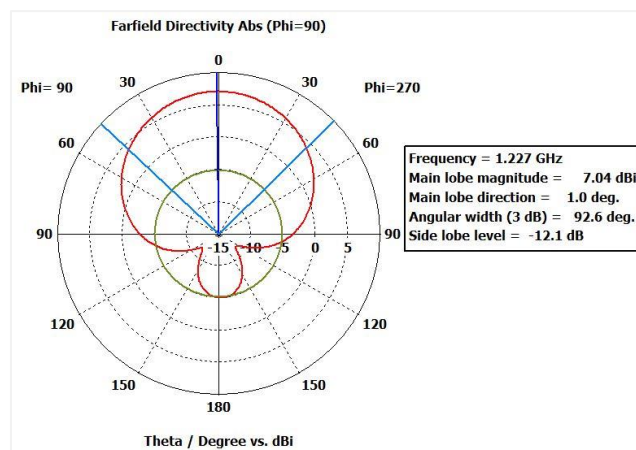
Table 4.13: Parametric study of antenna for GPS signals

Parameter	Slot Angle	L1	L2	L5
L (mm)	Z= 0°	44.71	57.49	59.95
	Z= 40°	44.5	57.67	60
	Z= 80°	44.61	57.75	60.18
W (mm)	Z= 0°	61	74.35	77.57
	Z= 40°	61	74.35	77.57
	Z= 80°	61	74.35	77.57
S11	Z= 0°	-17.279	-18.92	-20.33
	Z= 40°	-14.685	-19.32	-20.90
	Z= 80°	-21.556	-21.961	-22.932
VSWR	Z= 0°	1.316	1.255	1.213
	Z= 40°	1.452	1.242	1.198
	Z= 80°	1.18	1.17	1.15
BW (MHz)	Z= 0°	45.8	33.4	32.6
	Z= 40°	37.8	33.0	32.6
	Z= 80°	46.2	33.6	32.7
Main lobe magnitude (dBi)	Z= 0°	7.10	7.02	7.05
	Z= 40°	7.09	7.03	7.05
	Z= 80°	7.11	7.04	7.05
AW ($^\circ$)	Z= 0°	92.7	92.6	92.6
	Z= 40°	92.8	92.5	92.5
	Z= 80°	92.8	92.7	92.5
SLL (dB)	Z= 0°	-12.2	-12.0	-12.0
	Z= 40°	-12.1	-12.1	-12.0
	Z= 80°	-12.3	-12.1	-12.0

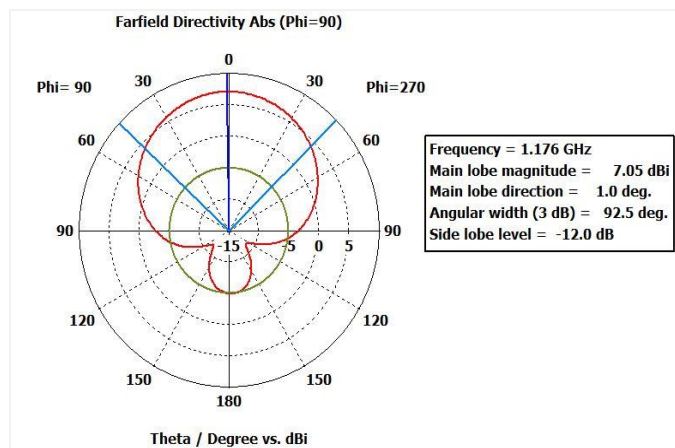
From the simulation results of GPS signals, it can be stated that the slot orientation $Z = 80^\circ$ provides the best performance among the other simulated angles. Radiation pattern variation due to $Z = 80^\circ$ angle for GPS signals are displayed in Fig. 4.31 (a ~ c).



(a)



(b)



(c)

Fig. 4.31: Far field radiation pattern (polar) for $Z = 80^\circ$ of (a) L1, (b) L2 and (c) L5

The S-parameter curves of the antenna for GPS frequencies indicate a good resonance in all the cases which are shown in Fig. 4.32 below.

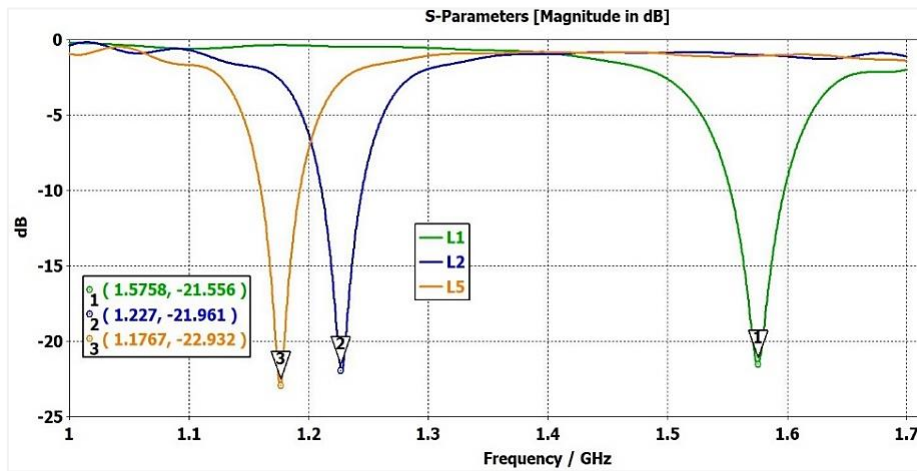


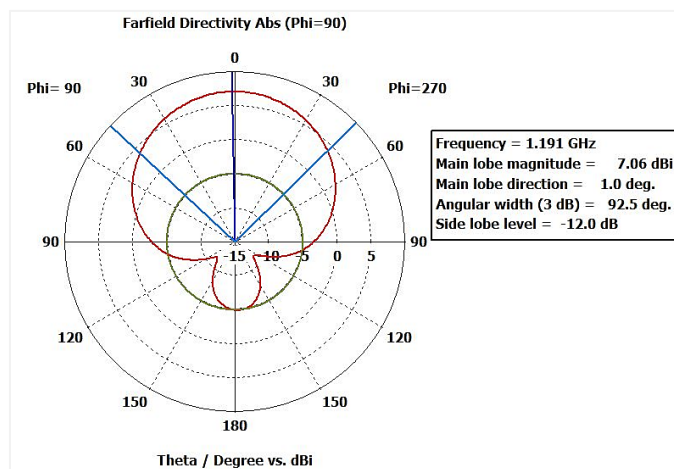
Fig. 4.32: S-parameters of the antenna for $Z = 80^0$ for GPS frequencies

Galileo (E5 and E6) and GLONASS (L3): Similarly, for both Galileo and GLONASS frequencies, the simulation is done and the important results are listed in Table 4.14 below to simplify the analysis.

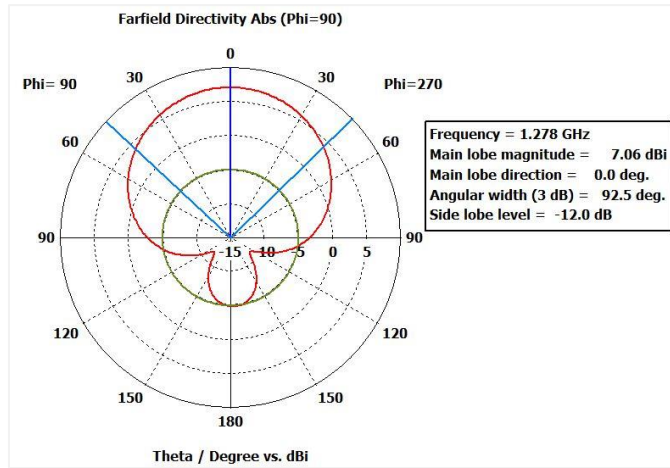
Table 4.14: Parametric study of antenna for Galileo and GLONASS signals

Parameter	Slot Angle	E5	E6	L3
L (mm)	Z=0 ⁰	59.09	54.55	58.54
	Z=40 ⁰	59.37	54.85	58.87
	Z=80 ⁰	59.4	54.87	58.7
W (mm)	Z=0 ⁰	71.1	71.38	75.96
	Z=40 ⁰	71.1	71.38	75.96
	Z=80 ⁰	71.1	71.38	75.96
S11	Z=0 ⁰	-19.57	-17.08	-19.089
	Z=40 ⁰	-20.013	-17.56	-19.54
	Z=80 ⁰	-22.223	-19.243	-20.606
VSWR	Z=0 ⁰	1.231	1.325	1.249
	Z=40 ⁰	1.221	1.305	1.235
	Z=80 ⁰	1.167	1.244	1.206
BW (MHz)	Z=0 ⁰	32.7	34.0	32.9
	Z=40 ⁰	33.1	34.7	32.8
	Z=80 ⁰	34.2	34.9	33.2
Main lobe magnitude (dBi)	Z=0 ⁰	7.05	7.05	7.06
	Z=40 ⁰	7.04	7.04	7.04
	Z=80 ⁰	7.06	7.06	7.06
A.W (°)	Z=0 ⁰	92.6	92.6	92.6
	Z=40 ⁰	92.5	92.5	92.5
	Z=80 ⁰	92.5	92.5	92.6
SLL (dB)	Z=0 ⁰	-11.9	-11.8	-11.9
	Z=40 ⁰	-12.0	-12.0	-12.0
	Z=80 ⁰	-12.0	-12.0	-11.9

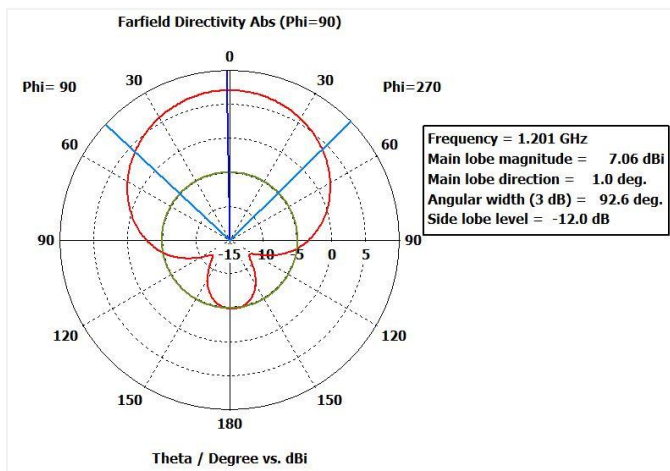
From the results, it can be observed that the slot angle $Z = 80^0$ provides the best performance among the other simulated angles in this case also. Radiation pattern variation due to $Z = 80^0$ angle for Galileo (E5, E6) and GLONASS (L3) are displayed in Fig. 4.33 (a ~ c).



(a)



(b)



(c)

Fig. 4.33: Far field radiation pattern (polar) for $Z = 80^\circ$ of (a) E5, (b) E6 and (c) L3

The S-parameter curves of the antenna for GPS frequencies are shown in Fig. 4.34 below.

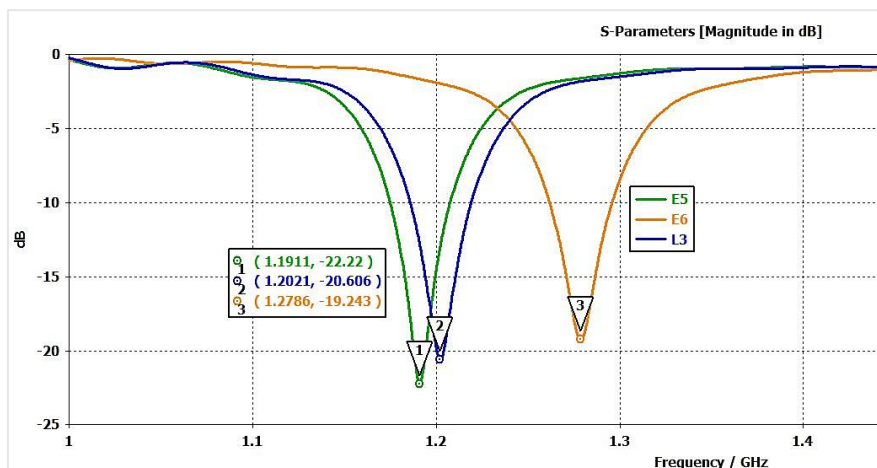


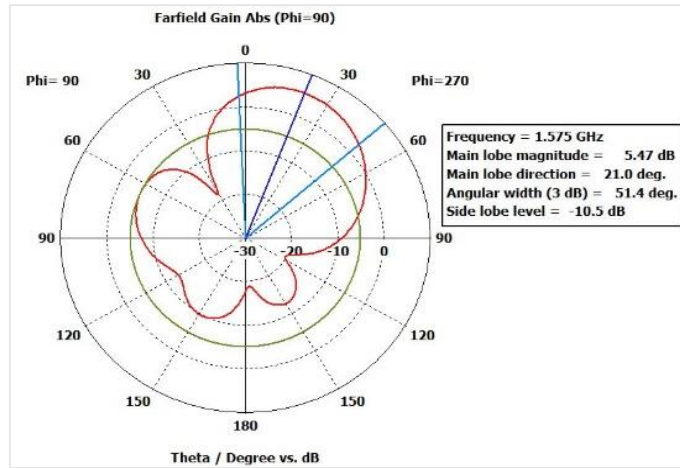
Fig. 4.34: S-parameters of the antenna for $Z = 80^\circ$ for Galileo and GLONASS frequencies

As the selection of better performing orientation has been achieved, the 2x2 phased array antenna is constructed to observe the desired beam steering. The beam steering capability for the GPS, Galileo and GLONASS constellation have been observed by changing the input scan angle of each antenna element. Among many simulation results of phased array antenna for GPS signals, some major outcomes are listed below in Table 4.15.

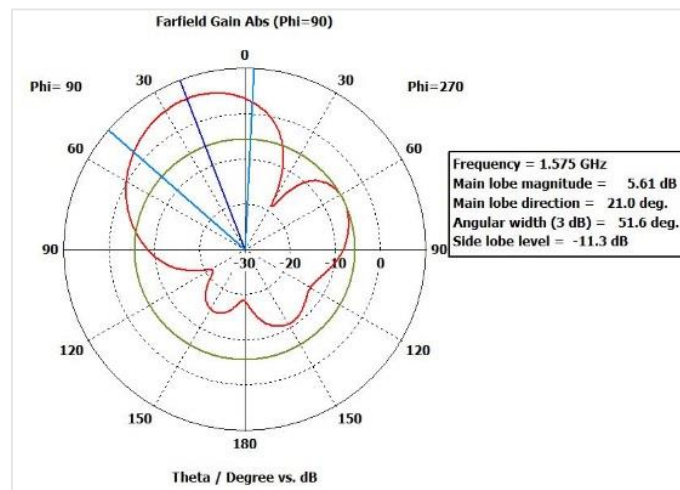
Table 4.15: 2x2 array antenna performance for GPS signals

Signal	Phase Variation of Input Signal ($^{\circ}$)	Scan Angle (θ)	Directivity (dBi)	Gain (dB)	SLL (dB)
L1	0, 0, 0, 0	0°	11.2	5.39	-21.6
	10, 20, 30, 40	7°	11.3	5.41	-20.7
	35, 70, 105, 140	21°	11.1	5.47	-10.5
	-20, -40, -60, -80	-13°	11.2	5.57	-17.1
	-35, -70, -105, -140	-21°	11.1	5.61	-11.3
L2	0, 0, 0, 0	0°	11.0	4.7	-24.8
	10, 20, 30, 40	7°	11.1	4.72	-21.6
	35, 70, 105, 140	21°	11.0	4.78	-10.9
	-20, -40, -60, -80	-14°	11.1	4.88	-17.8
	-35, -70, -105, -140	-21°	11.0	4.92	-11.6
L5	0, 0, 0, 0	0°	11.0	4.59	-24.9
	10, 20, 30, 40	7°	11.0	4.66	-21.7
	35, 70, 105, 140	21°	11.0	4.65	-10.9
	-20, -40, -60, -80	-14°	11.1	4.75	-17.9
	-35, -70, -105, -140	-21°	11.0	4.79	-11.6

From the above tables, it can be concluded that using the array antenna a scan angle range from -21° to $+21^{\circ}$ can be achieved. Also the gain value remains above 4.5 dB for all of the GPS signal frequencies. Amid the simulation results, the polar radiation pattern which shows the beam steering for the maximum angle $+21^{\circ}$ and minimum angle -21° of GPS L1 signal are shown in Fig. 4.35 (a ~ b) below.



(a)



(b)

Fig. 4.35: Radiation pattern (polar) of array antenna for GPS L1 (a) $\theta = +21^{\circ}$ and (b) $\theta = -21^{\circ}$

Now, similarly using the Galileo and GLONASS frequency the performance of the phased array antenna has been analyzed and major outcomes are listed below in Table 4.16.

Table 4.16: 2x2 array antenna performance for Galileo and GLONASS signals

Signal	Phase Variation of Input Signal ($^{\circ}$)	Scan Angle (θ)	Directivity (dBi)	Gain (dB)	SLL (dB)
E5	0, 0, 0, 0	0°	11.0	4.63	-25.0
	10, 20, 30, 40	7°	11.0	4.63	-21.7
	35, 70, 105, 140	21°	11.0	4.71	-11.0
	-20, -40, -60, -80	-13°	11.0	4.81	-18.1
	-35, -70, -105, -140	-21°	11.0	4.85	-11.7
E6	0, 0, 0, 0	0°	11.0	4.7	-24.8
	10, 20, 30, 40	7°	11.1	4.72	-21.6
	35, 70, 105, 140	21°	11.0	5.03	-10.9
	-20, -40, -60, -80	-14°	11.1	4.88	-17.8
	-35, -70, -105, -140	-21°	11.0	5.17	-11.6
L3	0, 0, 0, 0	0°	11.0	4.61	-24.9
	10, 20, 30, 40	7°	11.0	4.63	-21.7
	35, 70, 105, 140	21°	11.0	4.69	-10.9
	-20, -40, -60, -80	-14°	11.0	4.82	-18.0
	-35, -70, -105, -140	-21°	11.0	4.83	-11.6

Similarly, it can also be decided that using the array antenna a scan angle range from -21° to $+21^{\circ}$ can be attained for Galileo and GLONASS signals. Likewise the gain value remains above 4.5 dB for all of the signal frequencies. Amongst the simulation results, the polar radiation pattern that shows the maximum angle $+21^{\circ}$ and minimum angle -21° of Galileo E6 in Fig. 4.36 (a ~ b) and GLONASS L3 signals are shown in Fig. 4.37 (a ~ b).

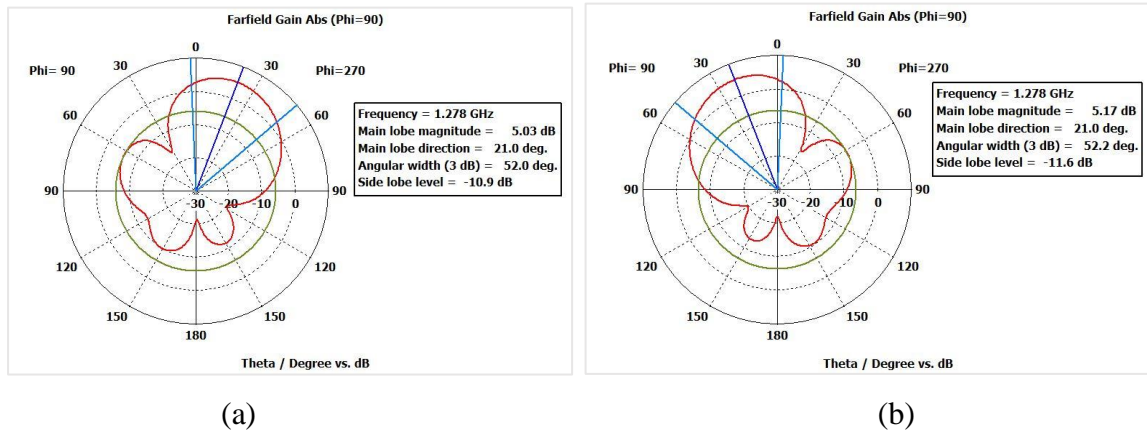


Fig. 4.36: Radiation pattern (polar) of array antenna for Galileo E6 (a) $\theta = +21^{\circ}$ and (b) $\theta = -21^{\circ}$

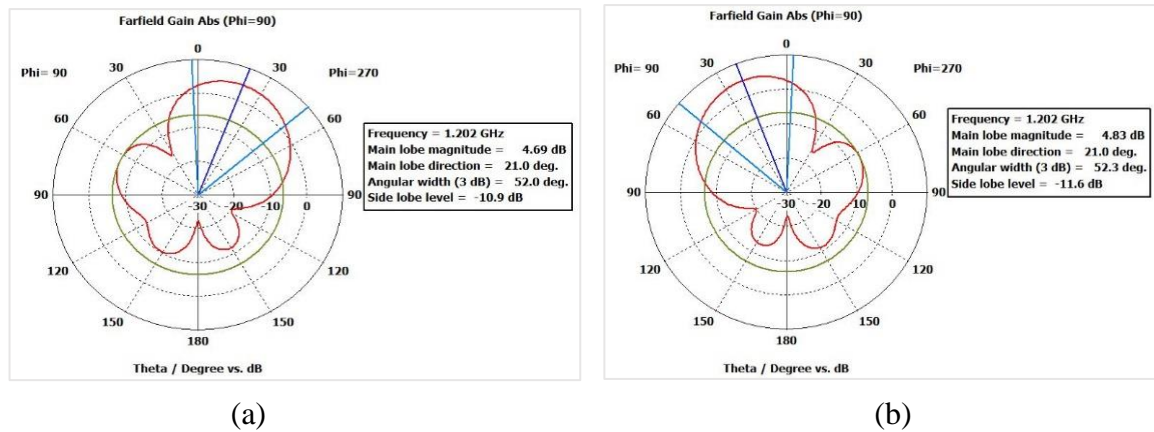


Fig. 4.37: Radiation pattern (polar) of array antenna for GLONASS L3, (a) $\theta = +21^\circ$ and (b) $\theta = -21^\circ$

In a nut shell, a FR-4 substrate to investigate the performance of the antenna for GPS, Galileo and GLONASS signal frequencies by revolving the angle of the slot. Comparing among the parameters such as bandwidth, reflection coefficient, VSWR, directivity etc., it is found that the slot angle $Z = 80^\circ$ is the optimum orientation. Then 2x2 phased array antenna are constructed for the GNSS signals to examine the array performance as well as beam steering. The variation in results has shown that a total steering angle of 42° (-21° to $+21^\circ$) has been achieved.

4.3.2 Simulation results of improved 2x3 phased array patch antenna to enhance the beam scanning range.

In order to increase the beam scanning angle, a 2x3 phased array antenna has been constructed and the design procedure has been discussed in Chapter 3. The simulation process of this antenna is the same as the previous one. Each of the element is fed with different phase angle signal and the major results are listed in Table 4.17 below.

Table 4.17: Scan angle determination of 2x3 phased array antenna

Phase Variation	Main Lobe Mag.	θ_s	AW	Side Lobe
0, 0, 0, 0, 0, 0	12.4	0^0	57.4^0	-28.0
0, 2, 4, 6, 8, 10	12.4	2^0	57.2^0	-25.6
5, 10, 15, 20, 25, 30	12.4	5^0	57.0^0	-22.8
10, 20, 30, 40, 50, 60	12.4	10^0	56.4^0	-19.5
15, 30, 45, 60, 75, 90	12.3	15^0	55.6	-17.1
20, 40, 60, 80, 100, 120	12.2	19^0	54.7^0	-14.5
25, 50, 75, 100, 125, 150	12.0	22^0	53.8^0	-11.5
27, 54, 81, 108, 135, 162	11.8	24^0	53.6^0	-10.5
30, 60, 90, 120, 150, 180	11.6	25^0	53.2^0	-9.1
-2, -4, -6, -8, -10, -12	12.4	-2^0	57.3^0	-26.9
-5, -10, -15, -20, -25, -30	12.4	-6^0	57.0^0	-24.0
-10, -20, -30, -40, -50, -60	12.4	-11^0	56.4^0	-20.5
-15, -30, -45, -60, -75, -90	12.3	-15^0	55.8^0	-17.9
-20, -40, -60, -80, -100, -120	12.2	-19^0	54.9^0	-15.2
-25, -50, -75, -100, -125, -150	12.0	-22^0	54.2^0	-12.2
-27, -54, -81, -108, -135, -162	11.9	-24^0	53.9^0	-11.2
-29, -58, -87, -116, -145, -174	11.7	-25^0	53.7^0	-10.2
-30, -60, -90, -120, -150, -180	11.0	-26^0	58.7^0	-9.80

From the above simulation outcomes, an overview of scan angle range can be judged. The results show that the scan angle varies from -26^0 to $+25^0$ and the other parameter values also differ with each phase combination. The maximum value of directivity is 12.4 dBi. Considering a good side lobe value which is below -10 dB, a scan angle range from -25^0 to

$+24^{\circ}$ can be estimated which gives a total scan range of 49° . Among the results, the radiation pattern of the maximum positive scan angle that is 24° is displayed in Fig. 4.38 (a ~ b).

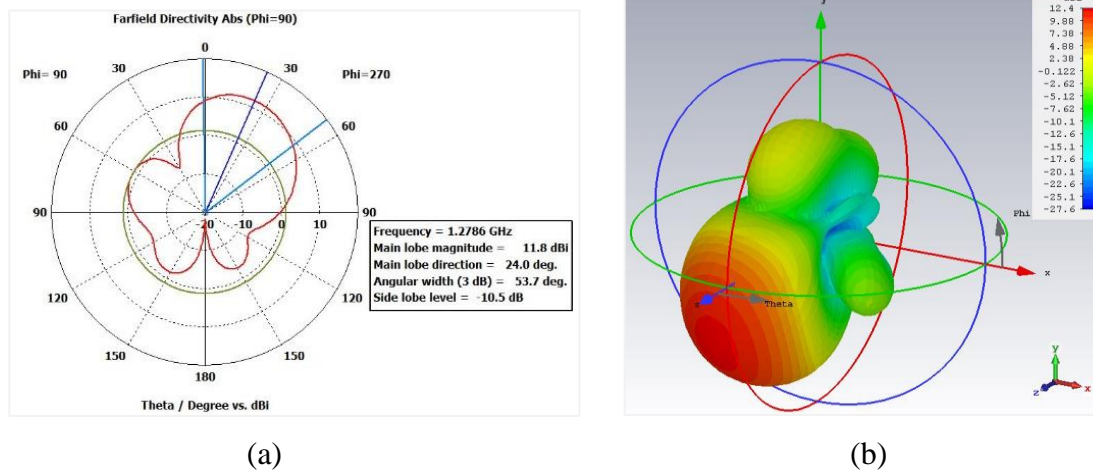


Fig. 4.38: (a) Far field polar radiation pattern and (b) 3D radiation pattern of the array antenna for $\theta = +24^{\circ}$

To display one of the results from the midrange value, the radiation pattern of the scan angle -15° is exhibited in Fig. 4.39.

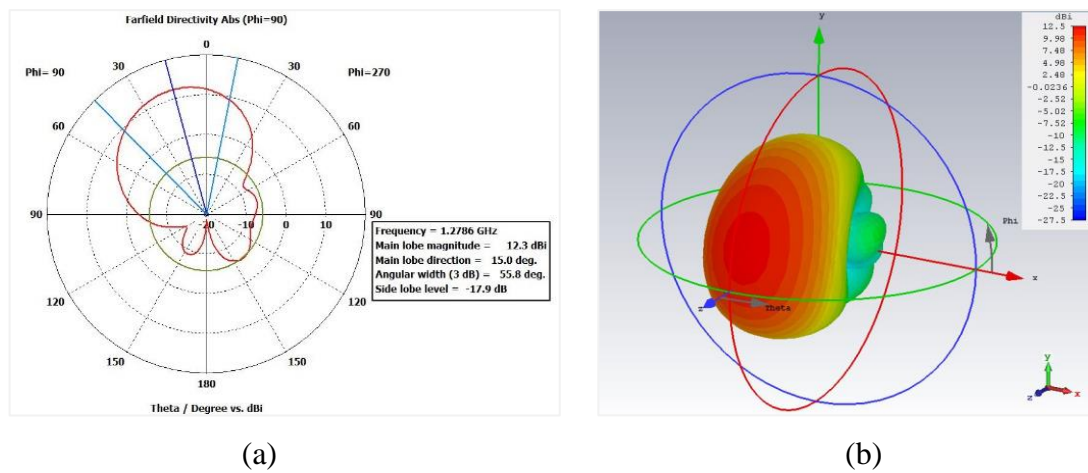


Fig. 4.39: (a) Far field polar radiation pattern and (b) 3D radiation pattern of the array antenna for $\theta = -15^{\circ}$

To display the minimum value of the range, the radiation pattern of the scan angle -25° is exhibited in Fig. 4.40.

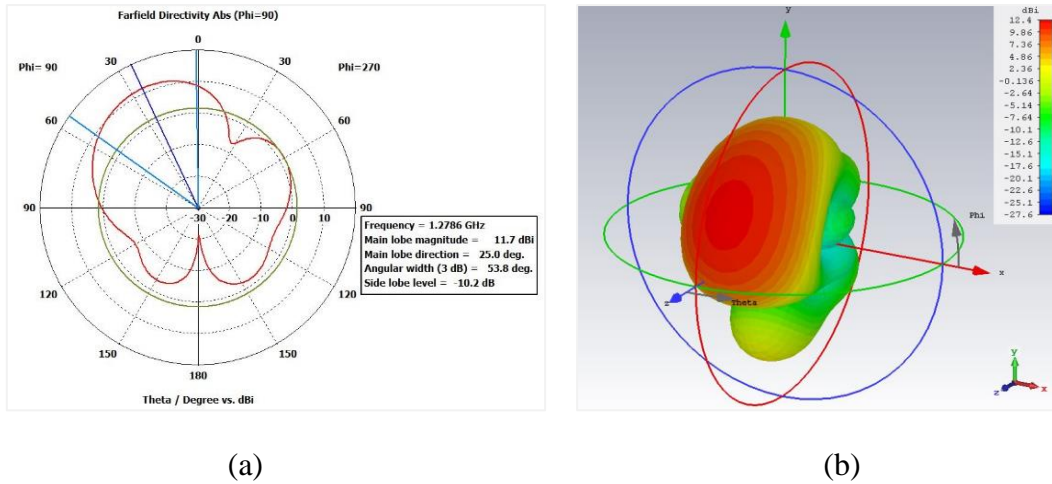


Fig. 4.40: (a) Far field polar radiation pattern and (b) 3D radiation pattern of the array antenna for $\theta = -25^\circ$

The antenna described above can be used for receiving and transmitting different GNSS signals as simulated above. If the number of element is increased, then the directivity of the antenna will increase as well as the scan angle. So, according to the requirement of directivity, these antennas can be modified for GNSS use.

4.4 Estimation of Atmospheric Factors of GNSS Signals over Bangladesh to Select Suitable Ground Station Location

In this section, the results from the atmospheric delay estimation will be displayed and discussed over five major cities of Bangladesh. The procedure of this analysis has been discussed largely in Chapter 3. The calculation of tropospheric scintillation fade depth (SFD), ionospheric delay and rainfall attenuation delay has been separately presented for each of the surveyed locations to make an assessment among them regarding the selection of ground station. The GNSS constellation frequencies are L1 and E5.

4.4.1 Tropospheric Scintillation Fade Depth (SFD)

As mentioned in Chapter 3, the variation of SFD will contain two set of values as maximum average temperature as well as minimum average temperature will be used separately. To see the variation of SFD due to the change in antenna elevation angle, the calculation is done for 5° , 10° and 15° .

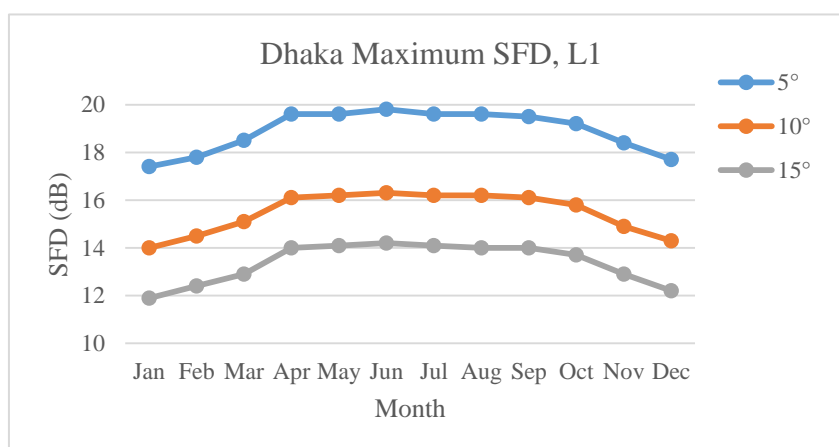
a) Dhaka SFD for L1 and E5 signals:

The calculated value of SFD both using maximum and minimum temperature using L1 signal for the chosen elevation angle is done and listed in Table 4.18.

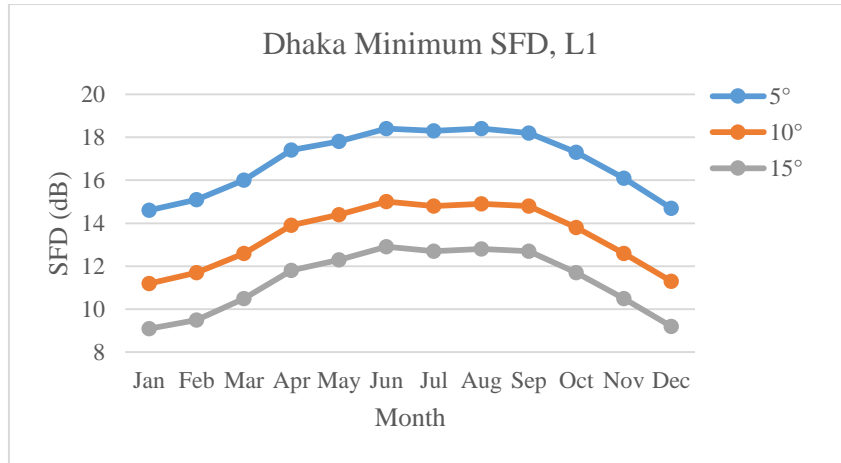
Table 4.18: SFD value of Dhaka using L1 for different elevation angle

Month	SFD (max) in dB			SFD (min) in dB		
	5 ⁰	10 ⁰	15 ⁰	5 ⁰	10 ⁰	15 ⁰
Jan	17.4	14.0	11.9	14.6	11.2	9.1
Feb	17.8	14.5	12.4	15.1	11.7	9.5
Mar	18.5	15.1	12.9	16.0	12.6	10.5
Apr	19.6	16.1	14.0	17.4	13.9	11.8
May	19.6	16.2	14.1	17.8	14.4	12.3
Jun	19.8	16.3	14.2	18.4	15.0	12.9
Jul	19.6	16.2	14.1	18.3	14.8	12.7
Aug	19.6	16.2	14.0	18.4	14.9	12.8
Sep	19.5	16.1	14.0	18.2	14.8	12.7
Oct	19.2	15.8	13.7	17.3	13.8	11.7
Nov	18.4	14.9	12.9	16.1	12.6	10.5
Dec	17.7	14.3	12.2	14.7	11.3	9.2

The maximum SFD and minimum SFD are shown graphically in Fig. 4.41 (a ~ b) below.



(a)



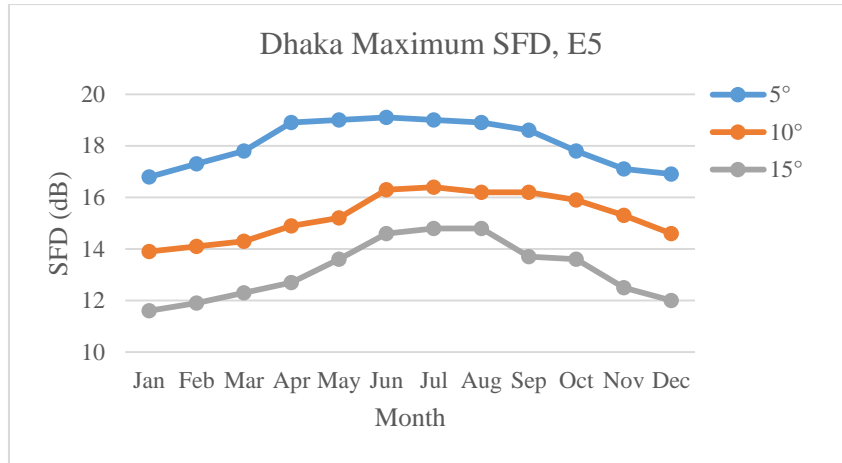
(b)

Fig. 4.41: SFD for different angle in Dhaka for L1 (a) Maximum and (b) Minimum

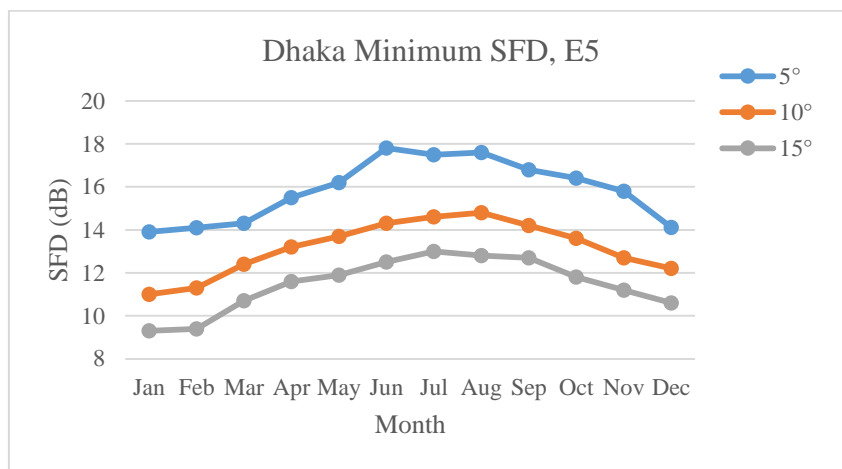
By analyzing the graphs, it is found that the maximum SFD due to the maximum temperature occurs in the month of June and minimum SFD for minimum temperature occurs in January. Also it is apparent from both the graphs that the value of SFD is less for an increased value of elevation angle. The minimum SFD value for 5^0 is 14.6 dB whereas for 15^0 it is 9.1 dB in Dhaka. Now, the calculated SFD values for E5 signal of Dhaka are listed in Table 4.19 are illustrated in Fig. 4.42 (a ~ b).

Table 4.19: SFD value of Dhaka using E5 for different elevation angle

Month	SFD (max) in dB			SFD (min) in dB		
	5^0	10^0	15^0	5^0	10^0	15^0
Jan	16.8	13.9	11.6	13.9	11	9.3
Feb	17.3	14.1	11.9	14.1	11.3	9.4
Mar	17.8	14.3	12.3	14.3	12.4	10.7
Apr	18.9	14.9	12.7	15.5	13.2	11.6
May	19	15.2	13.6	16.2	13.7	11.9
Jun	19.1	16.3	14.6	17.8	14.3	12.5
Jul	19	16.4	14.8	17.5	14.6	13
Aug	18.9	16.2	14.8	17.6	14.8	12.8
Sep	18.6	16.2	13.7	16.8	14.2	12.7
Oct	17.8	15.9	13.6	16.4	13.6	11.8
Nov	17.1	15.3	12.5	15.8	12.7	11.2
Dec	16.9	14.6	12	14.11	12.2	10.6



(a)



(b)

Fig. 4.42: SFD for different angle in Dhaka for E5 (a) Maximum and (b) Minimum

From the results of SFD using E5 signal for Dhaka, it can be denoted that the value of SFD is maximum in the middle quarter of the year with a maximum value of 19.1 dB. The minimum value of SFD if we consider all the results is 9.3 dB which is slightly higher than the minimum value of SFD for L1 signal. Like the previous results, the SFD value decreases as the elevation angle increases.

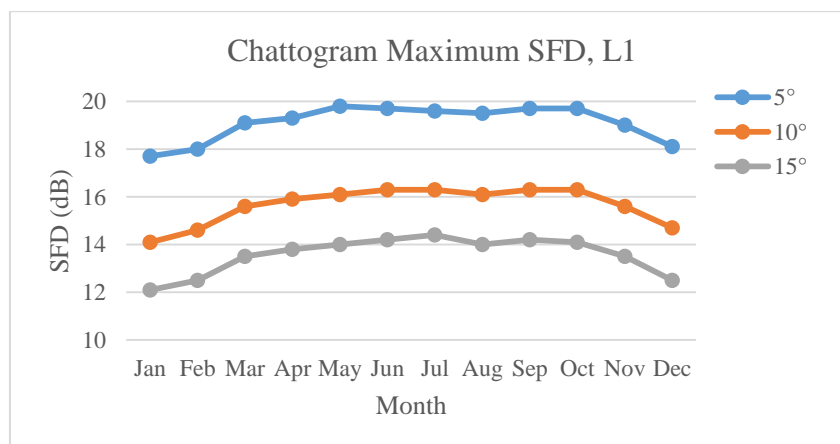
b) Chattogram SFD for L1 and E5 signals:

For Chattogram, the estimated value of maximum and minimum SFD using L1 signal for the chosen elevation angle is done and listed in Table 4.20.

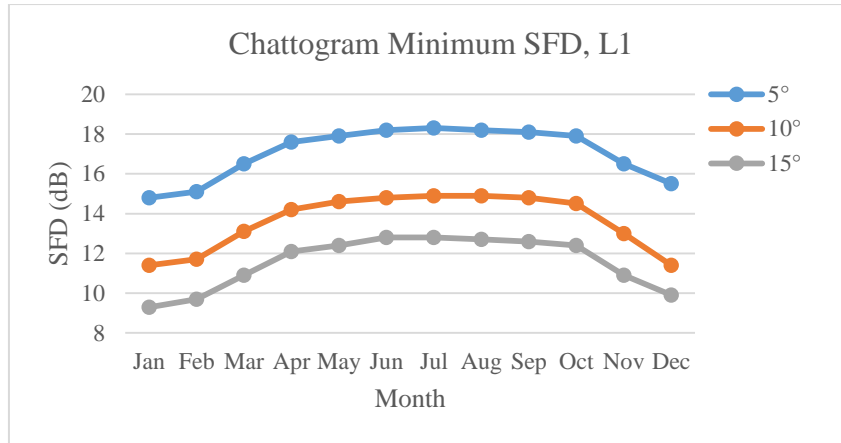
Table 4.20: SFD value of Chattogram using L1 for different elevation angle

Month	SFD (max) in dB			SFD (min) in dB		
	5 ⁰	10 ⁰	15 ⁰	5 ⁰	10 ⁰	15 ⁰
Jan	17.7	14.1	12.1	14.8	11.4	9.3
Feb	18	14.6	12.5	15.1	11.7	9.7
Mar	19.1	15.6	13.5	16.5	13.1	10.9
Apr	19.3	15.9	13.8	17.6	14.2	12.1
May	19.8	16.1	14	17.9	14.6	12.4
Jun	19.7	16.3	14.2	18.2	14.8	12.8
Jul	19.6	16.3	14.4	18.3	14.9	12.8
Aug	19.5	16.1	14	18.2	14.9	12.7
Sep	19.7	16.3	14.2	18.1	14.8	12.6
Oct	19.7	16.3	14.1	17.9	14.5	12.4
Nov	19	15.6	13.5	16.5	13	10.9
Dec	18.1	14.7	12.5	15.5	11.4	9.9

In Fig. 4.43 (a ~ b) below, results of the above table are shown using graphs. The maximum and minimum SFD for different angle are shown independently.



(a)



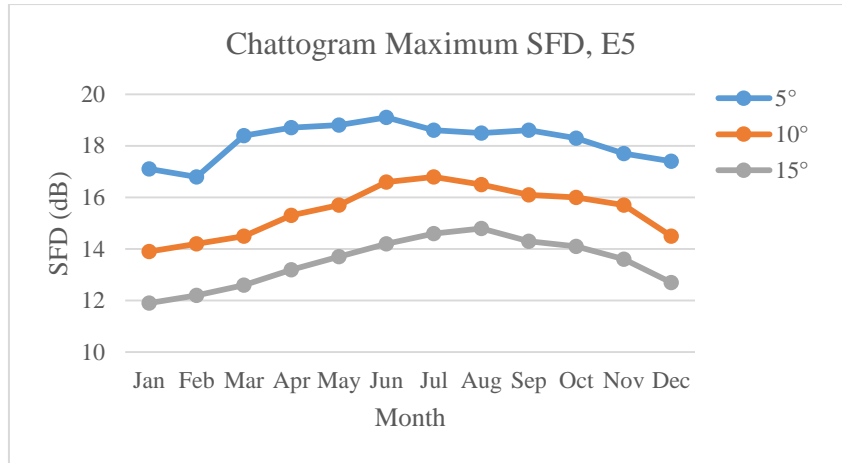
(b)

Fig. 4.43: SFD for different angle in Chattogram for L1 (a) Maximum and (b) Minimum

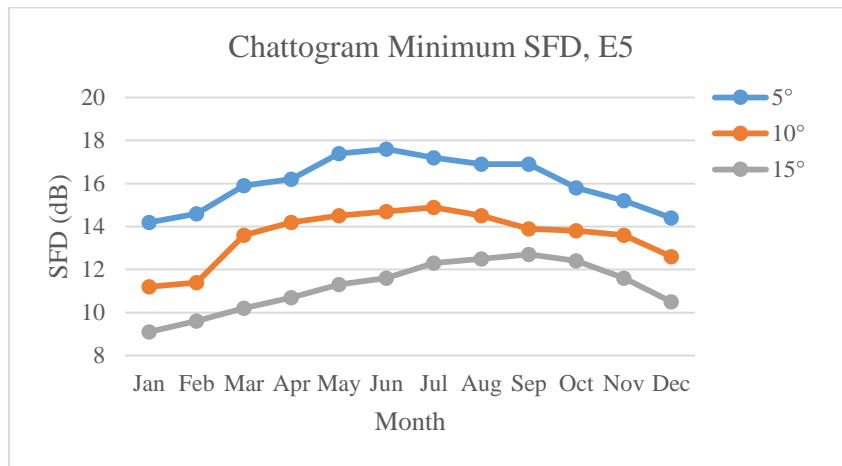
The graphs are examined and it can be found for 5° that the maximum SFD due to the maximum temperature is 19.8 dB that is recorded in May and minimum SFD for minimum temperature occurs in January with a value of 14.8 dB. Also, the change in the value of SFD due to the change in angle is also observed as the same as previous. Now, the calculated SFD values for E5 signal of Chattogram are listed in Table 4.21 and illustrated in Fig. 4.44 (a ~ b).

Table 4.21: SFD value of Chattogram using E5 for different elevation angle

Month	SFD (max) in dB			SFD (min) in dB		
	5°	10°	15°	5°	10°	15°
Jan	17.1	13.9	11.9	14.2	11.2	9.1
Feb	16.8	14.2	12.2	14.6	11.4	9.6
Mar	18.4	14.5	12.6	15.9	13.6	10.2
Apr	18.7	15.3	13.2	16.2	14.2	10.7
May	18.8	15.7	13.7	17.4	14.5	11.3
Jun	19.1	16.6	14.2	17.6	14.7	11.6
Jul	18.6	16.8	14.6	17.2	14.9	12.3
Aug	18.5	16.5	14.8	16.9	14.5	12.5
Sep	18.6	16.1	14.3	16.9	13.9	12.7
Oct	18.3	16	14.1	15.8	13.8	12.4
Nov	17.7	15.7	13.6	15.2	13.6	11.6
Dec	17.4	14.5	12.7	14.4	12.6	10.5



(a)



(b)

Fig. 4.44: SFD for different angle in Chattogram for E5 (a) Maximum and (b) Minimum

The fluctuation of SFD for 5° elevation angle is more than the other two elevation angles in both maximum and minimum cases for E5 signal. The highest calculated SFD value is 19.1 dB and 17.6 dB for maximum and minimum temperature respectively.

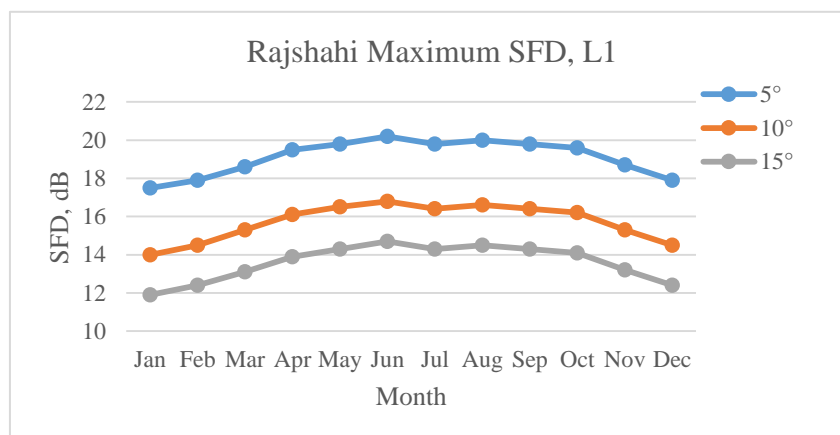
c) Rajshahi SFD for L1 and E5 signals:

The calculation of SFD is also done for Rajshahi using L1 signal for the chosen elevation angle to observe and analyze the data and the data is listed in Table 4.22.

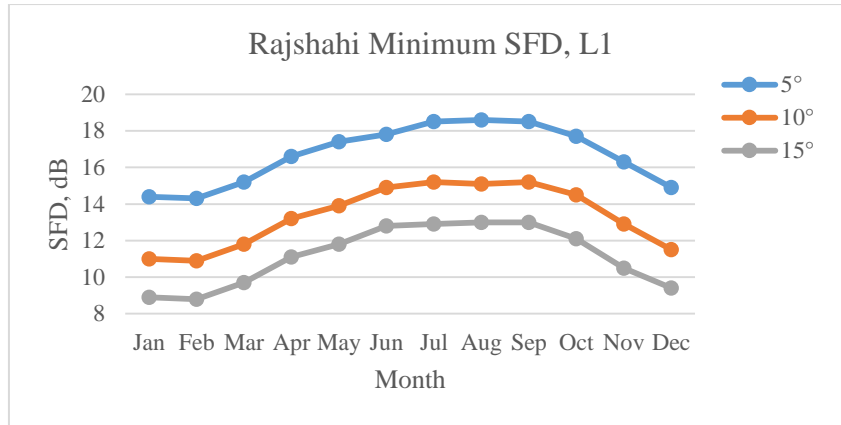
Table 4.22: SFD value of Rajshahi using L1 for different elevation angle

Month	SFD (max) in dB			SFD (min) in dB		
	5 ⁰	10 ⁰	15 ⁰	5 ⁰	10 ⁰	15 ⁰
Jan	17.5	14	11.9	14.4	11	8.9
Feb	17.9	14.5	12.4	14.3	10.9	8.8
Mar	18.6	15.3	13.1	15.2	11.8	9.7
Apr	19.5	16.1	13.9	16.6	13.2	11.1
May	19.8	16.5	14.3	17.4	13.9	11.8
Jun	20.2	16.8	14.7	17.8	14.9	12.8
Jul	19.8	16.4	14.3	18.5	15.2	12.9
Aug	20	16.6	14.5	18.6	15.1	13
Sep	19.8	16.4	14.3	18.5	15.2	13
Oct	19.6	16.2	14.1	17.7	14.5	12.1
Nov	18.7	15.3	13.2	16.3	12.9	10.5
Dec	17.9	14.5	12.4	14.9	11.5	9.4

The maximum and minimum SFD for different angle are illustrated graphically in Fig. 4.45 (a ~ b) below.



(a)



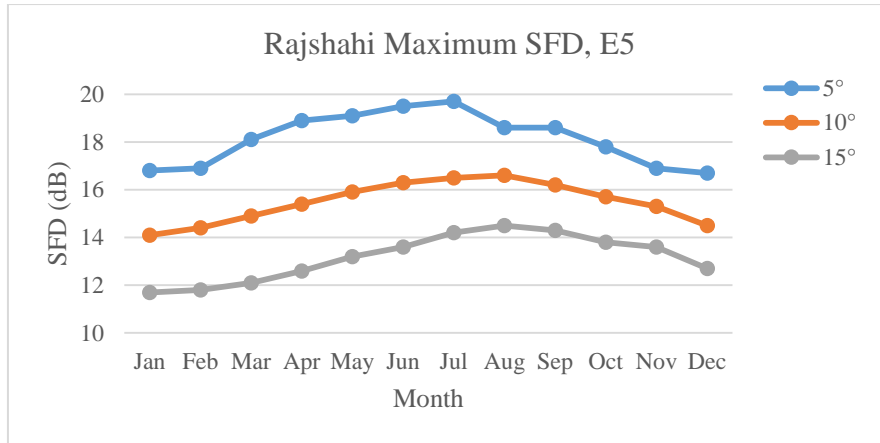
(b)

Fig. 4.45: SFD for different angle in Rajshahi for L1 (a) Maximum and (b) Minimum

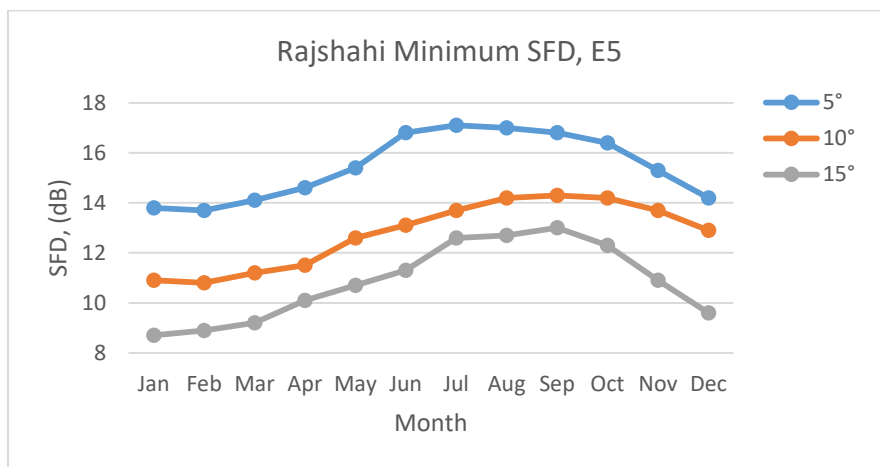
The graphs are studied and it is observed that the SFD value in Rajshahi is the highest among all the surveyed locations above. The maximum value of SFD is 20.2 dB and the minimum value of SFD is 8.8 dB which is also the lowest value of SFD till now. The calculated SFD values for E5 signal are listed in Table 4.23 and separately illustrated in Fig. 4.46 (a ~ b).

Table 4.23: SFD value of Rajshahi using E5 for different elevation angle

Month	SFD (max) in dB			SFD (min) in dB		
	5°	10°	15°	5°	10°	15°
Jan	16.8	14.1	11.7	13.8	10.9	8.7
Feb	16.9	14.4	11.8	13.7	10.8	8.9
Mar	18.1	14.9	12.1	14.1	11.2	9.2
Apr	18.9	15.4	12.6	14.6	11.5	10.1
May	19.1	15.9	13.2	15.4	12.6	10.7
Jun	19.5	16.3	13.6	16.8	13.1	11.3
Jul	19.7	16.5	14.2	17.1	13.7	12.6
Aug	18.6	16.6	14.5	17	14.2	12.7
Sep	18.6	16.2	14.3	16.8	14.3	13
Oct	17.8	15.7	13.8	16.4	14.2	12.3
Nov	16.9	15.3	13.6	15.3	13.7	10.9
Dec	16.7	14.5	12.7	14.2	12.9	9.6



(a)



(b)

Fig. 4.46: SFD for different angle in Rajshahi for E5 (a) Maximum and (b) Minimum

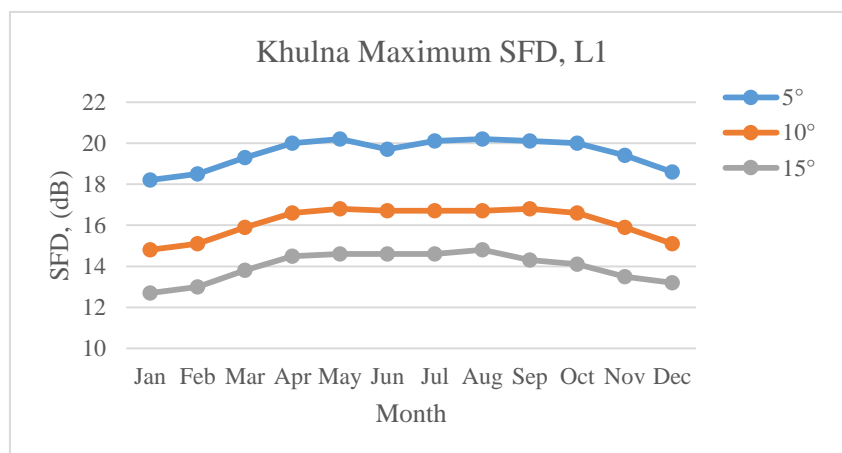
For E5 signal, the highest values of SFD are observed in the middle months of the year and the maximum SFD is 19.7 dB and the minimum SFD is 8.7 dB. The relation between SFD and elevation angle remains the same as before.

d) Khulna SFD for L1 and E5 signals:

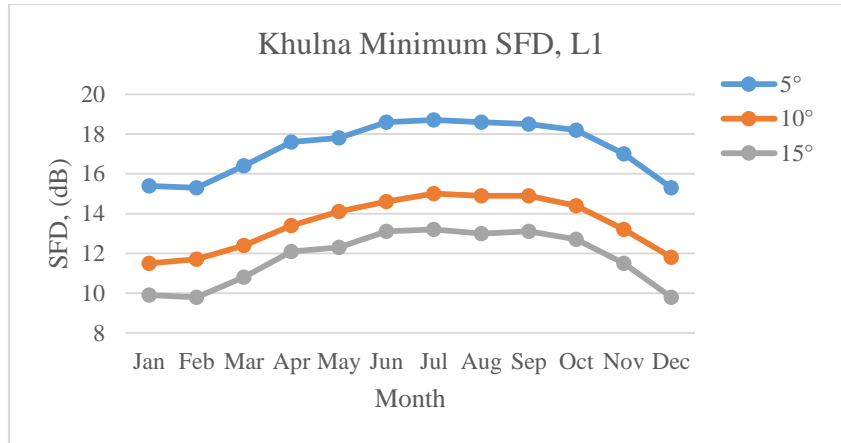
Table 4.24 below registers the maximum and minimum SFD for Khulna using L1 signal for the selected elevation angle to observe and analyze the data. Also the data set are represented graphically in Fig. 4.47 (a ~ b).

Table 4.24: SFD value of Khulna using L1 for different elevation angle

Month	SFD (max) in dB			SFD (min) in dB		
	5 ⁰	10 ⁰	15 ⁰	5 ⁰	10 ⁰	15 ⁰
Jan	18.2	14.8	12.7	15.4	11.5	9.9
Feb	18.5	15.1	13	15.3	11.7	9.8
Mar	19.3	15.9	13.8	16.4	12.4	10.8
Apr	20	16.6	14.5	17.6	13.4	12.1
May	20.2	16.8	14.6	17.8	14.1	12.3
Jun	19.7	16.7	14.6	18.6	14.6	13.1
Jul	20.1	16.7	14.6	18.7	15	13.2
Aug	20.2	16.7	14.8	18.6	14.9	13
Sep	20.1	16.8	14.3	18.5	14.9	13.1
Oct	20	16.6	14.1	18.2	14.4	12.7
Nov	19.4	15.9	13.5	17	13.2	11.5
Dec	18.6	15.1	13.2	15.3	11.8	9.8



(a)



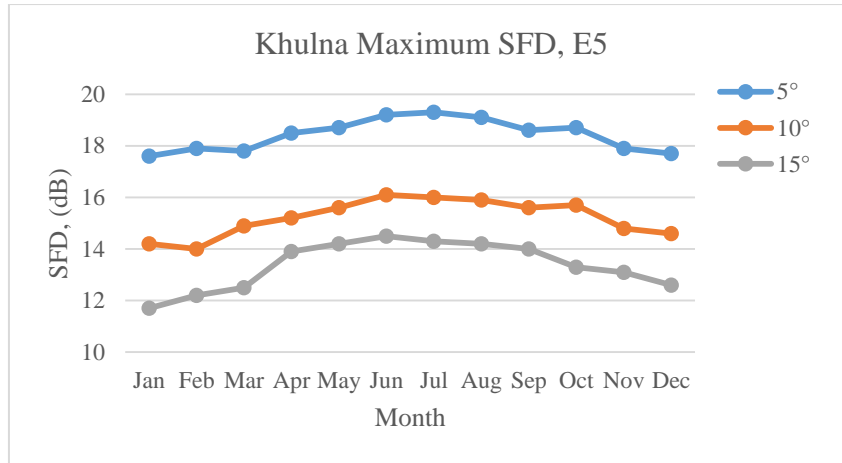
(b)

Fig. 4.47: SFD for different angle in Khulna for L1 (a) Maximum and (b) Minimum

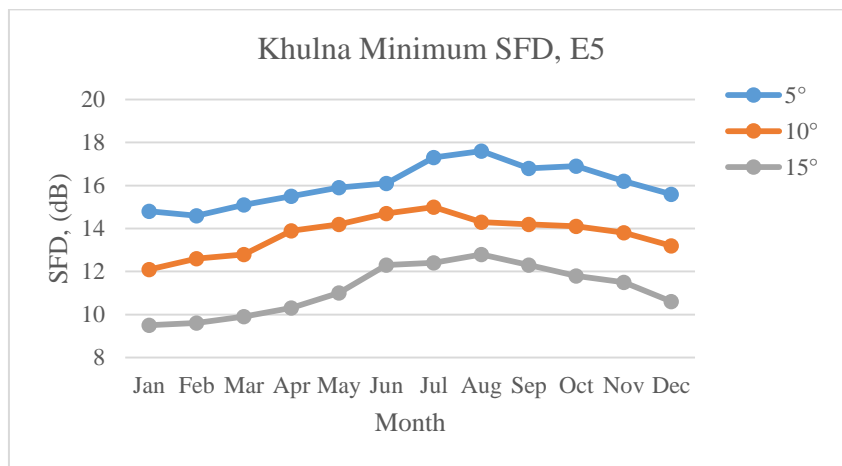
The maximum SFD value for Khulna is similar to Rajshahi which is 20.2 dB that occurs in May for a 5° elevation angle. The minimum SFD value among the outcomes is 9.8 which occurs in the month of February for an elevation angle of 15°. The calculated SFD values for E5 signal of Khulna are written down in Table 4.25 and graphs are shown in Fig. 4.48 (a ~ b).

Table 4.25: SFD value of Khulna using E5 for different elevation angle

Month	SFD (max) in dB			SFD (min) in dB		
	5°	10°	15°	5°	10°	15°
Jan	17.6	14.2	11.7	14.8	12.1	9.5
Feb	17.9	14	12.2	14.6	12.6	9.6
Mar	17.8	14.9	12.5	15.1	12.8	9.9
Apr	18.5	15.2	13.9	15.5	13.9	10.3
May	18.7	15.6	14.2	15.9	14.2	11
Jun	19.2	16.1	14.5	16.1	14.7	12.3
Jul	19.3	16	14.3	17.3	15	12.4
Aug	19.1	15.9	14.2	17.6	14.3	12.8
Sep	18.6	15.6	14	16.8	14.2	12.3
Oct	18.7	15.7	13.3	16.9	14.1	11.8
Nov	17.9	14.8	13.1	16.2	13.8	11.5
Dec	17.7	14.6	12.6	15.6	13.2	10.6



(a)



(b)

Fig. 4.48: SFD for different angle in Khulna for E5 (a) Maximum and (b) Minimum

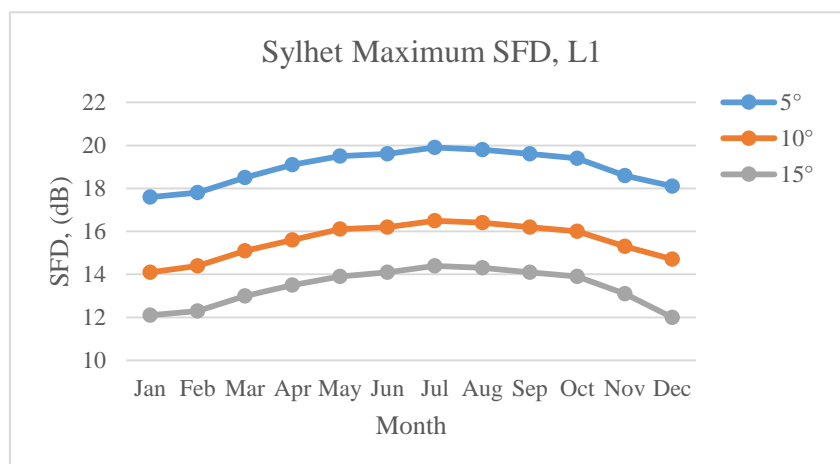
The maximum SFD values are calculated in the months of June to August for E5 signal. The maximum SFD values are 19.3 dB, 16.1 dB and 14.5 dB for 5° , 10° and 15° respectively. Amongst the minimum values, 9.5 dB is the lowest calculated in the month of January.

e) Sylhet SFD for L1 and E5 signals:

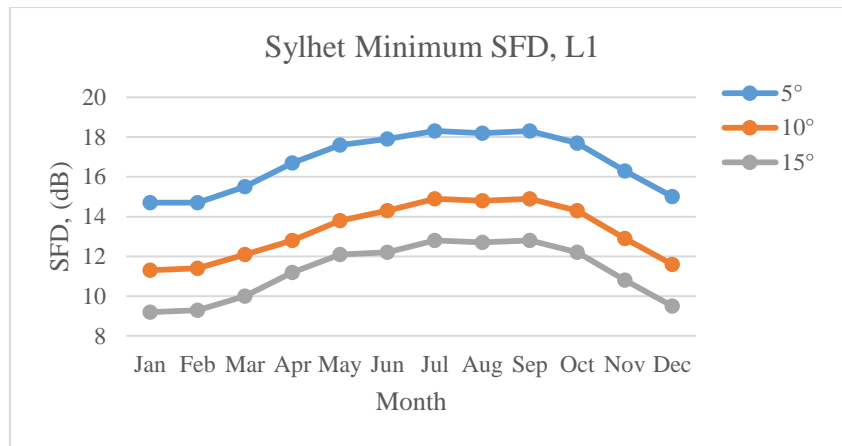
The maximum and minimum SFD for Sylhet by means of L1 signal for the estimated. All the results are documented in Table 4.26. Also the data set are portrayed graphically in Fig. 4.49 (a ~ b).

Table 4.26: SFD value of Sylhet using L1 for different elevation angle

Month	SFD (max) in dB			SFD (min) in dB		
	5 ⁰	10 ⁰	15 ⁰	5 ⁰	10 ⁰	15 ⁰
Jan	17.6	14.1	12.1	14.7	11.3	9.2
Feb	17.8	14.4	12.3	14.7	11.4	9.3
Mar	18.6	15.1	13	15.5	12.1	10
Apr	19.2	15.6	13.5	16.7	12.8	11.2
May	19.5	16.1	13.9	17.6	13.8	12.1
Jun	19.6	16.2	14.1	17.9	14.3	12.2
Jul	19.9	16.5	14.4	18.3	14.9	12.8
Aug	19.8	16.4	14.3	18.2	14.8	12.7
Sep	19.6	16.2	14.1	18.3	14.9	12.8
Oct	19.4	16	13.9	17.7	14.3	12.2
Nov	18.6	15.3	13.1	16.3	12.9	10.8
Dec	18.1	14.7	12	15	11.6	9.5



(a)



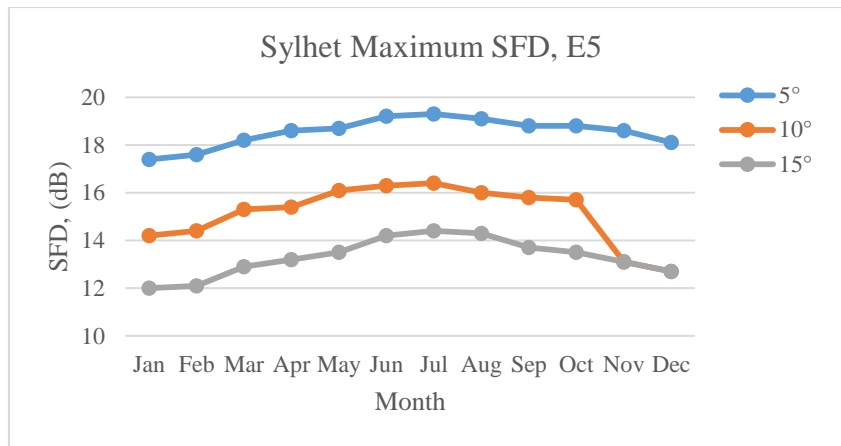
(b)

Fig. 4.49: SFD for different angle in Sylhet for L1 (a) Maximum and (b) Minimum

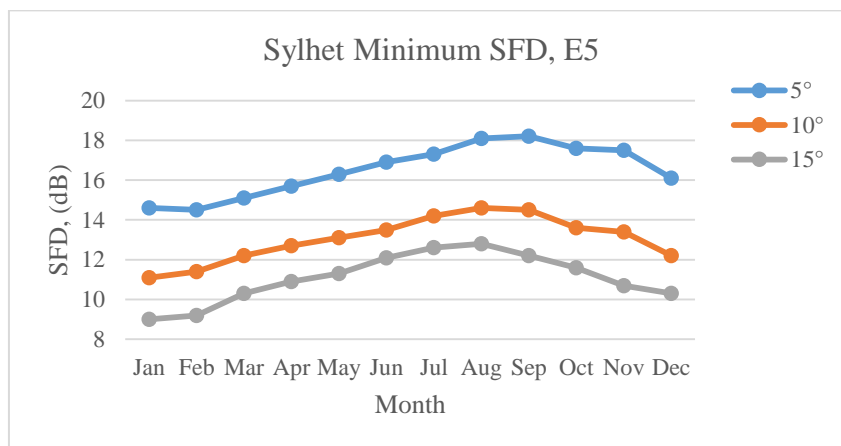
The maximum SFD value for Sylhet is 19.9 dB and minimum SFD value is 9.2 dB for 5° elevation angle which are also the highest and lowest value of SFD amid the outcomes. The evaluated SFD values for E5 signal are listed in Table 4.27 and graphs are individually shown in Fig. 4.50 (a ~ b).

Table 4.27: SFD value of Sylhet using E5 for different elevation angle

Month	SFD (max) in dB			SFD (min) in dB		
	5°	10°	15°	5°	10°	15°
Jan	17.4	14.2	12	14.6	11.1	9
Feb	17.8	14.4	12.1	14.5	11.4	9.2
Mar	18.2	15.3	12.9	15.1	12.2	10.3
Apr	18.6	15.4	13.2	15.7	12.7	10.9
May	18.7	16.1	13.5	16.3	13.1	11.3
Jun	19.2	16.3	14.2	16.9	13.5	12.1
Jul	19.3	16.4	14.4	17.3	14.2	12.6
Aug	19.1	16	14.3	18.1	14.6	12.8
Sep	18.8	15.8	13.7	18.2	14.5	12.2
Oct	18.8	15.7	13.5	17.6	13.6	11.6
Nov	18.6	13.1	13.1	17.5	13.4	10.7
Dec	18.1	12.7	12.7	16.1	12.2	10.3



(a)



(b)

Fig. 4.50: SFD for different angle in Sylhet for E5 (a) Maximum and (b) Minimum

Finally, from the table and graphs above, the SFD value for Sylhet can be perceived. The maximum SFD value and minimum SFD value are 19.3 dB and 9 dB respectively.

4.4.2 Discussion on the results:

The analysis above shows the variation of tropospheric SFD in the surveyed locations for GPS and Galileo constellations. It is evident from the results that SFD value is not the same throughout the process and this is due to the dissimilarities of temperature, pressure and humidity among the locations. These facts result in the signal condition to change. Also the elevation angle has been proven to be an important factor as it controls the value of SFD. The higher the angle the better the value of SFD in all the surveyed locations. Also, the value of SFD for Galileo constellation is on the better side than GPS constellation. To compare among the locations in terms of SFD, the average maximum SFD and average

minimum SFD for 5^0 elevation angle (as it will predict the worst condition) are calculated and Table 4.28 is constructed.

Table 4.28: Average SFD comparison among the locations per year

Location	Average SFD (max)		Average SFD (min)	
	L1	E5	L1	E5
Dhaka	18.9	18.1	16.9	15.8
Chattogram	19.1	18.1	17.0	16.0
Rajshahi	19.1	18.1	16.7	15.4
Khulna	19.5	18.4	17.3	16.0
Sylhet	18.9	18.5	17.1	16.5

The table above provides a more compact picture of SFD condition in the selected locations. Khulna has the worst SFD value that means the signal fading due to troposphere is more than other locations followed by Chattogram. Rajshahi has the best value of SFD succeeded by Dhaka.

4.4.3 Ionospheric delay estimation:

The estimation of ionospheric delay per km of the individual locations are done where maximum TEC of the specific locations are exploited. The ionospheric delay is calculated using the GPS (L1), Galileo (E5) and GLONASS (L3) frequency to get a comparative analysis. The results are registered in Table 4.29. Also the results due to L1, E5 and L3 signal for all the locations are displayed using Fig. 4.51 to Fig. 4.53.

Table 4.29: Ionospheric delay of all the locations for L1, E5 and L3

Month	Dhaka			Chattogram			Rajshahi			Khulna			Sylhet		
	L1	E5	L3	L1	E5	L3	L1	E5	L3	L1	E5	L3	L1	E5	L3
Jan	2.7	4.7	4.8	2.7	4.7	4.9	2.6	4.6	4.8	2.9	5.1	5.3	2.6	4.5	4.8
Feb	2.9	5.2	5.3	3.1	5.4	5.6	3.3	5.7	5.8	3.6	6.3	6.5	3.4	5.9	6
Mar	4.9	8.8	8.9	4.7	8.4	8.5	3.8	6.7	6.8	4.2	7.3	7.4	3.8	6.6	6.7
Apr	6.1	10.7	10.8	5.2	9.1	9.2	5.8	10.1	10	6	10.5	9.9	5.4	9.4	9.5
May	5.9	10.3	10.3	3.7	6.5	6.7	3.9	6.8	6.9	3.9	6.9	7.1	3.7	6.5	6.6
Jun	4	7	7.1	3.9	6.8	6.9	3.5	6.2	6.4	3.6	6.3	6.4	3.4	6.1	6.2
Jul	3.7	6.5	6.6	3.6	6.3	6.5	3.5	6.2	6.4	3.8	6.6	6.7	3.5	6.2	6.4
Aug	4.2	7.4	7.6	4.1	7.1	7.3	3.4	6	6.1	3.5	6.1	6.3	3.3	5.8	5.9
Sep	3.9	6.9	7.1	3.8	6.7	6.9	4	7.1	7.3	4.1	7.2	7.4	4.2	7.4	7.5
Oct	3.2	5.6	5.8	3.1	5.4	5.6	2.9	5.2	5.4	3.2	5.7	5.9	2.7	4.7	4.9
Nov	3.9	5.6	5.8	3.1	5.4	5.5	2.8	4.9	5	2.8	4.9	5.2	2.6	4.6	4.7
Dec	3.2	5.1	5.3	2.7	4.8	4.9	2.5	4.7	4.8	2.7	4.8	5	2.4	4.3	4.4

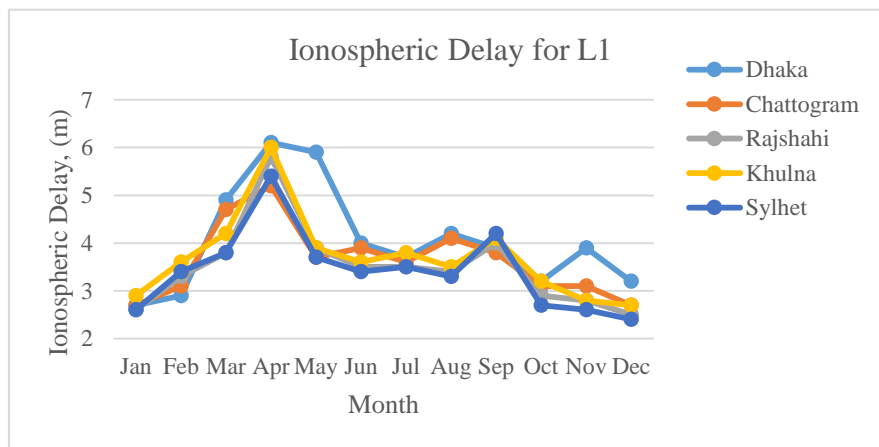


Fig. 51: Ionospheric delay for L1

A variation in the outcomes of ionospheric delay can be observed from Fig. 4.51. The highest value of ionospheric delay occurs in Dhaka with a value of 6.1m. In both Rajshahi and Sylhet, the lowest value of 2.6 m is calculated. April is the month when the maximum ionospheric delay happens for all the locations. If we do the average of the ionospheric delay values of the total surveyed period, we find that Dhaka has an average value of 4.05 m which is the highest and Sylhet has an average value of 3.4 m which is the lowest. The

average values of ionospheric delay of Sylhet and Rajshahi are 19% and 15% lower than Dhaka.

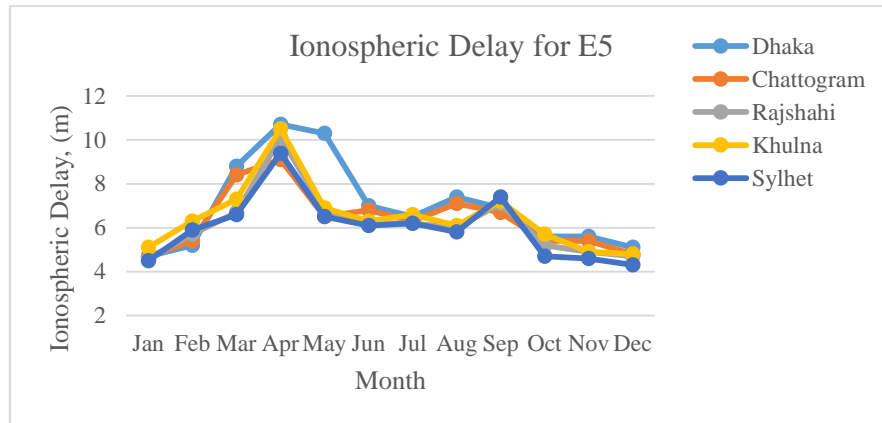


Fig. 4.52: Ionospheric delay for E5

The results of ionospheric delay for E5 signal has greater values than the delay for L1 signal. The highest values are 10.7 m and 10.5m in Dhaka and Khulna respectively. The average value of the ionospheric delay in Sylhet is 16% lower than Dhaka which has the highest average value followed by Rajshahi which is 12.9% lower.

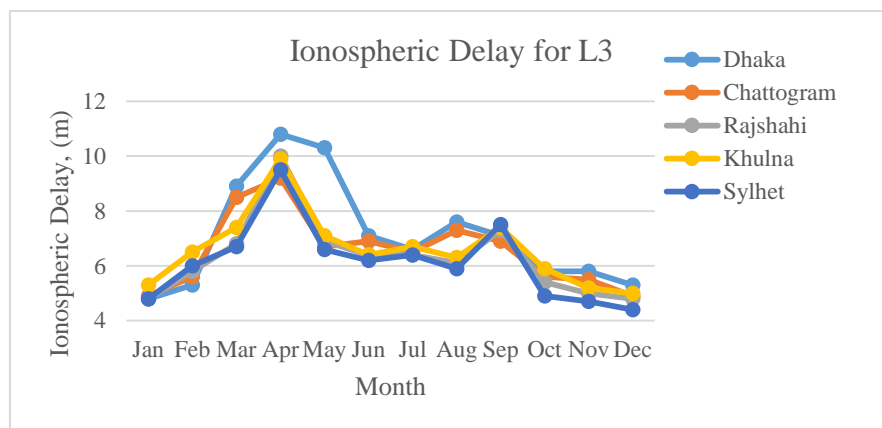


Fig. 4.53: Ionospheric delay for L3

Ionospheric delay outcomes for L3 signal has slightly higher values than the delay for E5 signal. 10.8 m meter and 10.1 m are the highest values in Dhaka and Rajshahi respectively. The lowest value is 4.8m in Chattogram.

4.4.4 Discussion on the results:

The ionospheric delay analysis, executed above, indicates that there are variation in the value in different regions. The main factor regarding this delay calculation has been the total electron content. The value of TEC is not the same throughout the day as well as month. It reaches a peak during certain times of the day. Moreover, the weather condition of different regions also result in different value of TEC. Thus the final ionospheric delay value is not alike in the surveyed regions. From the analysis, it has been observed that during April the ionospheric delay is highest and it tends to decrease at the end of the year. Furthermore, the signals from different constellations has also resulted in dissimilar values of ionospheric delay due to the difference in frequency. It has been observed that for higher frequency signal, the delay is lower.

The assessment among the locations regarding the ionospheric delay is done in the Table 4.30 below by taking the average values.

Table 4.30: Average ionospheric delay comparison among the locations per year

Location	Average Ionospheric Delay (m)		
	L1	E5	L3
Dhaka	4.1	6.9	7.1
Chattogram	3.6	6.3	6.5
Rajshahi	3.5	6.2	6.3
Khulna	3.7	6.5	6.5
Sylhet	3.4	6.0	6.1

From the above table, it can be observed that Sylhet is the best location in terms of lower ionospheric delay followed by Rajshahi while Dhaka is the worst location among the considered locations for analysis. Also, GPS signal has provided better results than the other simulated constellation signals.

4.4.5 Rainfall attenuation:

Finally, the rainfall attenuation for the individual locations are calculated considering the rain rate of the locations. The calculated value of the rain attenuation is listed in Table 4.31 below.

Table 4.31: Rain attenuation (db/km) of individual locations

Month	Dhaka	Chattogram	Rajshahi	Khulna	Sylhet
Jan	3.57	3.41	4.68	6.09	6
Feb	8.27	6.6	6	13.66	9.79
Mar	16.15	14.39	8.27	15.18	24.78
Apr	29.21	27.48	16.9	21.44	51.2
May	46	39.8	38.69	37.45	73.67
Jun	56.25	76.7	51.9	52.9	93.2
Jul	57.2	90.2	59.3	52.3	90.8
Aug	50.9	71.9	49.3	51.6	77.7
Sep	45.9	44.7	44.3	43.9	66.2
Oct	31.8	37.8	30.2	27.9	40.77
Nov	10.9	14.4	6.6	10.9	10.74
Dec	3.9	5.68	3.57	3.57	4.3

To understand and visualize the variation of rain attenuation of different locations better, the results are accumulated in a graph in Fig. 4.54 below.

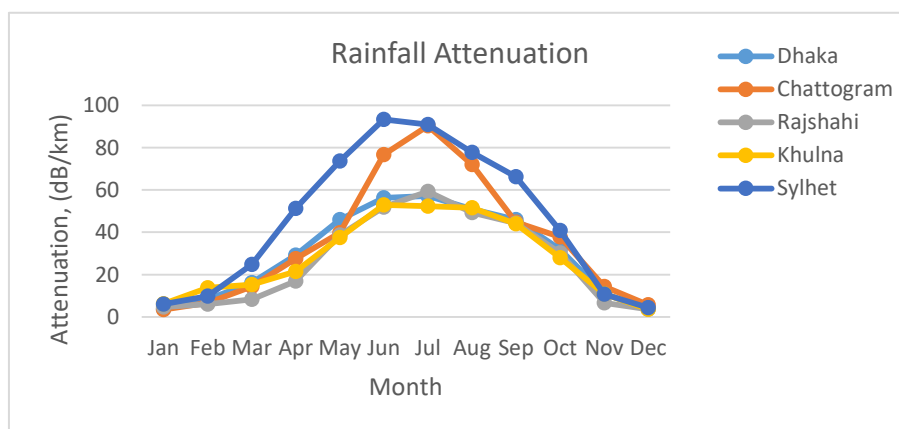


Fig. 4.54: Rainfall attenuation delay over different locations

The graph shows that the rain attenuation is much higher in the middle months of the year. The maximum rain attenuation that is 93.2 db/km occurs in Sylhet in June. Also in Sylhet, highest rain attenuation is calculated throughout the year followed by Chattogram where the maximum value is 90.2 db/km.

4.4.6 Discussion on the results:

The attenuation due to rainfall analysis has been shown above. A number of facts can be pointed from the study. As the rain rate is not the same throughout the country, the fluctuation in the result has been observed. The attenuation is highest during the monsoon time in Bangladesh which is from June to August. Also, the attenuation is on the higher side in those regions which are mainly hilly areas like Chattogram and Sylhet. To make a contrast among the locations, the average of the rain attenuation is taken and Table 4.32 is constructed.

Table 4.32: Average rainfall attenuation comparison among the locations per year

Location	Average Rainfall Attenuation (db/km)
Dhaka	30.0
Chattogram	38.1
Rajshahi	26.7
Khulna	28.1
Sylhet	45.7

The table shows the average value of the rainfall attenuation of the surveyed locations and from the table it is observed that the least average rainfall attenuation occurs in Rajshahi as the rain rate is lower in that region. Due to the higher rain rate, the attenuation is highest in Sylhet followed by Chattogram.

4.4.7 Evaluation of the outcomes:

From the calculated data of section 4.4, it has been observed that the atmospheric factors are not the same at all. Due to this reason, the performance of the ground station will not be similar. To make an assessment of the locations, the comparison Table 4.33 has been listed below.

Table 4.33: Overall comparison among the locations on environmental factors

Parameter	Dhaka	Chattogram	Rajshahi	Khulna	Sylhet
Scintillation Fade Depth	Good	Average	Best	Worst	Not Good
Ionospheric Delay	Worst	Average	Good	Not Good	Best
Rainfall Attenuation	Average	Not Good	Best	Good	Worst

4.5 Estimation of Uplink and Downlink Loss over the Locations

In this section, the results of the uplink and downlink loss have been presented considering the free space path loss and atmospheric loss. The uplink and downlink loss calculation have been displayed in Fig. 4.55 and Fig. 4.56 for GPS, Galileo and GLONASS respectively.

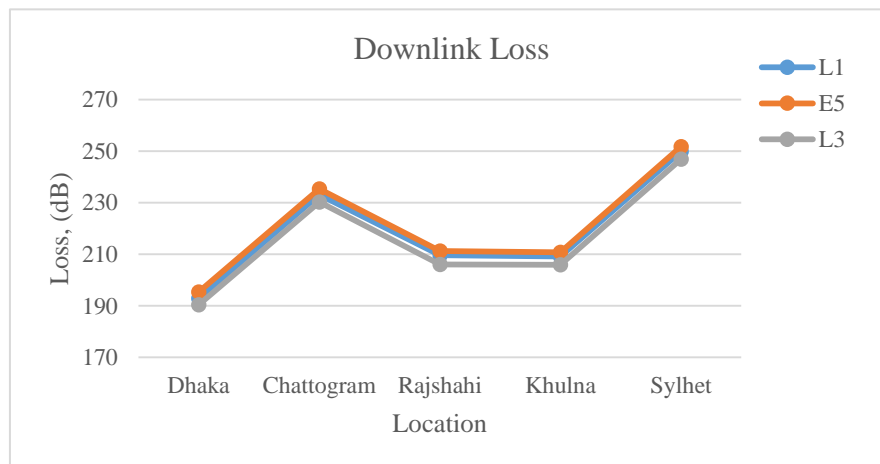


Fig. 4.55: Downlink loss over different locations

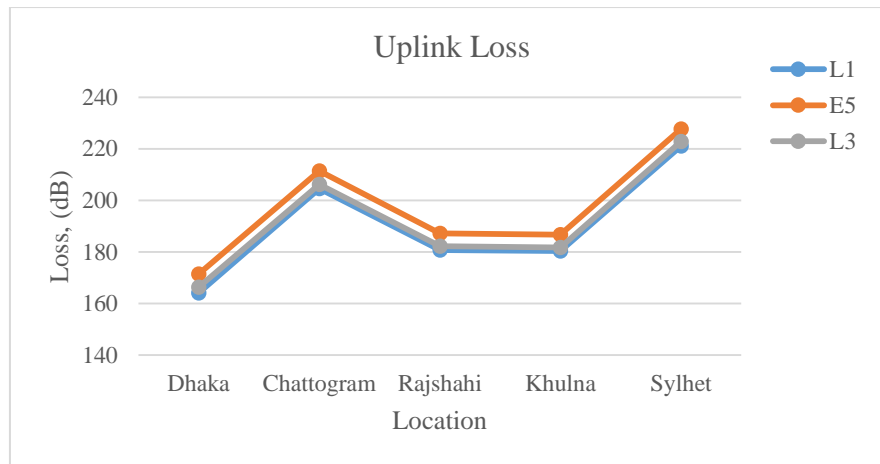


Fig. 4.56: Uplink loss over different locations

4.5.1 Discussion on the results:

The calculated losses displayed in the graphs above indicates that due to variation in atmospheric conditions, the losses also varies. As free space path loss has also been considered, the losses has been fluctuating. The uplink loss and downlink loss are not similar as well. Also the loss of different constellations differ from each other as the frequency of the signals are not the same. The loss for GPS signal is lower than the other signals whereas loss of Galileo signal is on the higher side. It has been observed that Dhaka has the lowest loss value. On the other hand Sylhet exhibits the highest loss value.

CHAPTER 5

CONCLUSION AND FUTURE RECOMMENDATION

5.1 Conclusion

In this research work, some major criteria of developing a SBAS for Bangladesh have been investigated over five different locations in Bangladesh which are Dhaka, Chattogram, Rajshahi, Khulna and Sylhet. GNSS constellation parameters such as MDB, MDE, GDOP, BNR, number of visible satellites and accuracy have been investigated for GPS and Galileo constellation. Also, a number of GNSS reference station antennas have been designed to observe the performance of GNSS signals and achieve beam scanning. Moreover, the environmental factors such as tropospheric scintillation, ionospheric delay and rainfall attenuation have been investigated using the atmospheric data of 20 years. A number of widely recognized models have been used to calculate the atmospheric factors. These studies have been done to aid in making an evaluation among the location to select ideal reference station sites for SBAS. Finally, uplink and downlink loss have been calculated for the surveyed locations.

5.2 Significance of the Research

In this research, the variation of different GNSS parameters has been observed among the locations and the results have been organized in tabular form to understand the dissimilarities. The major findings and their significance are:

- a) The research is the first of its kind ever done in Bangladesh focusing on the establishment of SBAS which will improve the satellite navigation sector of Bangladesh in near future.
- b) In the case of comparison among GPS and Galileo, the latter has performed better than the other. This will aid to choose between the constellations for further work. Also, we have observed that Khulna has the best performance in terms of the simulated parameters, preceded by Chattogram. These results can be helpful in establishing the ground station on different locations.
- c) In terms of accuracy the best results have been observed in Dhaka followed by Chattogram. From assisting to select site for ground station to select location for major establishment such as defense base, these results can be proven important.

- d) As in various fields of communication such as satellite and radar, beam steering not only provides superior performance but also heightens the overall integrity of the communication system. Focusing on beam steering, a part of this research is carried out by designing and improving a phased array antenna using microstrip patch which has a scan angle range of 49° . This antenna array can be utilized in constructing the earth station antenna for wider scan angle.
- e) The analysis of tropospheric scintillation, ionospheric delay and rainfall attenuation have shown the fluctuation in values and from the result it can be said that Rajshahi has the best results among the others. Also, the results of ionospheric delay for Galileo is greater than GPS. These simulation results will definitely help to locate ideal ground station locations. Also, what type of model needs to be used to mitigate the delay and where to use can be analyzed from the results.
- f) The maximum loss is recorded in Sylhet followed by Chattogram. On the other hand, Dhaka has the minimum loss value. As link budget calculation is one of the most essential works in designing SBAS, the loss estimation in this work can be resourceful.

To summarize, this research can give a visionary direction in order to establish an SBAS for Bangladesh which will bring a radical change from the geopolitical point of view.

5.3 Scope for Future Work

The work of developing a SBAS for Bangladesh is not over with this research as there are still more opportunity. A more widespread research can be done in future to make the whole system feasible as well as validated from the international authorities. The requirements at present and in future should be considered before designing such a system which will help Bangladesh leverage its economic progress. Since augmentation system escalates the major performance criteria of GNSS system, a comprehensive approach needs to be taken for developing the overall system to avail its full advantage.

- a) Performance parameters of GPS and Galileo has been investigated in this research work which are the major constellations. More constellations such as GLONASS, BeiDou etc. can be explored in order to have a clear view of GNSS condition over Bangladesh.

- b) It is advised to increase the number of location in future which will increase the chance of establishing the SBAS ground station in a much better location. Not only that, the number of analytical parameters can be increased so that the study becomes more impactful and effective.
- c) Since one of the most important factors in SBAS development is the atmospheric condition, more focus can be placed on various types of models so that a comparison can be made.
- d) In addition to that, the interoperability of different types of SBAS can be another future scope. In parallel to the development of the SBAS for Bangladesh, a study can be commenced on the established SBAS of the neighboring countries to understand the mechanism of merging both the systems.
- e) Research on other components of ground station such as power system, control system, communication system between reference stations etc. are also recommended.
- f) Lastly, research on the rules and regulations aspect of creating an SBAS can be conducted. These rules may be national or international in nature, and they should be crafted with both the interests in mind.

LIST OF PUBLICATIONS

1. **A. A. M. Shah Sadman** and Md Hossam-E-Haider, "An Analysis on GNSS Parameters over Bangladesh Intended for Developing a SBAS", *2nd International Conference on Robotics, Electrical and Signal Processing Techniques 2021 (ICREST 2021)*, AIUB, pp. 215 – 220, 5 – 7 January, 2021, Dhaka, Bangladesh.
2. **A. A. M. Shah Sadman** and Md Hossam-E-Haider, "Design of a 2x3 Microstrip Patch Phased Array Antenna for GNSS Augmentation", *23rd International Conference on Computer and Information Technology (ICCIT 2020)*, Ahsanullah University of Science and Technology, pp. 1 – 6, 19 – 21 December, 2020. [**Ranked no 1, Best Paper Award**]
3. **A. A. M. Shah Sadman** and Md Hossam-E-Haider, "Design and Performance Analysis of a Slotted Microstrip Patch Antenna for Different GNSS Frequencies", *2020 IEEE 7th International Conference on Engineering Technologies and Applied Sciences (ICETAS)*, 18 – 20 December, 2020, Kuala Lumpur, Malaysia.
4. **A. A. M. Shah Sadman** and Md Hossam-E-Haider, "GNSS Position Accuracy Considering GDOP and UERE for Different Constellation over Bangladesh" *22nd International Conference on Computer and Information Technology (ICCIT 2019)*, South East University, pp. 1 – 5, 18 – 20 December, 2019.

LIST OF REFERENCES

- [1] L. S. Lawal and C. R. Chatwin, "A review of GNSS and augmentation systems," *Journal of Electrical and Electronics Engineering*, vol. 5, issue 3, pp. 1 – 21, March 2019.
- [2] E. D. Kaplan and C. J. Hegarty, *Understanding GPS Principles and Applications*. 2nd ed. Boston: Artech House, 2006.
- [3] W. Y. Ochieng, K. Sauer, D. Walsh, G. Brodin, S. Griffin and M. Denney, "GPS integrity and potential impact on aviation safety," *The Journal of Navigation*, vol. 56, issue 1, pp. 51 – 65, June 2003.
- [4] K. N. S. Rao, "GAGAN - The Indian satellite based augmentation system," *Indian Journal of Radio & Space Physics*, vol. 36, pp. 293 – 302, August 2007.
- [5] JICA, "Ex-Ante evaluation for Hazrat Shahjalal International Airport expansion project," August 13, 2020.
- [6] M. G. Hussain, P. Failler and S. Sarker, "Future importance of maritime activities in Bangladesh," *Journal of Ocean and Coastal Economics*, vol. 6, issue 2, art. 3, Bangladesh, October 2019.
- [7] L. L. Arnold, "Positional accuracy of the wide area augmentation system," M. S. thesis, College of Geography, Univ. of New Mexico, Mexico, 2009. Accessed on: June 10, 2020.
- [8] L. Gauthier, P. Michel, J. Benedicto and J. Ventura, "EGNOS: The first step in Europe's contribution to the Global Navigation Satellite System," *ESA Publications Bulletin*, vol. 105, pp. 35 – 43, January 1, 2004. Accessed on: June 10, 2020.
- [9] European Space Agency, "EGNOS Open Service (OS) service definition document," October 3, 2017.
- [10] R. Singh, "Satellite communications: the Indian scenario," *International Journal of Engineering Research and Applications*, vol. 4, issue 5, pp. 41 – 49, May 2014.
- [11] A. S. Ganeshan, A. Kartik, S. Nirmala and G. Ramesh, "India's Satellite-Based Augmentation System GAGAN - redefining navigation over the Indian region," *Inside GNSS*, January 2016.
- [12] D. S. Ilcev, "Architecture of African satellite augmentation system (ASAS) for Africa and middle east," *International Journal of Engineering & Technology*, vol. 8, issue 4, pp. 567 – 571, 2019.

- [13] S. Choy, J. Kuckartz, A. G. Dempster, C. Rizos and M. Higgins, “GNSS satellite-based augmentation systems for Australia,” *GPS Solutions*, vol. 21, issue 3, pp. 835 – 848, 2017.
- [14] “SBAS safety assessment guidance related to anomalous ionospheric conditions,” ICAO Asia and Pacific office, July 2016.
- [15] ICAO, “Global Navigation Satellite System (GNSS) Manual,” June 2012.
- [16] M. Tsai, K. Chiang, M. Yang and H. Chen, “The accuracy and reliability analysis for future GNSS in Taiwan region,” *Journal of Photogrammetry and Remote Sensing*, vol. 13, no.1, pp. 57 – 65, March 2008.
- [17] Z. Zhou and Y. Wu, “System model bias processing approach for regional coordinated states information involved filtering,” *Mathematical Problems in Engineering*, vol. 2016, pp. 1 – 7, March 2016.
- [18] A. Grant, P. Williams, G. Shaw, M. D. Voy and N. Ward, "Understanding GNSS availability and how it impacts maritime safety," *Proceedings of the 2011 International Technical Meeting of The Institute of Navigation*, pp. 687 – 695, San Diego, CA, January 2011,
- [19] C. S. Chen, Y. J. Chiu, C. T. Lee and J. M. Lin, “Calculation of weighted geometric dilution of precision,” *Journal of Applied Mathematics*, vol. 13, pp. 1 - 10, September 2013.
- [20] R. B. Langley, “Dilution of precision,” *GPS World*, vol. 10, no. 5, pp. 52 – 59, May 1999.
- [21] J. Januszewski, “Sources of error in satellite navigation positioning,” *The International Journal on Marine Navigation and Safety of Sea Transportation*, vol. 11, no. 3, pp. 419 – 423, September 2017.
- [22] M. Tahsin, S. Sultana, T. Reza, M. Haider “Analysis of DOP and its preciseness in GNSS position estimation”, *Int’l Conf. on Electrical Engineering and Information & Communication Technology (iCEEiCT)*, vol. 2, pp. 12 – 17, May, 2015, Dhaka, Bangladesh.
- [23] J. J. H. Wang, “Antennas for global navigation satellite system (GNSS), ” *Proceedings of the IEEE*, vol. 100, no. 7, pp. 2349 – 2355, July 2012.
- [24] C. A. Balanis, *Antenna Theory: Analysis and Design*, 4th ed., Hoboken, NJ, USA: Wiley, 2016.

- [25] F. Gulbrandsen, "Design and analysis of an X-band phased array patch antenna", M. S. thesis, Department of Electronics and Telecommunications, Norwegian University of Science and Technology, Norway, June 2013.
- [26] D. A. Ritchie, "Factors that affect the global positioning system and global navigation satellite system in an urban and forested environment," M. S. thesis, Department of Technology, East Tennessee State University, UA, May 2017.
- [27] C. Y. Chen and M. J. Singh "Comparison of tropospheric scintillation prediction models of the Indonesian climate," *Earth, Planets and Space*, vol. 66, pp. 1 – 12, July 2014.
- [28] G. N. Ezeh, N. Chukwunke and U. H. Diala "Effects of rain attenuation on satellite communication link," *Advances in Science and Technology Research Journal*, vol. 8, no. 22, pp. 1 – 11, June 2014.
- [29] C. J. R. Capela, "Protocol of communications for vorsat satellite," M. S. thesis, College of Electrical Engineering, Univ. of Porto, Portugal, 2012.
- [30] M. S. Islam, M. I. Ibrahimy, S. M. A. Motakabber and A. K. M. Hossain, "A rectangular inset-fed patch antenna with defected ground structure for ISM band," *International Conference on Computer and Communication Engineering (ICCCCE)*, vol. 7, pp. 104 – 108, September 2018.
- [31] A. Rani and R. K. Dawre, "Design and analysis of rectangular and U slotted patch for satellite communication," *International Journal of Computer Applications*, vol. 12, no. 7, pp. 36 – 40, December 2010.
- [32] G. Anjaneyulu and J. S. Varma, "Design and simulation of multi band microstrip antenna array for satellite applications," *International Conference on Electronics, Communication and Aerospace Technology (ICECA)*, vol. 2, pp. 2386 – 2389, March 2018.
- [33] International Telecommunication Union: Propagation Data and Prediction Methods Required for the Design of Earth-Space Telecommunication Systems, Recommendation ITU-R P.618-10, October 2009.
- [34] I. E. Otung, "Prediction of tropospheric amplitude scintillation on a satellite Link," *IEEE Transaction on Antenna and Propagation*, vol. 44, no. 12, pp. 1600 – 1608, December 1996.

- [35] Y. Karasawa, M. Yamada and J.F. Allnutt, "A new prediction method for tropospheric scintillation on earth-space paths," *IEEE Transaction on Antenna and Propagation*, vol. 36, no. 11, pp. 1608 – 1614, November 1988.
- [36] M. S. Hossain and M. A. Samad, "The tropospheric scintillation prediction of earth-to-satellite link for Bangladeshi climatic condition," *Serbian Journal of Electrical Engineering*, vol. 12, no. 3, pp. 263 – 273, October 2015.